Polymer-Based Analytical Devices and Systems

塑膠基材分析元件與系統

December 2nd, 2020

Introduction

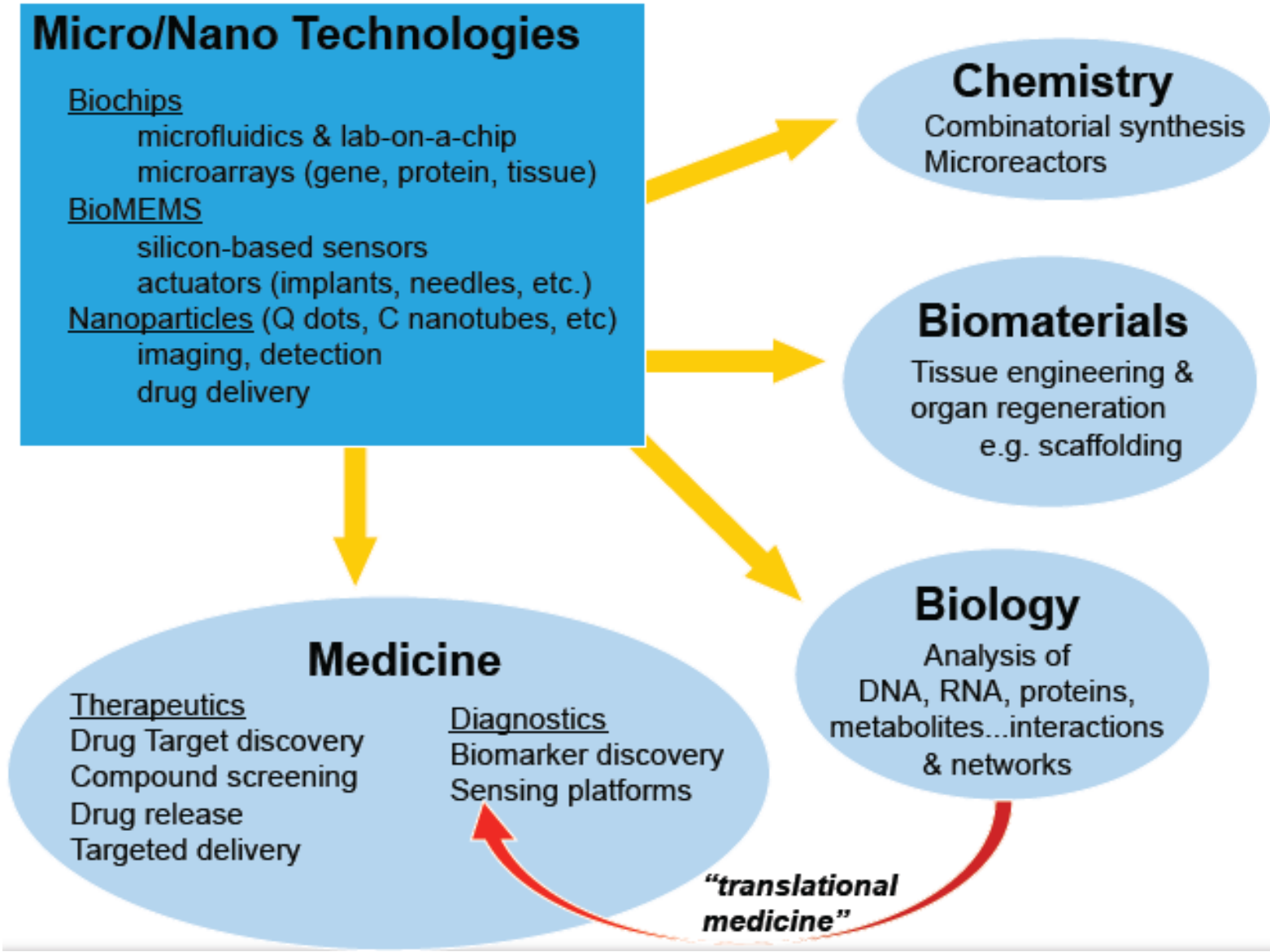

Lab-on-a-Chip vs. Microfluidics

Microfluidics is a microtechnological field dealing with the precise transport of fluids (liquids or gases) in small amounts (e.g. microliters, nanoliters or even picoliters).

A Lab-on-a-Chip (LOC) is a device that integrates one or several laboratory functions on a single chip of only millimeters to a few square centimeters in size.

LOCs deal with the handling of extremely small fluid volumes down to less than pico liters. Lab-on-a-Chip devices are a subset of MEMS devices and often indicated by "Micro Total Analysis Systems" (µTAS) as well.

However, strictly regarded "Lab-on-a-Chip" or "µTAS" indicate generally the scaling of single or multiple lab processes to perform chemical analysis.

The term "Lab-on-a-Chip" was introduced later on when it turned out that µTAS technologies were more widely applicable than only for analysis purposes.

History

At beginning of the 1990's, the LOC research started to seriously grow as a few research groups in Europe developed micropumps, flowsensors and the concepts for integrated fluid treatments for analysis systems.

These μTAS concepts demonstrated that integration of pre-treatment steps, usually done at lab-scale, could extend the simple sensor functionality towards a complete laboratory analysis, including e.g. additional cleaning and separation steps.

A big boost in research and commercial interest came in the mid 1990's, when μTAS technologies turned out to provide interesting tooling for genomics applications, like capillary electrophoresis and DNA microarrays. A big boost in research support also came from the military, especially from DARPA (Defense Advanced Research Projects Agency), for their interest in portable bio/chemical warfare agent detection systems.

Point of care diagnostics.

Timeline

1800

Electrophoresis 1809 Rcoss

≈

1900

Chromatography 1906 M.S. Tswett
(**Liquid Chromatography, Adsorption Chromatography)**

Moving Boundary Electrophoresis 1930 A.W.K.Tiselius 1948 Nobel Prize

Ion-Exchanged Chromatography 1940s' Manhattan Project

Partition Chromatography 1941 A. J. P. Martin and R. L. M. Synge 1952 Nobel Prize

Gas Chromatography 1947 Fritz Prior

1950

Affinity Chromatography 1953

Size-Exclusive Chromatography 1955 G. H. Lathe and C. R Ruthven

High-Performance Liquid Chromatography (HPLC) 1967 C. G. S. R. Lipsky

Isoelectric Focussing 1968 C. Wrigley

Two-Dimensional Polyacrylamide Gel Electrophoresis (2-D PAGE) O'Farrell 1975

Lab on a Chip 1975 S.C. Terry

MALDI-MS 1987 K. Tanaka 2002 Nobel Prize

ESI-MS 1988 J. B. Fenn 2002 Nobel Prize

µ-TAS 1990' DAPRA

2000

Global Health Program

http://www.fiscalliteracy.com

http://science.howstuffworks.com

http://www.h2o2.com/

http://aglaw.blogspot.tw

http://pocd.com.au/

http://www.agilent.com

www.afap.org

www.birthday-party-resource.com

Point of Care - Commercial Available Products

Glucose meter

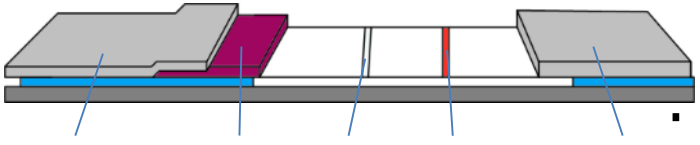

Lateral flow immunoassay

Dipstick

Abbott
A Promise for Life

i-STAT Analyzer

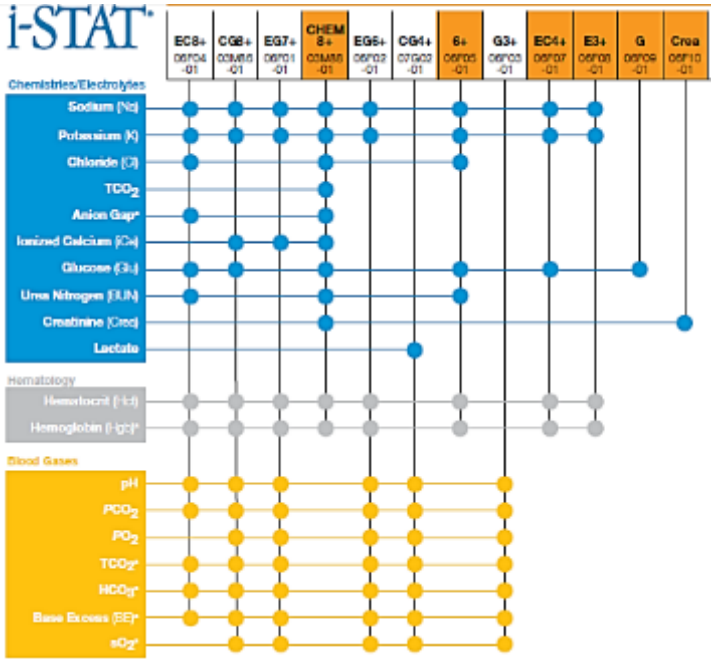

The array of rapid tests

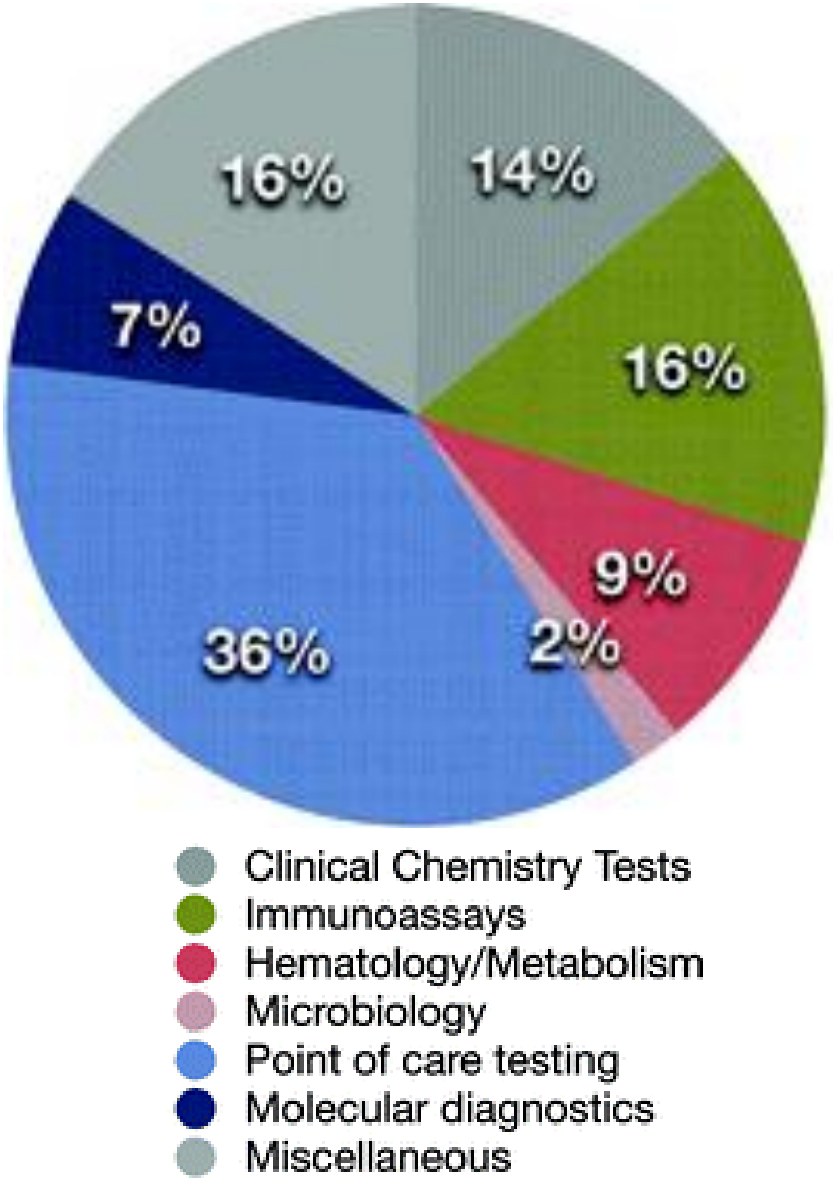

In vitro Diagnostics Market Segments

A. K. Yetisen, *Lab Chip,* 2013.

Lab-on-a-Chip Integration

- **Low fluid volumes consumption**
- **Faster analysis and response times**
- **Better process control**
- **Compactness of the systems**
- **Lower fabrication costs**
- **Safer platform**

- Miniaturize

- Automate

- Integrate

- Silicon

- Glass

- Polymer

- Paper

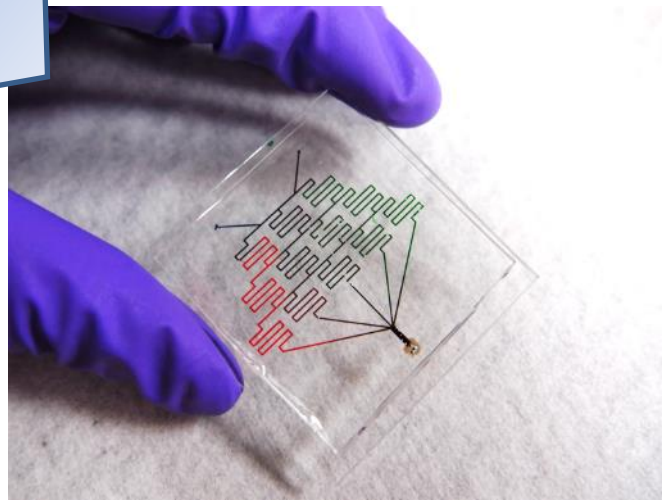

Size Scale

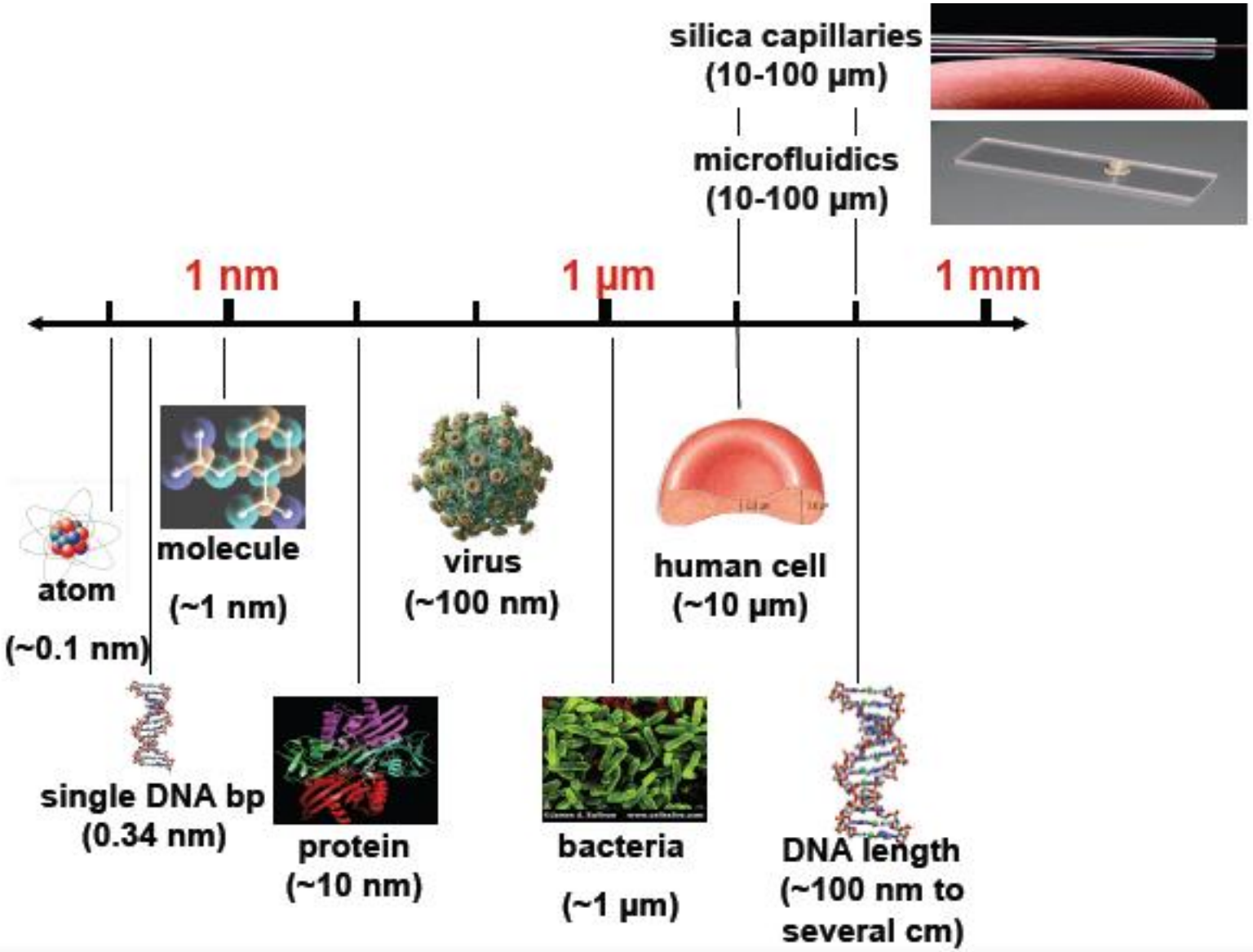
silica capillaries
(10-100 µm)
microfluidics
(10-100 µm)
1 nm
1 µm
1 mm
atom
(~0.1 nm)
molecule
(~1 nm)
virus
(~100 nm)
human cell
(~10 µm)
single DNA bp
(0.34 nm)
protein
(~10 nm)
bacteria
(~1 µm)
DNA length
(~100 nm to
several cm)

Portable Miniaturized Analytical System

Low-Cost Miniaturized Analysis Systems

Silicon

Polymer

Paper

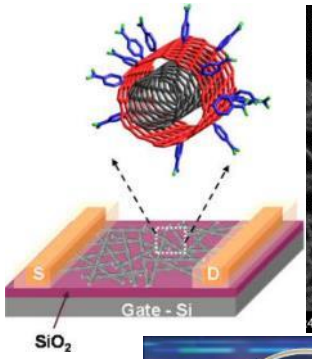

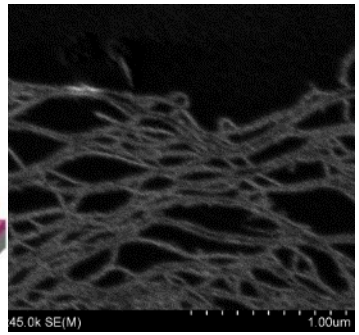

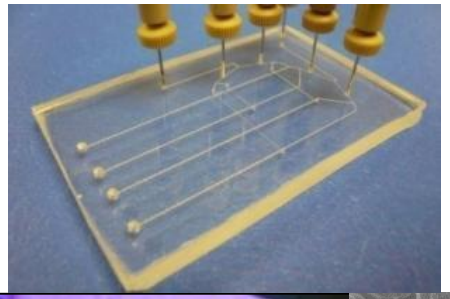

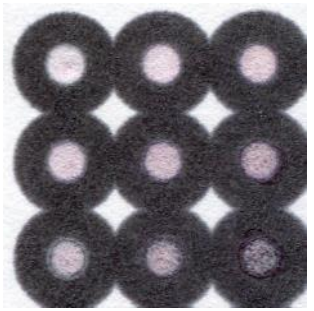

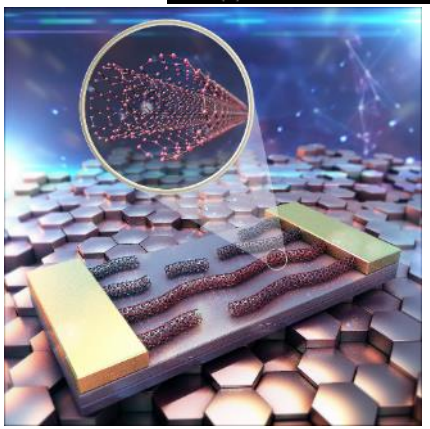

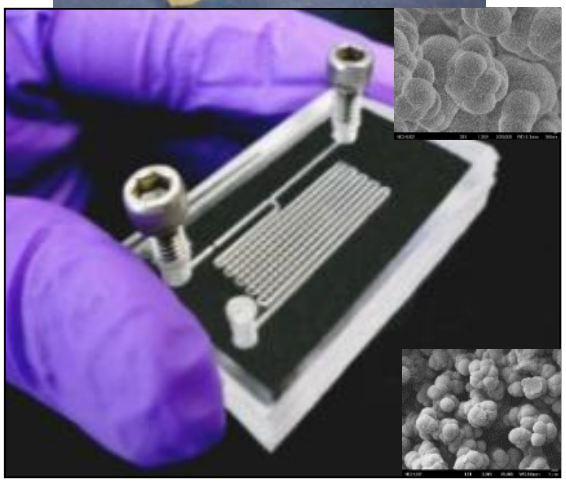

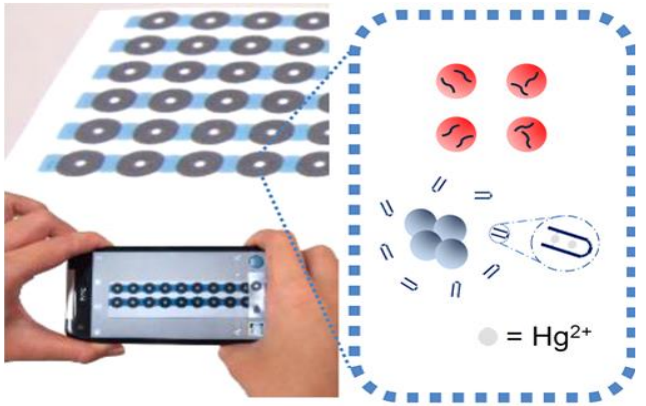

FET Biosensor

Thermoplastic Device

Paper Diagnosis

Basic Principles - Molecular Diagnostics

Enzyme-Linked Immunosorbent Assay (ELISA)

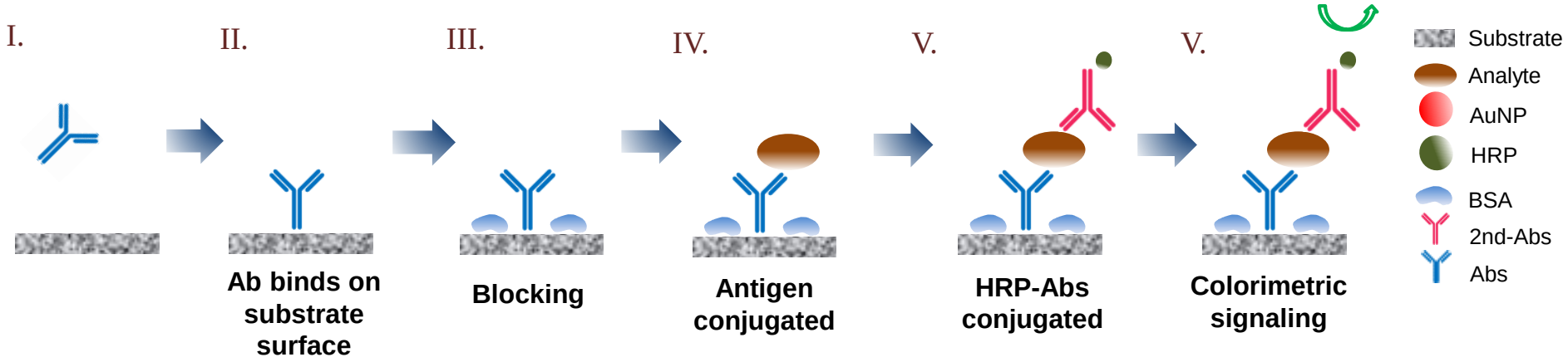

DNA hybridization or Aptamer binding

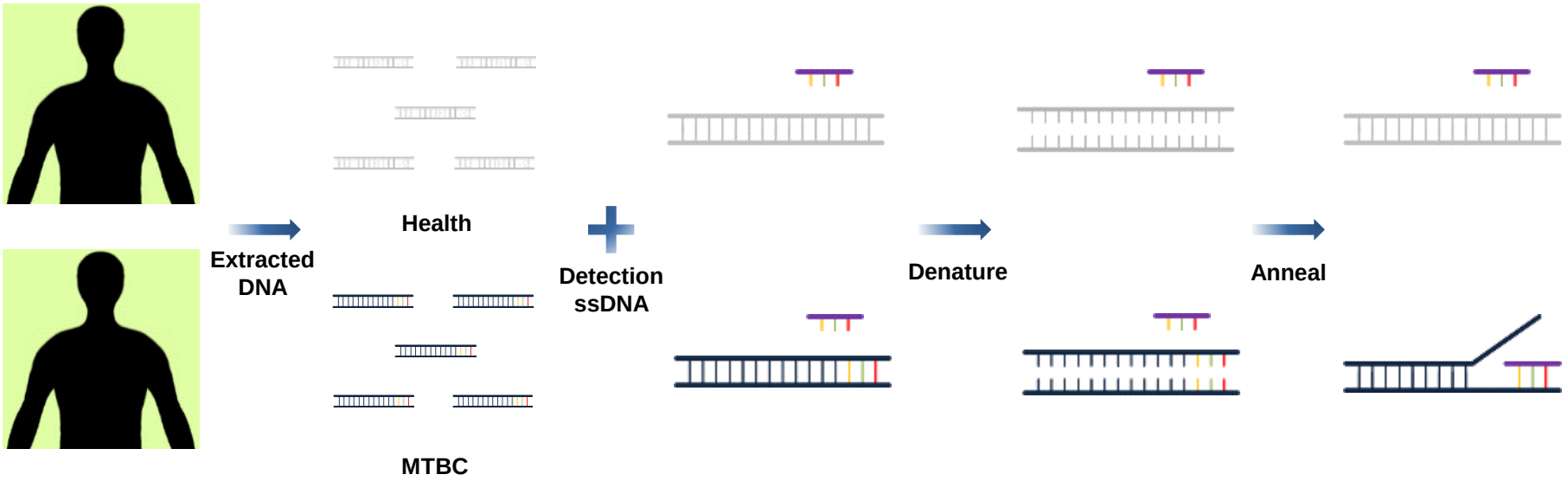

Enzyme-linked immunosorbent assay (ELISA)

- **Direct and Indirect ELISA**

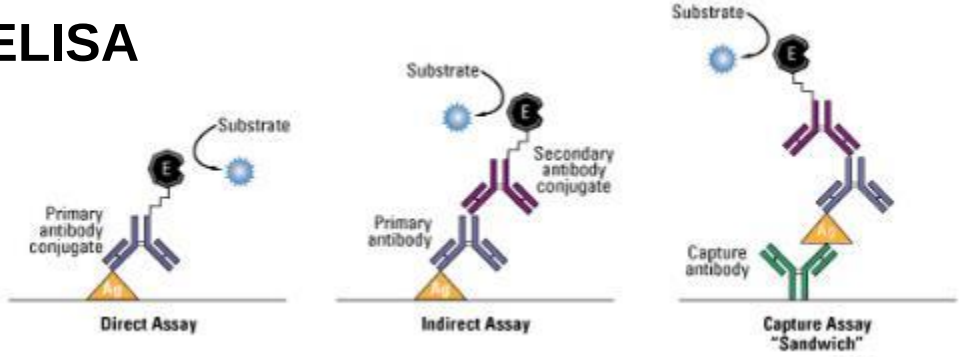

- **Sandwich ELISA**

- **Competitive ELISA**

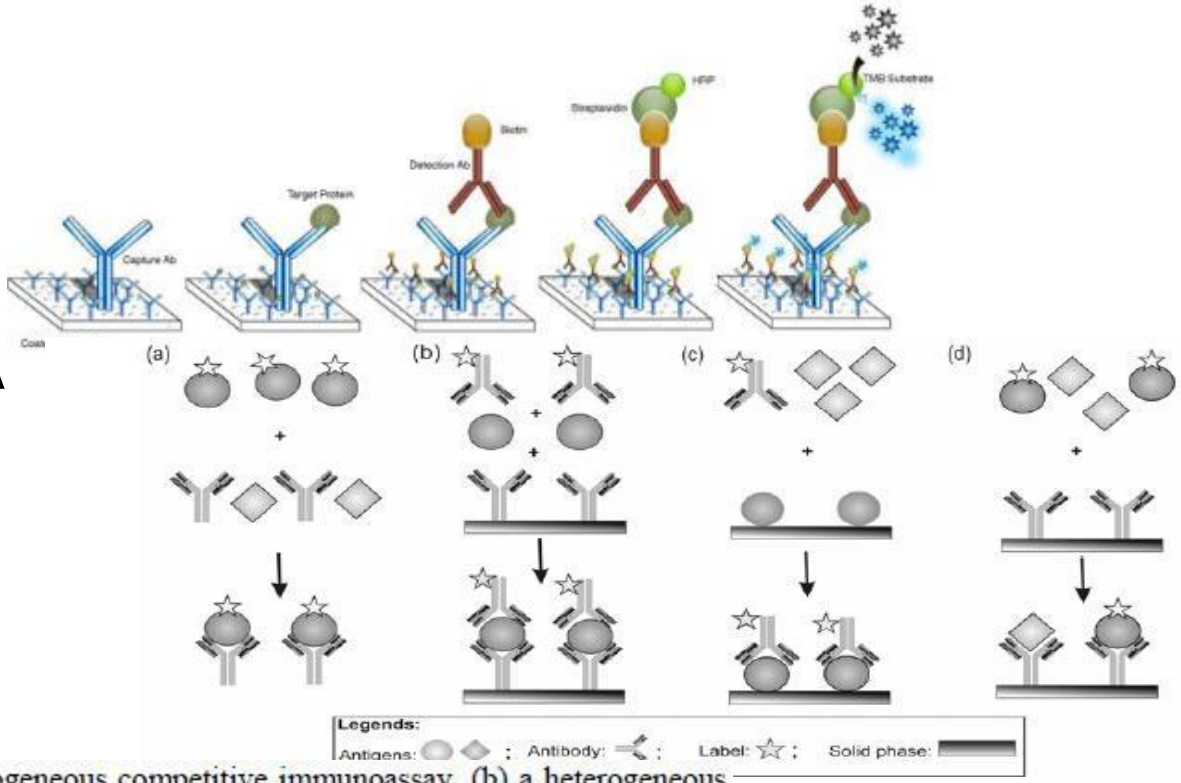

Figure 1: Generally used formats: (a) a homogeneous competitive immunoassay, (b) a heterogeneous non-competitive immunoassay, (c) a heterogeneous competitive immunoassay and (d) a heterogeneous competitive immunometric assay.

Commercial POC NAT Platforms

Platform	Manufacturer	Sample prep included?	Amplification	Detection	Time to result (min)[a]	Website
GeneXpert	Cepheid	Y	PCR	RTF	<120	www.cepheid.com
Liat Analyzer	IQuum	Y	PCR	RTF	<60	www.iquum.com
MDx	Biocartis	Y	PCR	RTF	Unknown	www.biocartis.com
FL/ML	Enigma	Y	PCR	RTF	<45	www.enigmadiagnostics.com
FilmArray	Idaho technologies	Y	PCR	RTF	60	www.idahotech.com
Razor	Idaho technologies	N	PCR	RTF	<60	www.idahotech.com
R.A.P.I.D.	Idaho technologies	N	PCR	RTF	<30	www.idahotech.com
LA-200	Eiken	N	Isothermal (LAMP)	RTT	< 60	www.eiken.co.jp
Twista	TwistDX	N	Isothermal (RPA)	RTF	< 20	www.twistdx.co.uk
BART	Lumora	N	Isothermal (LAMP)	RTB	< 60	lumora.co.uk/
Genie II	Optigene	N	Isothermal (LAMP)	RTF	< 20	www.optigene.co.uk
SAMBA	Diagnostics for the Real World	N	Isothermal (similar to NASBA)	NALF	> 60	Not available
BESt Cassette[b]	BioHelix/ Ustar Biotech	N	Not included, but typically isothermal	NALF	N/A	www.biohelix.com; www.bioustar.com

[a]Time to result depends upon the particular assay. Longer times may be required for assays with a reverse transcriptase step.

[b]Device sold by BioHelix in the USA; manufactured and sold by Ustar Biotech in China.Abbreviations: RTB real-time bioluminescence; RTF real-time fluorescence; RTT real-time turbidimetry.

Example POC NAT platforms that are commercially available or close to market.

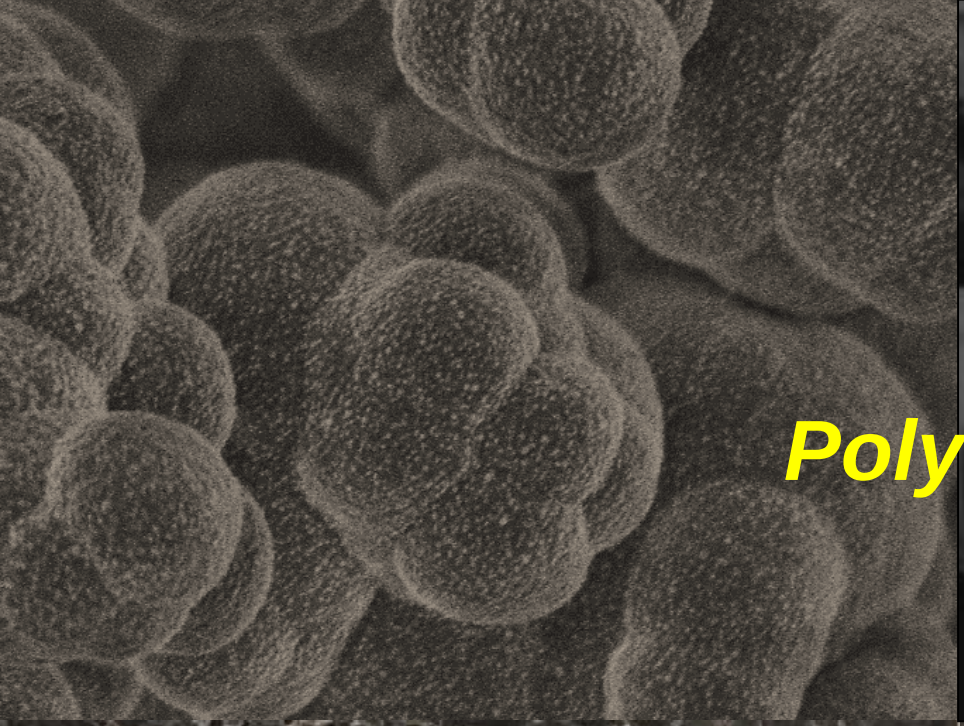

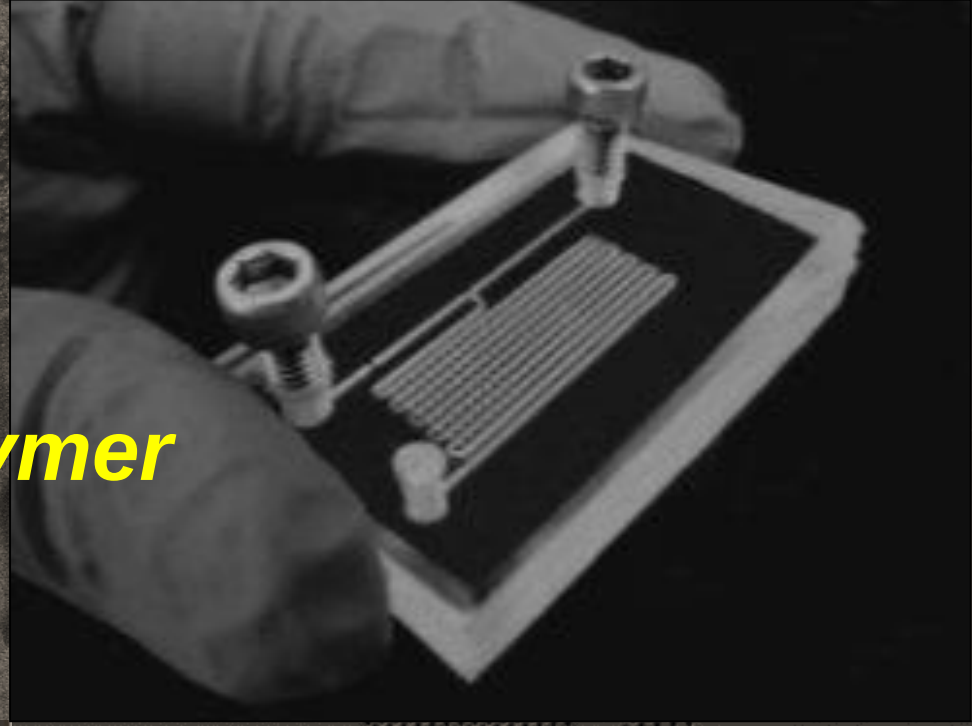

Polymer

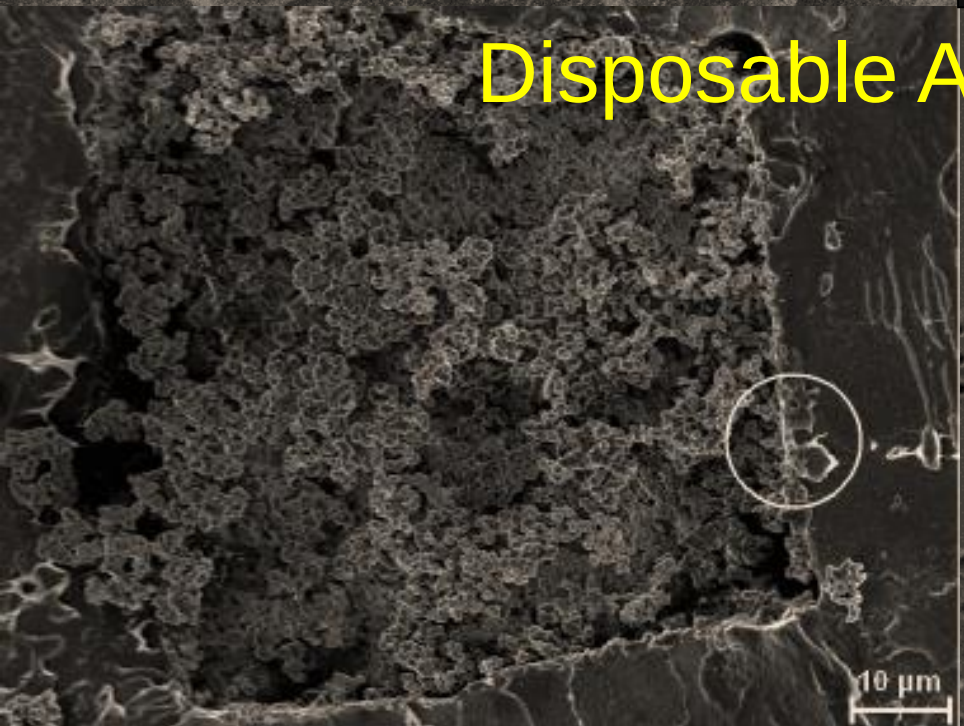

Disposable Analytical Chips

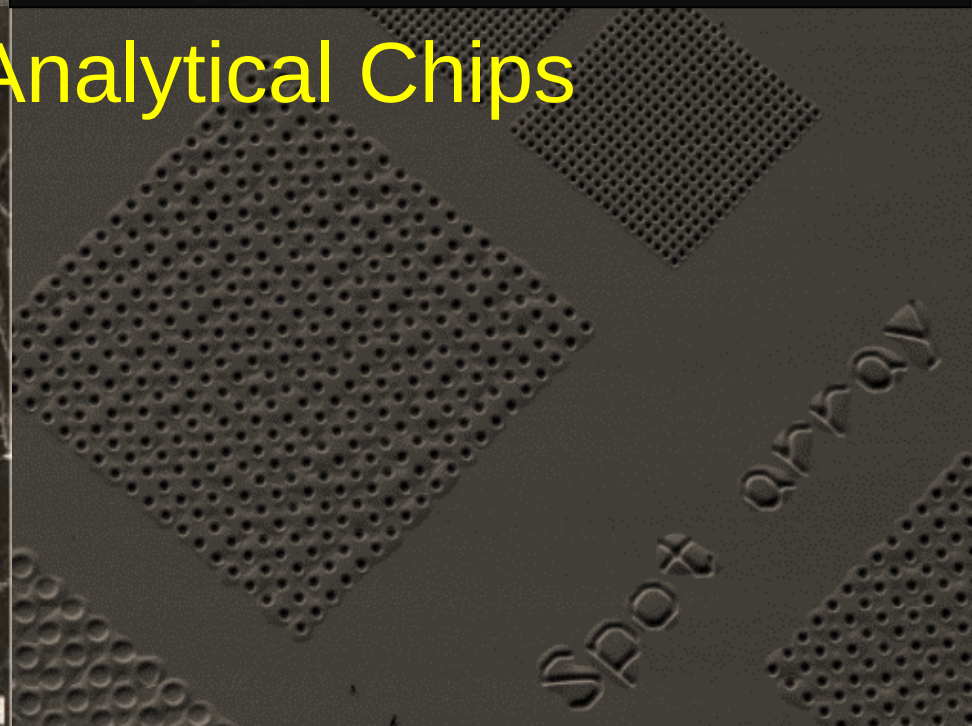

Examples

- Point-of-care systems
- PoC can accurately cover ~70% of requested tests.

Abbott
A Promise for Life

i-STAT Analyzer

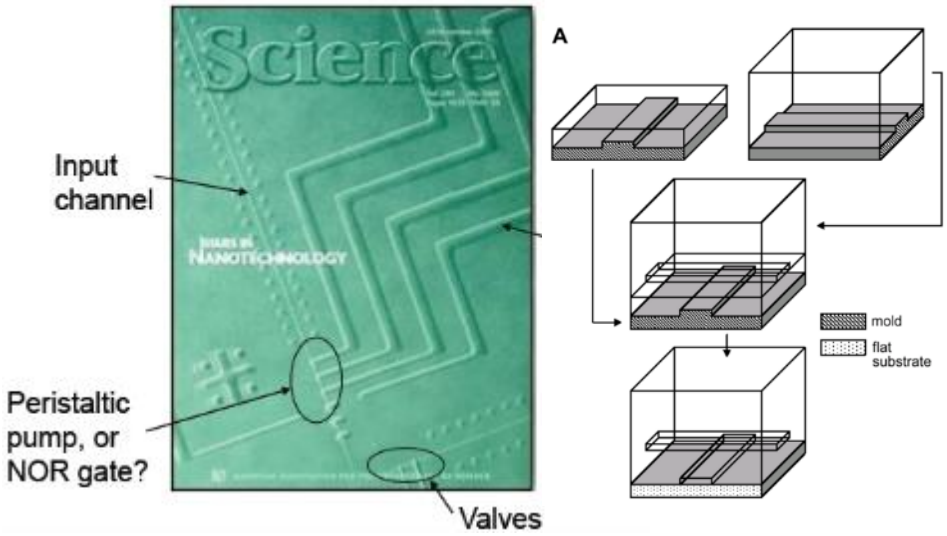

Fluidigm—the largest commercial μTAS technology company currently in the market—build their microfluidic systems using deformable elastomers (NanoFlex valves).

Advantages

- **Scalable**
- Simple fabrication
- Rapid diagnosis
- Real time
- **Cost effective**
- Portable
- Disposable
- Multiplex diagnosis (arrays)
- User friendly
- High sensitive (Automatic, digital readout)
- **Flexible**
- Easy to store
- Avoid damage during transportation
- The wettablility of paper help biosensing without external follow control systems
- Directly sensing (not depends on enzyme reaction)
- Enhance the healthcare in extreme places such as developing world and battle fields.

- 2.2. Selection of Polymer Materials
- 2.2.1. Polydimethylsiloxane
- 2.2.2. Cyclic Olefin Copolymer
- 2.3. Fabrication of Polymer Devices
- 2.3.1. Structure Formation
- 2.3.1.1. Soft Lithography
- 2.3.1.2. Injection Molding
- 2.3.1.3. Hot Embossing
- 2.3.1.4. Nanoimprint Lithography
- 2.3.1.5. Direct Machining
- 2.3.1.6. Laser-Printed
- 2.3.2. Device Sealing
- 2.3.2.1. Adhesive Bonding
- 2.3.2.2. Thermal Bonding
- 2.3.2.3. Solvent Bonding
- 2.3.2.4. Welding
- 2.3.3. World-to-Chip Interface
- 2.4. Fluidic Control Components
- 2.4.1. Valve
- 2.4.2. Pump
- 2.4.3. Mixer

Properties of Common Polymeric Materials

Polymer	Acronym	Tg (^{0}C)	CTE (10^{-60}C^{-1})	Water absorption (%)	Solvent resistance	Acid/base resistance	Biocompatibility	Optical transmissivity	
								Visible	UV
Polydimethylsiloxane	PDMS	-125--122	300-310	0.03	Poor	Good	Excellent	Excellent	Excellent
Cyclo olefin polymer	COP	70-163	60-70	0.01	Good	Good	Excellent	Excellent	Good
Cyclic olefin copolymer	COC	80-180	60-70	0.01	Good	Good	Excellent	Excellent	Good
Poly(methyl methacrylate)	PMMA	100-122	70-150	0.3-0.6	Good	Good	Excellent	Excellent	Good
Polycarbonate	PC	140-148	60-70	0.12-0.34	Good	Good	Excellent	Excellent	Poor
polystyrene	PS	92-106	10-150	0.02-0.15	Poor	Good	Excellent	Excellent	Poor

CTE: coefficient of thermal expansion

The variance of these parameters is based on the different grades of polymer.

Soft Lithography

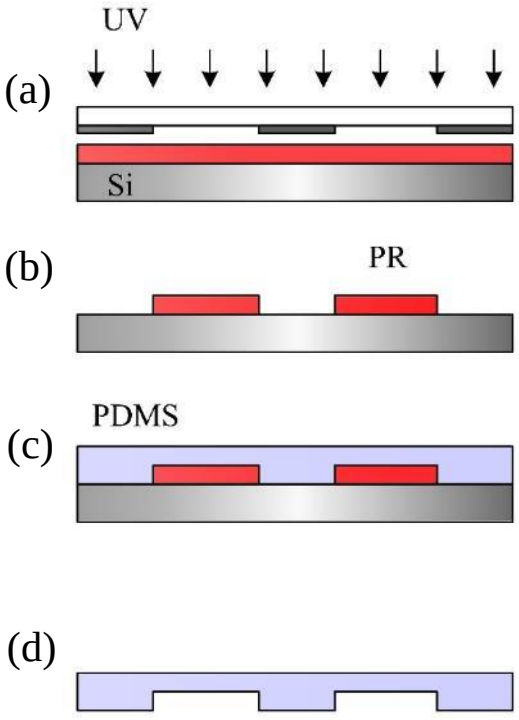

Spincoated photoresist on a silicon wafer followed by photolithography processes

A silicon wafer with patterned photoresist as a master

Poured and then thermally cured PDMS on a master

The peeling-off layer of inverted PDMS slab

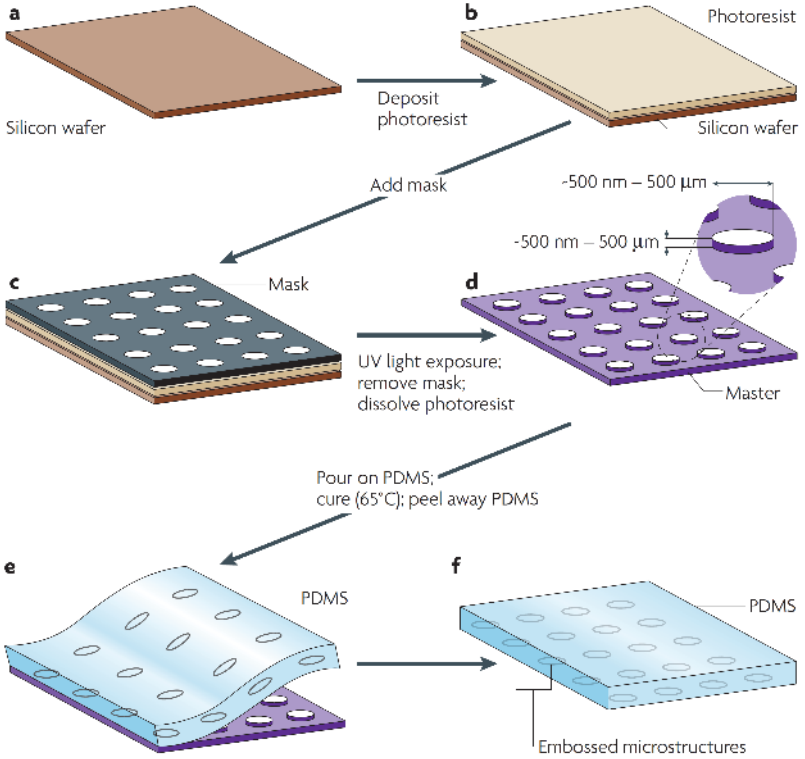

The fabrication of PDMS slab using soft lithography. (ab) Master is first formed by spincoated photoresist on a silicon wafer followed by photolithography processes. (c) PDMS mixture is then poured on the master and cured thermally. (d) The peeling-off layer of PDMS slab has invert microstructures to the master.

The fabrication of micropatterned slabs of PDMS. (a–d) Photoresist is spincoated on a silicon wafer followed by photolithography processes. As a result, the master consists of a silicon wafer with features of photoresist in bas-relief. (e) PDMS is poured on the master and then cured thermally. (f) The peeling-off layer of PDMS has invert microstructures embossed in its surface.

D. B. Weibel, W. R. DiLuzio and G. M. Whitesides, *Nature Reviews Microbiology*, 2007, **5**, 209-218.

Typical Micromachining Process

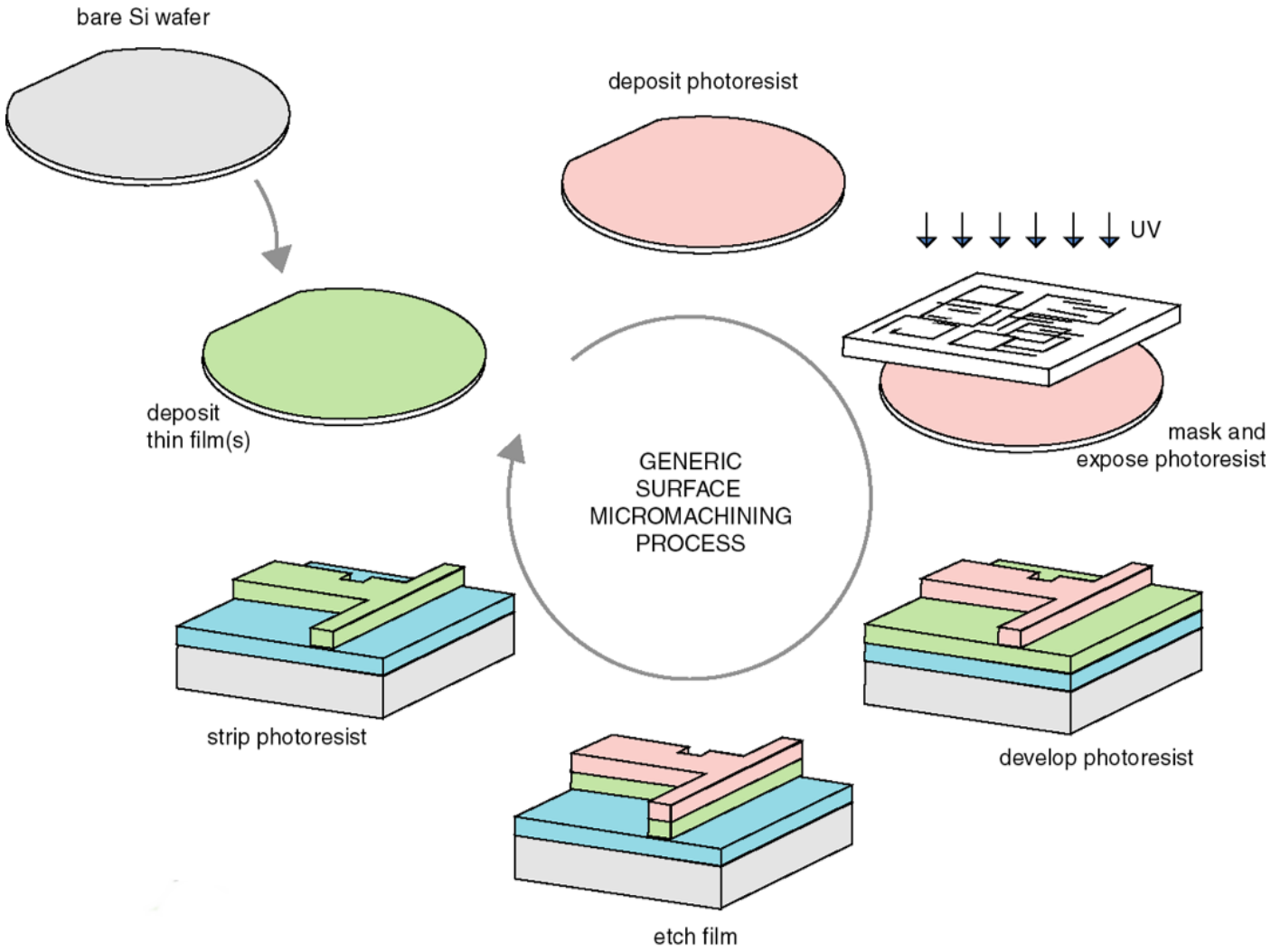

Positive and Negative Photoresist

Different chemicals may be used for permanently giving the material the desired property variations:

- Poly(methyl methacrylate) (PMMA)
- Poly(methyl glutarimide) (PMGI)
- Phenol formaldehyde resin (DNQ/Novolac)
- SU-8.

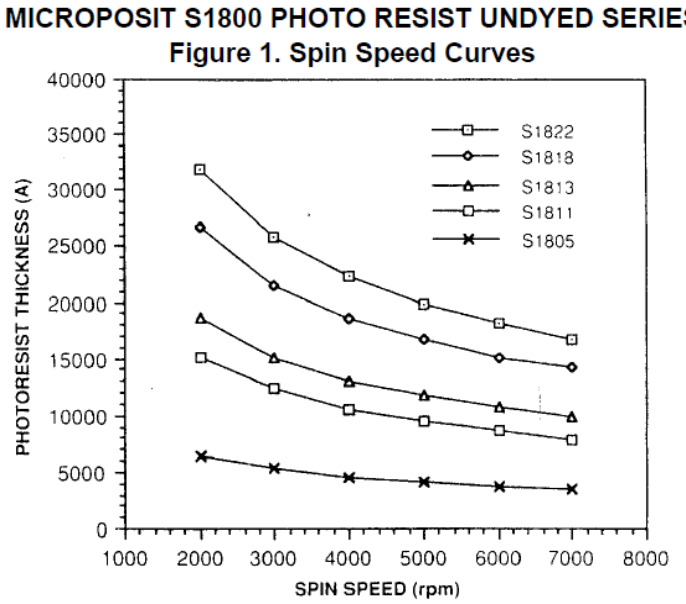

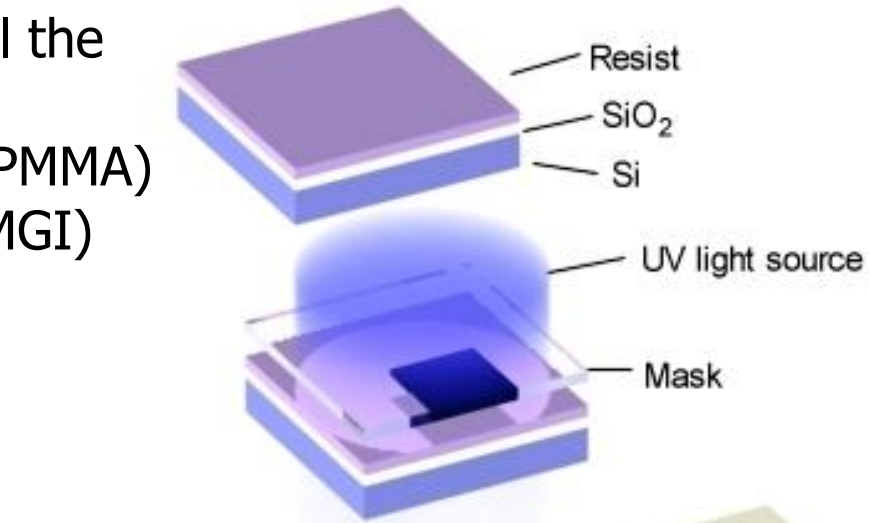

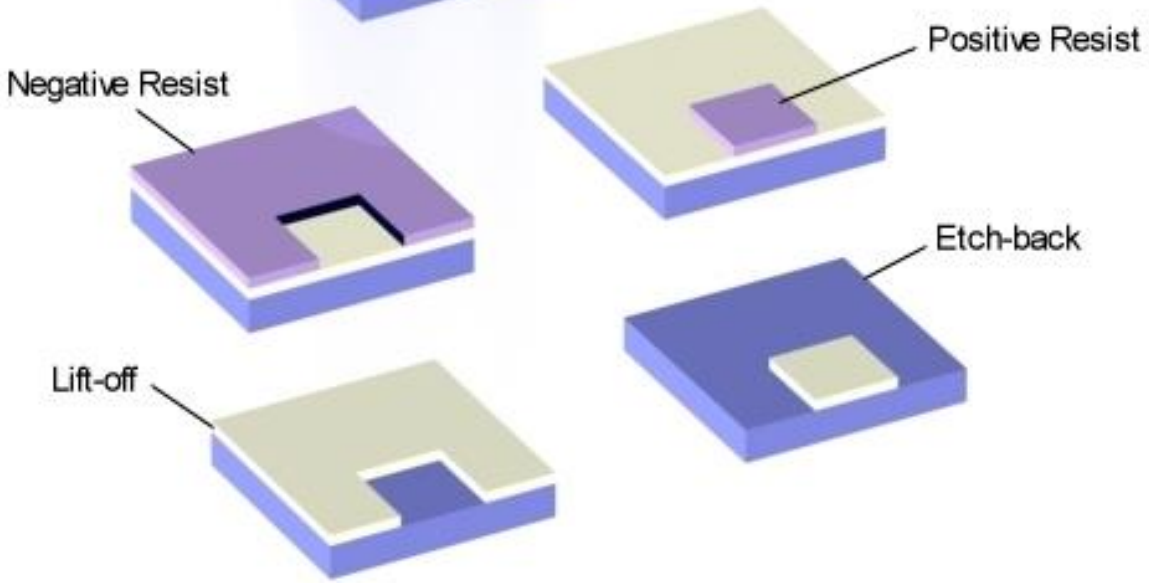

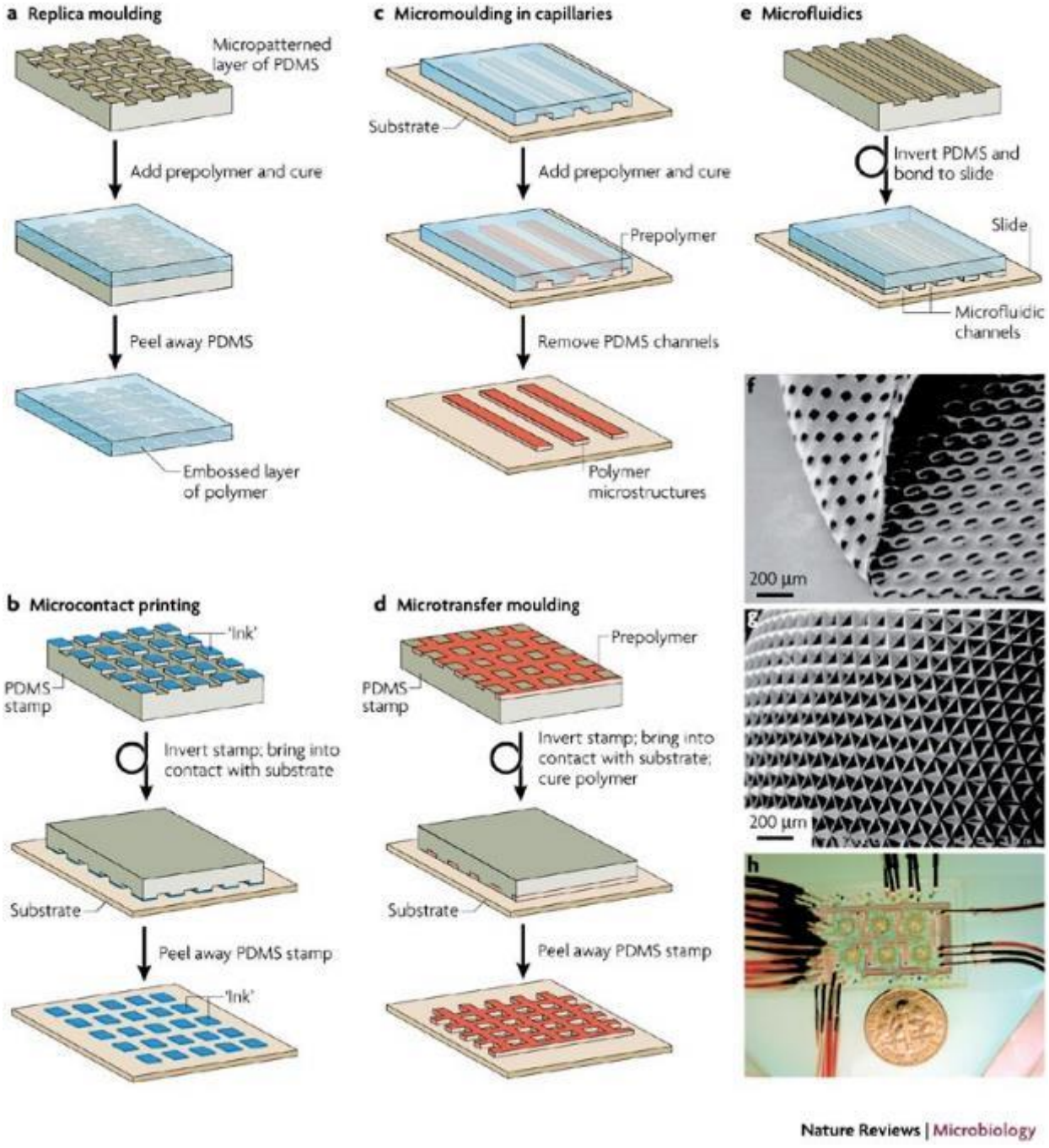

The key stages of each of the following techniques are shown: a | replica moulding; b | microcontact printing; c | micromoulding in capillaries; d | microtransfer moulding; and e | microfluidics. f | A PDMS membrane with microfabricated holes created by replica moulding from a master with circular posts. g | A curved layer of micropatterned polyurethane created by bending a micropatterned layer of PDMS and then replica moulding against it. h | A microfluidic chemostat for the growth and culture of microbial cultures. The device incorporates six reactors with an intricate network of plumbing, in a footprint that is approximatley 5 cm^2. PDMS, poly(dimethylsiloxane).

D. B. Weibel, W. R. DiLuzio and G. M. Whitesides, *Nature Reviews Microbiology*, 2007, **5**, 209-218.

Quake Valve by Steven Quake

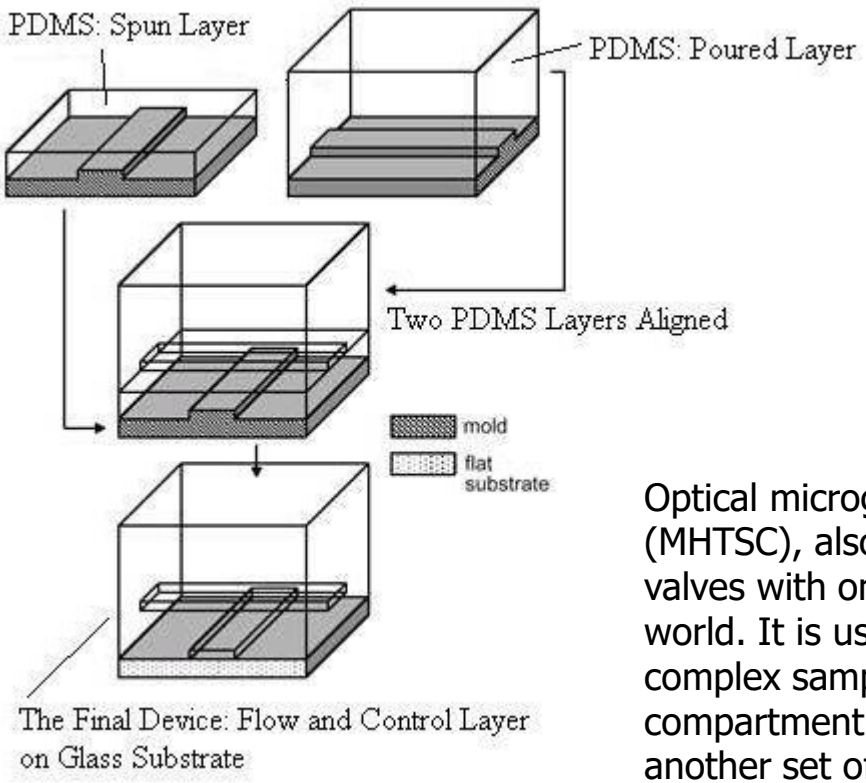

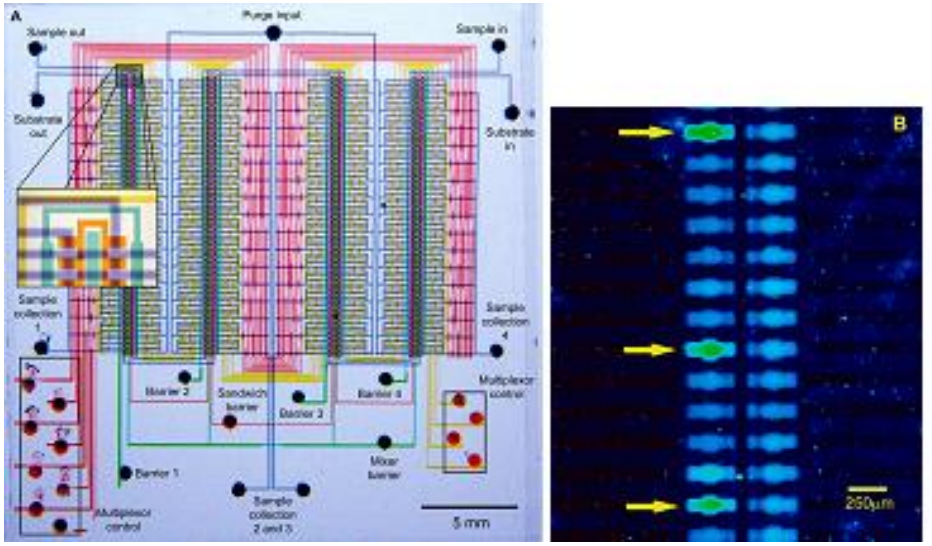

Optical micrograph of the Multiwell High Throughput Screening Chip (MHTSC), also referred to as a comparator array. This chip has 2,056 valves with only 18 valve control lines needed to interface to the outside world. It is used in high throughput screening applications and allows a complex sample to be segmented into many compartments; each compartment can then be assayed individually by pairwise mixing with another set of compartments containing, for example, fluorescent substrate. The chip occupies a total area of one square inch. This chip (without food dyes) was shown on the cover of the October 18, 2002 issue of Science . B. Portion of an image of the MHTSC chip taken with a DNA array scanner. A dilute sample of E. Coli bacteria expressing cytochrome C peroxidase (CCP) was segmented and then allowed to mix pairwise with the substrate Amplex Red.

http://thebigone.stanford.edu/publications_home.htm

PDMS Valve Actuation Mechanisms

(a)

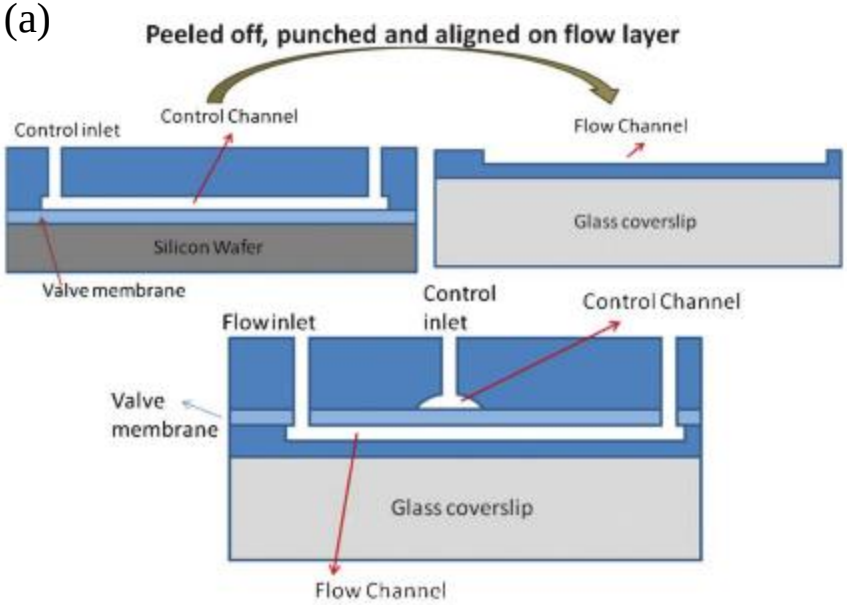

(b)

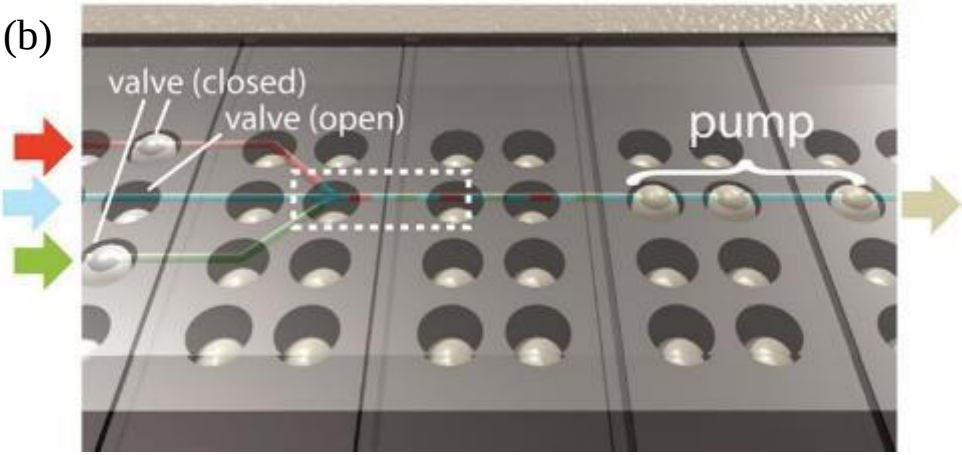

(c)

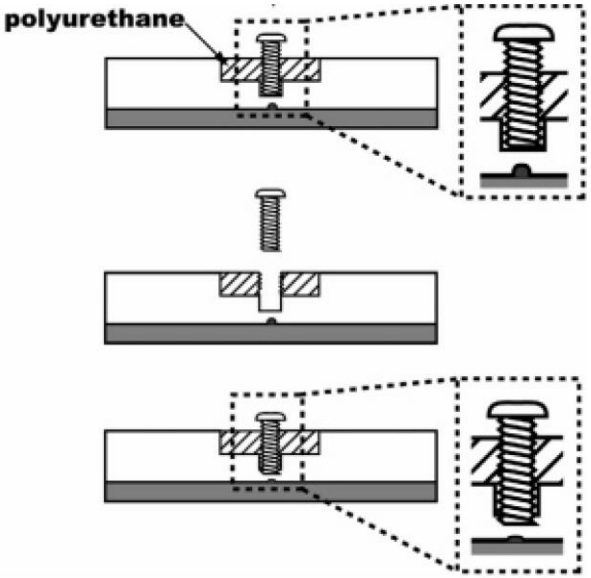

(a) Intermediate fabrication steps (top) and cross section (bottom) of the three-layer PDMS valve integration. There are three types of actuation mechanisms utilized to enclose the PDMS channels, they are gas, (b) braille display and (c) screws, respectively.

1. EmreáAraci, *Lab on a Chip*, 2012, **12**, 2803-2806.
2. W. Gu et al, *Proceedings of the National Academy of Sciences of the United States of America*, 2004, **101**, 15861-15866.
3. D. B. Weibel et al, *Analytical chemistry*, 2005, **77**, 4726-4733.

On-Chip CE/LC

Capillary Electrophoresis (CE)

Flux électrophorétique

$$\mu_{ep} = \frac{q}{6.\pi.\eta.r}$$

q : charge de l'ion

r : rayon de l'ion

η : viscosité de la solution

Flux électrosmotique

$$\mu_{eo} = \frac{\varepsilon.\zeta}{4\pi.\eta}$$

ε: constante diélectrique

ζ : potentiel zetâ

η : viscosité de la solution

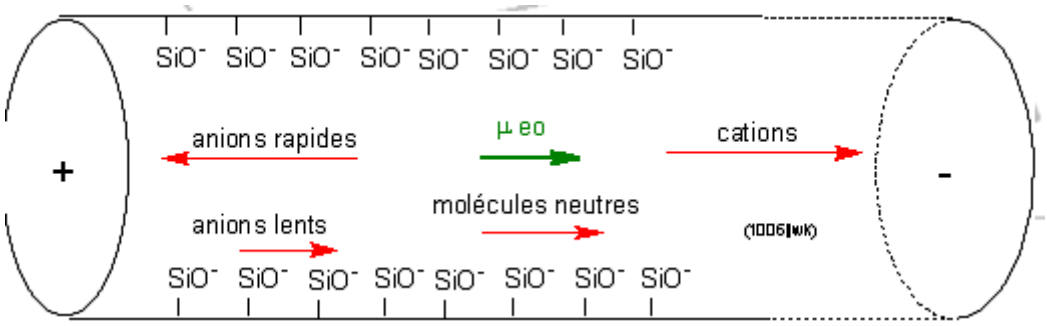

Lab-on-a-Chip for Electrophoresis

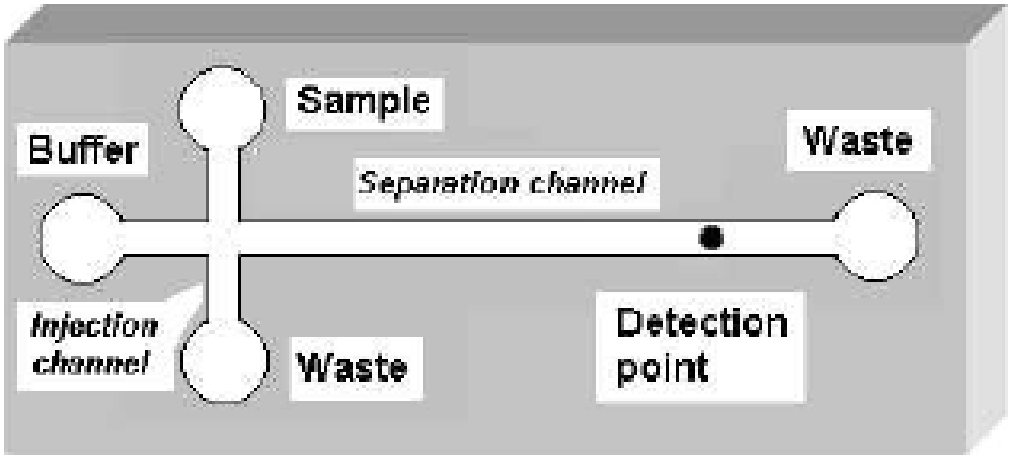

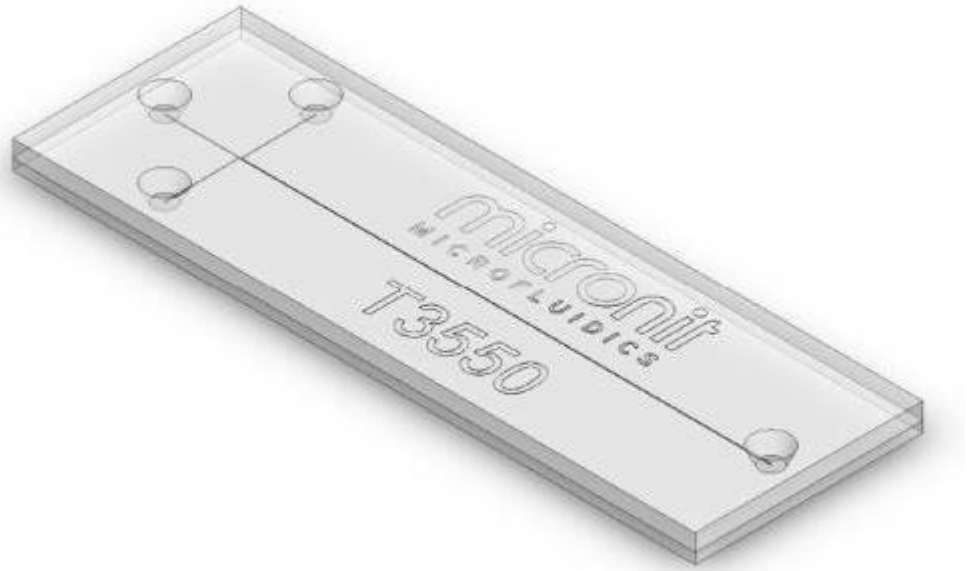

Micronit CE Chip

http://www.berkeley.edu/

Lab-on-a-Chip-Based Mass Spectrometry

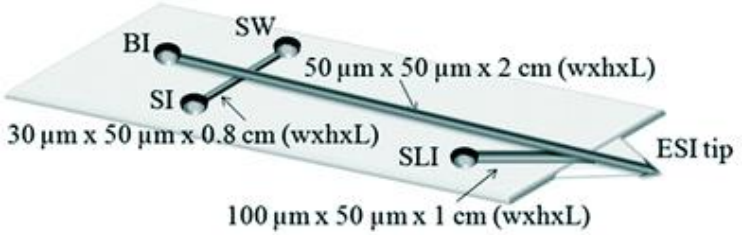

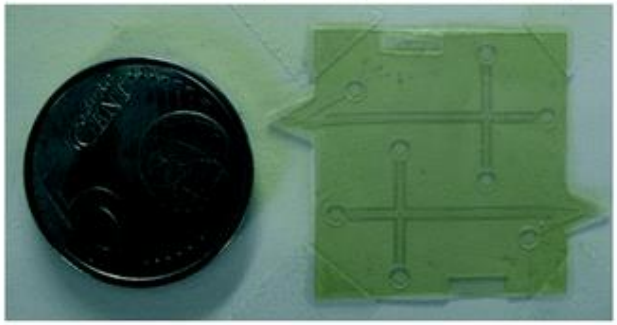

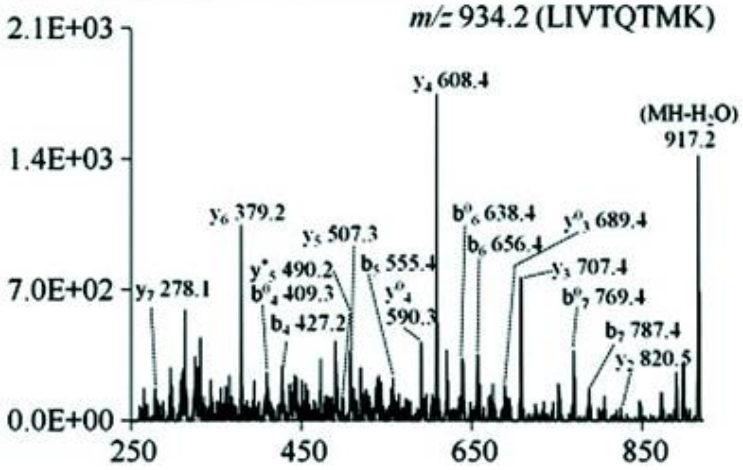

All-SU-8-based CZE-ESI chip. Top: description of chip. Middle: the SU-8 chip showing inlets, channels and ESI tip. Bottom: mass spectrum obtained from the study using the peptide β-lactoglobulin.

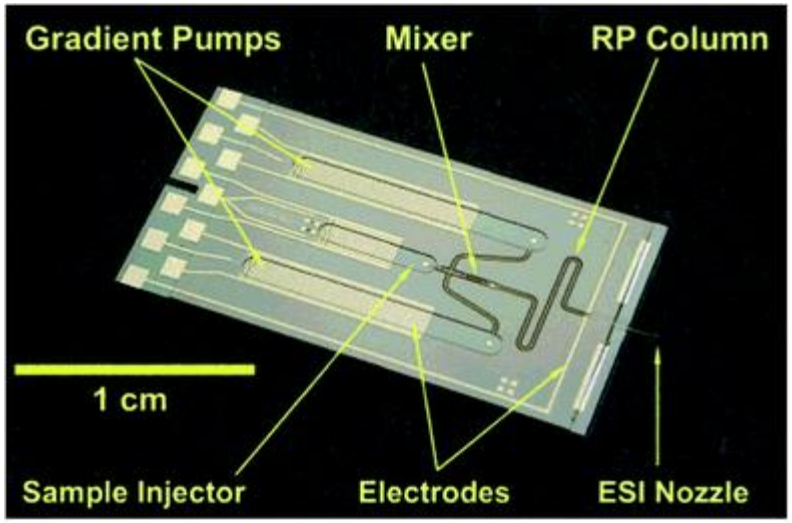

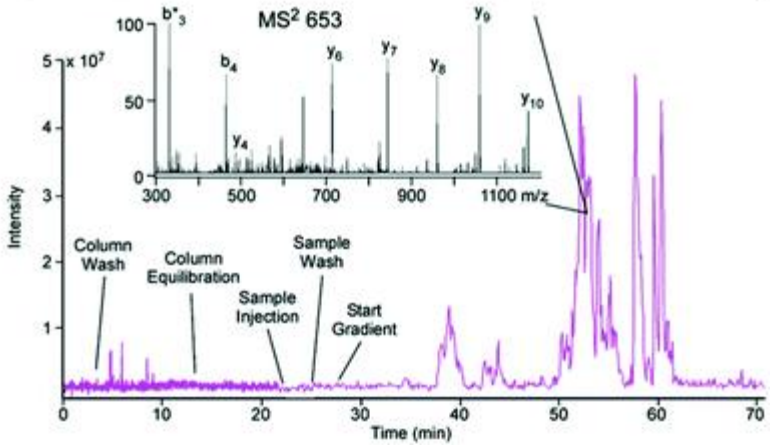

ESI chip using a multi-material approach including SU-8 as a structural component. Top: the chip and its components. Bottom: base peak chromatogram obtained from the study. The inset shows the MS/MS spectrum.

High-Pressure Thermoplastic Device Fabrication

I. Polymer-Based Microstructure Fabrication

- *Hot Embossing Lithography*
- *Injection Molding*
- *Mechanical Milling*

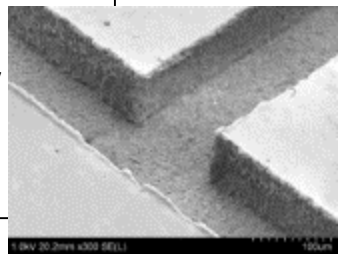

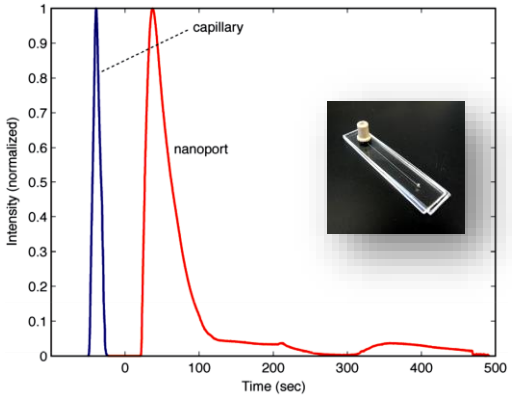

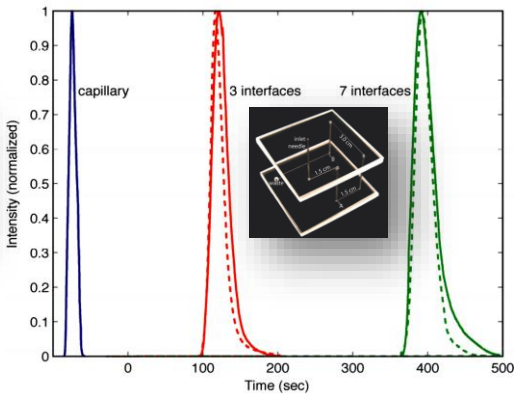

II. Thermal Plastic Bonding Techniques

- *Thermal Bonding*
- *Solvent Bonding*
- *Surface modification*

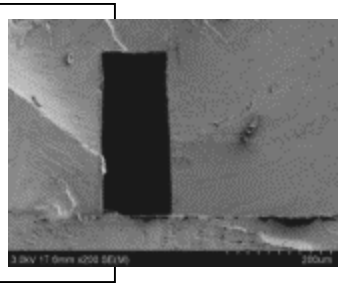

Diffusion length

$P_e = LU/D \quad D_e = D(1+P_e^2/192) \quad \sigma = (2D_e t)^{1/2}$

	Nanoport	Point A	Point B
Total path length	2 cm	8.6 cm	18.2 cm
σ^2 theoretical/cm^2	0.07	0.29	0.62
	>500%		
σ^2 measured/cm^2	0.36	52%	
σ^2 measured, planar/cm^2		0.36	0.58
			70%
σ^2 measured, 2-layer/cm^2		0.44	1.05
Cost (USD)	>30	1	

III. World-to-Chip Interfaces

- *Integrated Interconnector*

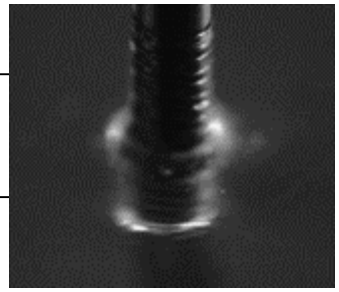

Optimized size compatibility
Resistance > 20 MPa (~ 200 atm)

Lab on a Chip, 2009, 2009, 9, 50-55.

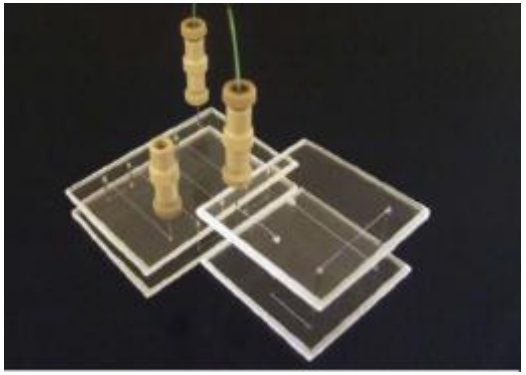

High-pressure polymer devices

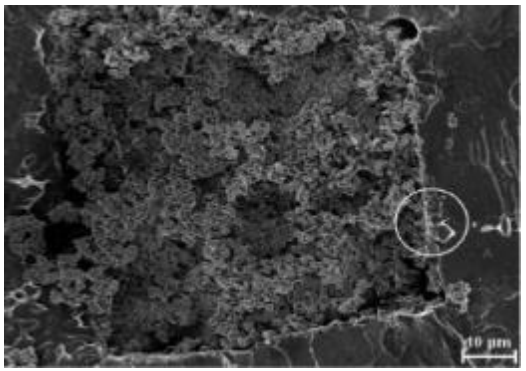

Porous monoliths

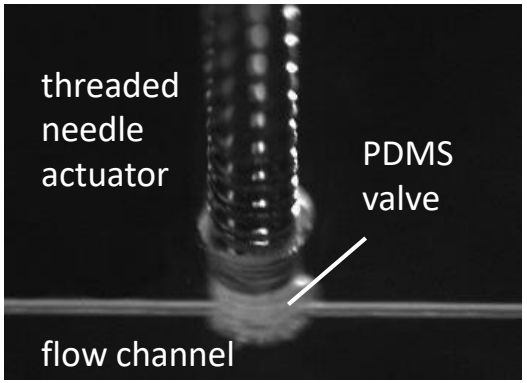

On-chip valve

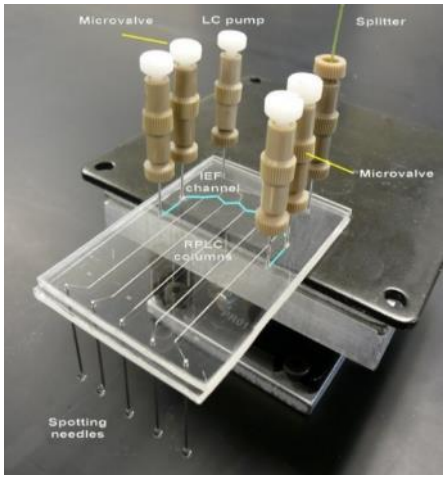

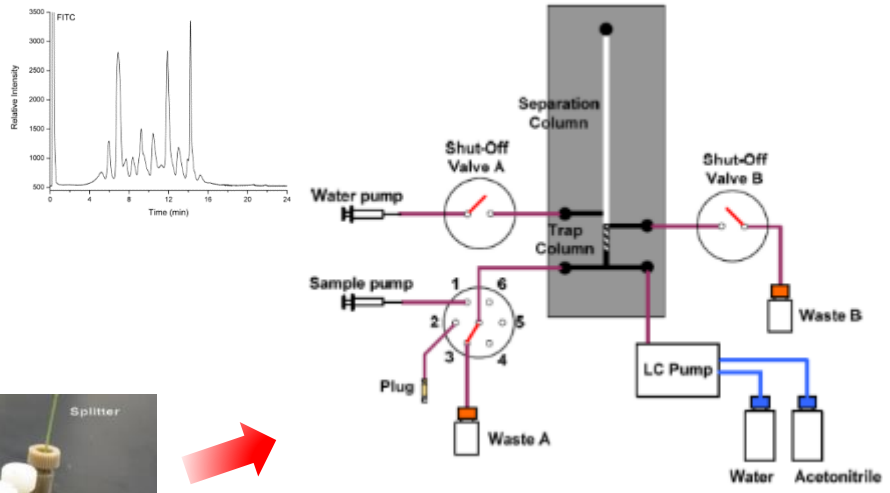

Solid-phase extraction – liquid chromatography (SPE-LC)

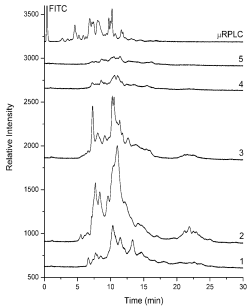

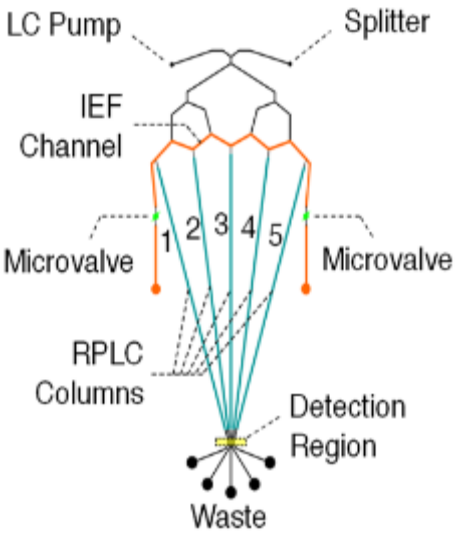

Isoelectric focusing – liquid chromatography (IEF-LC)

C. F. Chen, *Lab on a Chip*, 2009
J. Liu, *Analytical Chemistry*, 2009
C. F. Chen, *Lab on a Chip*, 2009
J. Liu, *Lab on a Chip*, 2010
C. W. Tsao, *Microfluid Nanofluid*, 2010

Hot embossing process

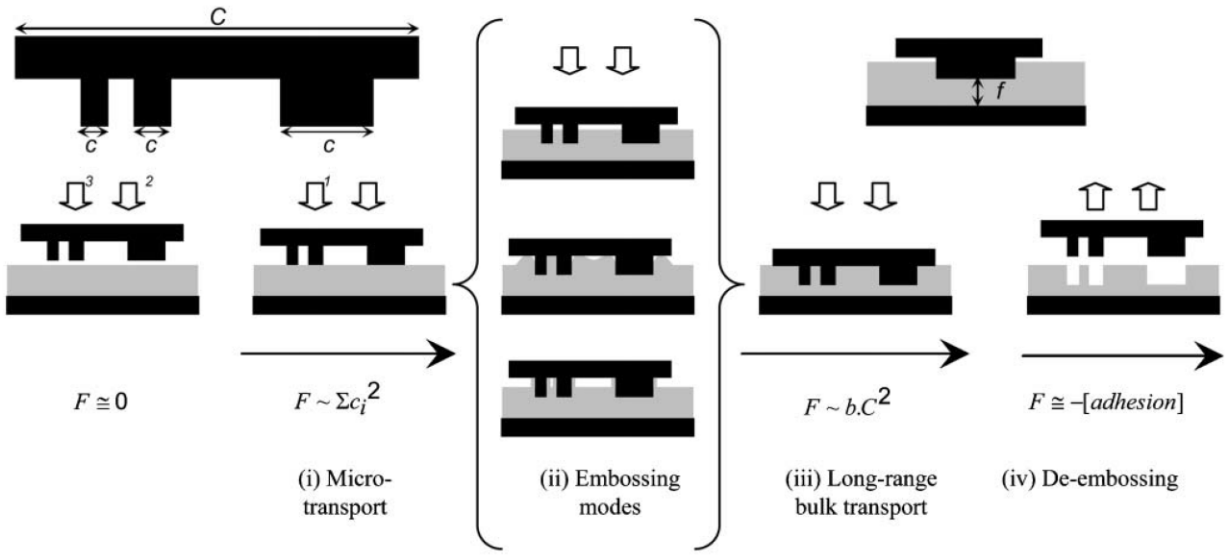

The schematic hot embossing process. The total force (F) required to emboss a thermoplastic polymer depends on the polymer's viscosity, contact area of the stamp features with the polymer (c), surface area of the entire stamp (C) and temperature. N. S. Cameron, H. Roberge, T. Veres, S. C. Jakeway and H. J. Crabtree, *Lab on a Chip*, 2006, **6**, 936-941.

Directly Milling & Laser Ablation

Directly Milling

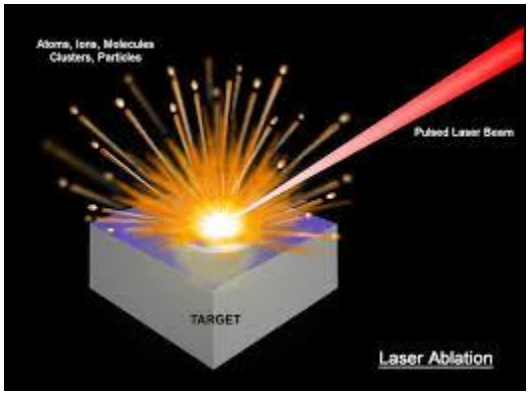

Laser Ablation

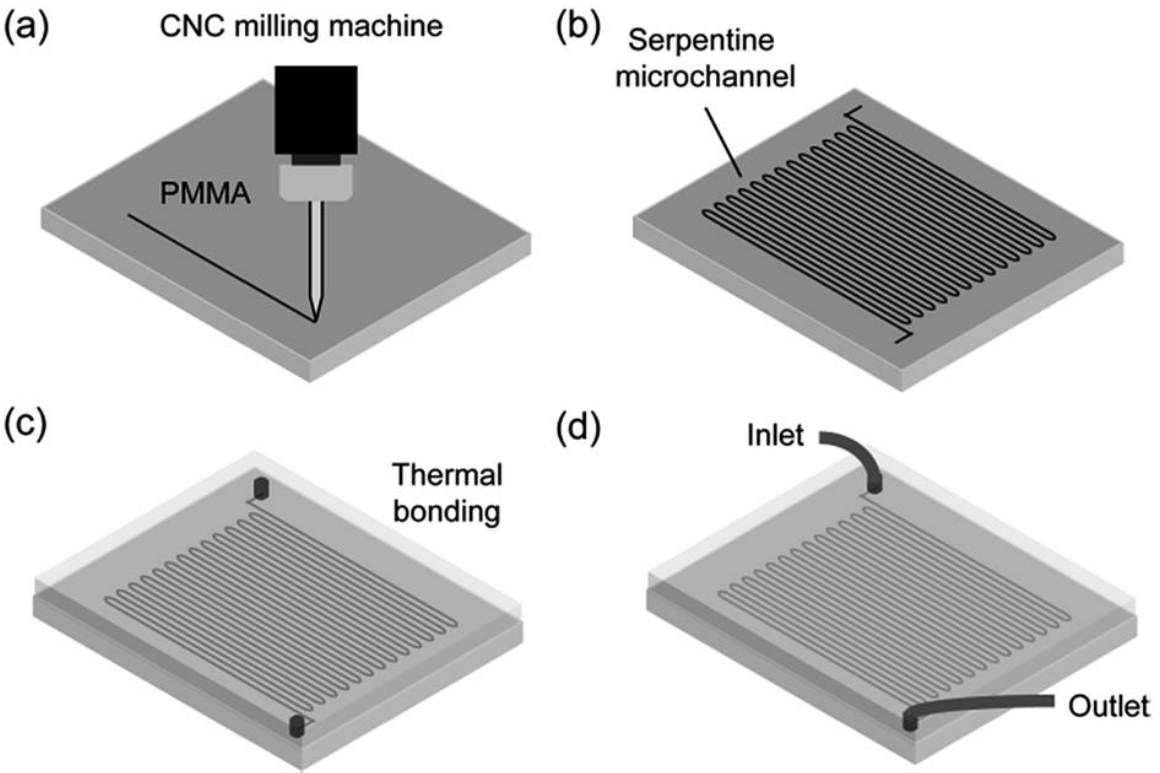

(a) Fabrication of a serpentine microchannel on PMMA using a CNC milling machine. (b) Serpentine microchannel engraved on one PMMA substrate. (c) Punching inlet and outlet ports on a flat PMMA substrate, followed by thermal bonding. (d) Insertion of silicone tubes into the inlet and outlet ports.

2015 Lab Chip

Stationary Phase

Commercial Available

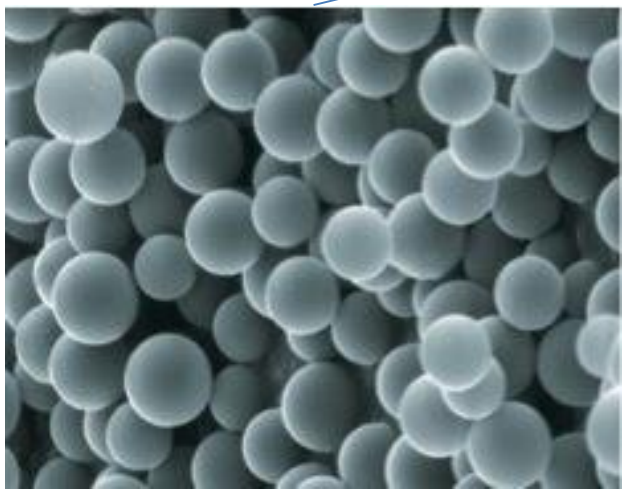

packing beads

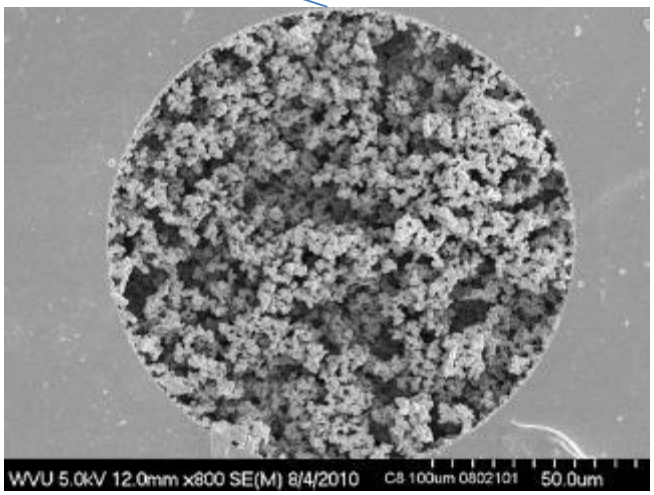

Porous monoliths

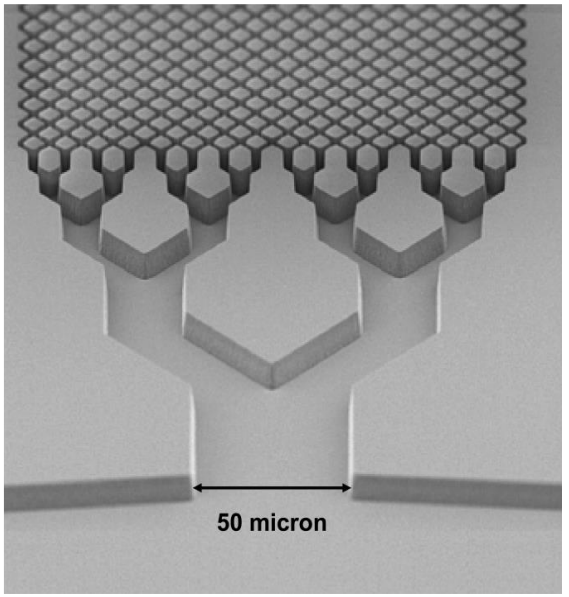

Micropillar

Formed via water bath, UV irradiation or microwave etc.

(micromachined pillars of 5 µm diameter which were coated with a monolayer of C18)

They found reduced plate heights between 0.2 (k' = 0) and 1.0 (k' = 2.17), i.e. close to the theoretical minimum for non-porous pillar columns

A Perfect Column - a Perfectly Ordered Column

$$h = \frac{B}{v} + Av^{1/3} + Cv$$

A, B and C are constants and v is the reduced velocity equal to ud_p/D_m with u (m s^{-1}) the mobile phase flow velocity, d_p (m) the particle diameter and D_m (m^2 s^{-1}) the diffusion coefficient of the analyte in the mobile phase. The value of B is determined by analyte diffusion in the axial direction of the column, the value of A by packing inhomogeneities that cause different flow paths for the mobile phase and the value of C by slow mass transfer in the stationary zone (either in pores or in the stationary phase)

Lab Chip, 2007, 7, 815–817

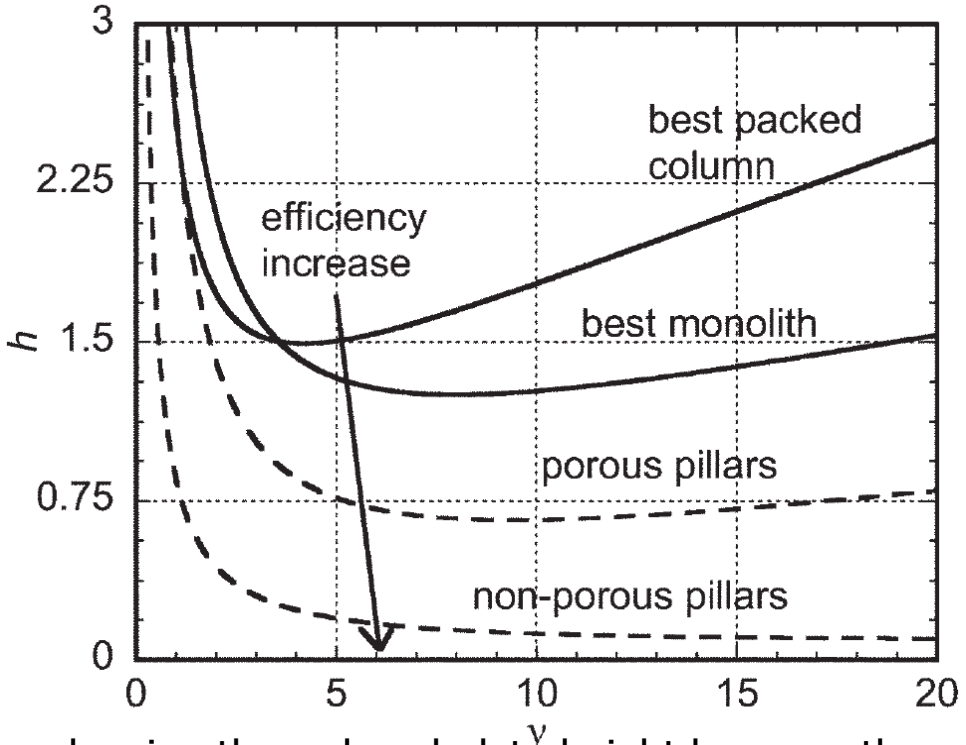

Curves showing the reduced plate height h versus the reduced mobile phase flow velocity v. Measured curves (drawn lines) for the best packed column (A = 0.5, B = 2 and C = 0.05) and the best monolith with a porosity of 0.8 (A = 0.32, B = 3.3 and C = 0.025); calculated curves (dotted lines) for a porous pillar array with a porosity of 0.8 and k' = 1.25 (A = 0.094, B = 2.495 and C = 0.021)13 and for an array of non-porous pillars with a porosity of 0.4 (A = 0.014, B = 0.84 and C = 0.001).

Porous Photopolymerized Monoliths

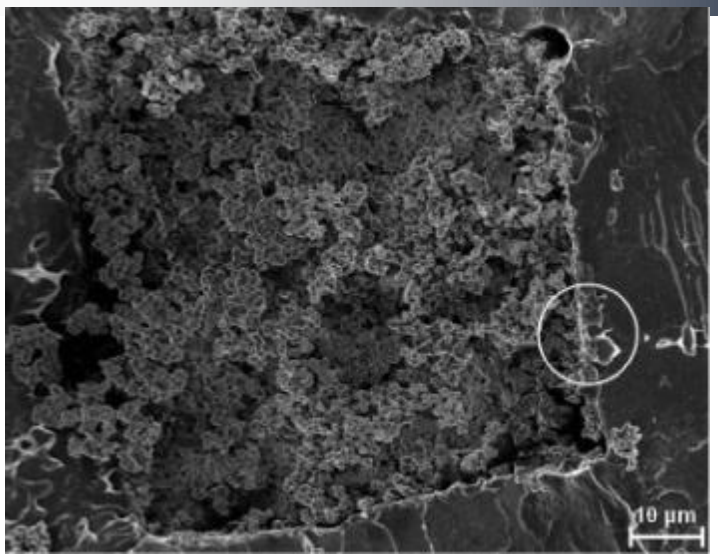

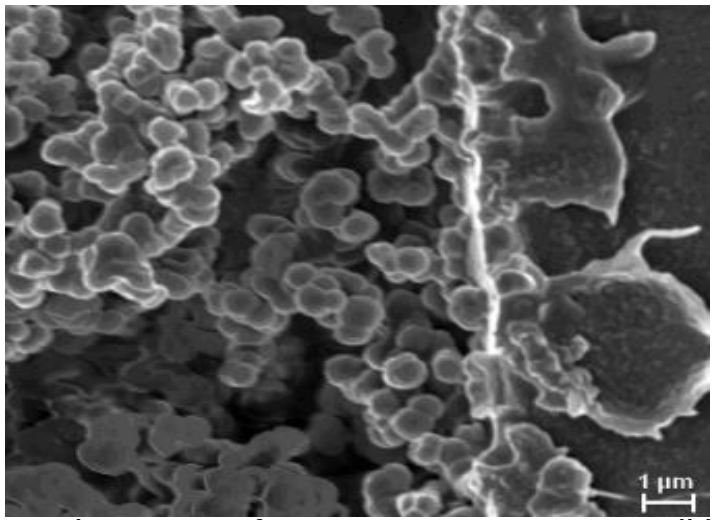

SEM images of BMA-TMPTMA monolith. Magnification of the circular area revealing apparent covalent attachment of monolith to the COP channel surface.

Cyclic olefin coplymer

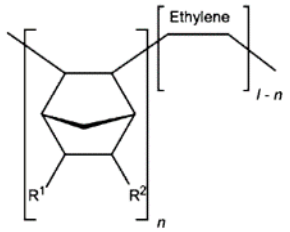

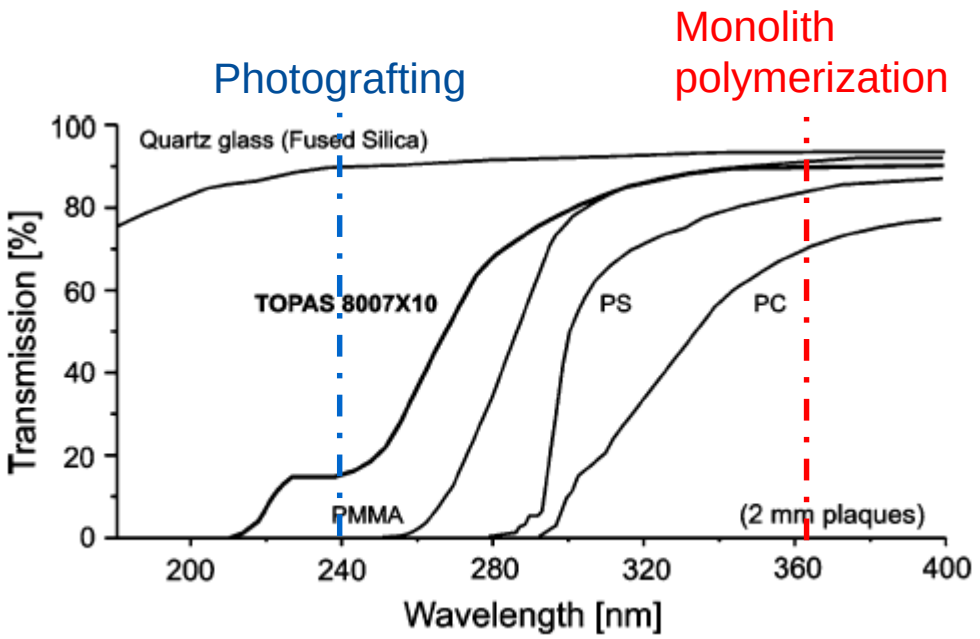

The surface bound initiators are formed by abstracting hydrogen from the COC surface

Monolith covalently bound to COC surface

P. S. Nunes, *Microfluid Nanofluid*, 2010

World-to-Chip Interfaces

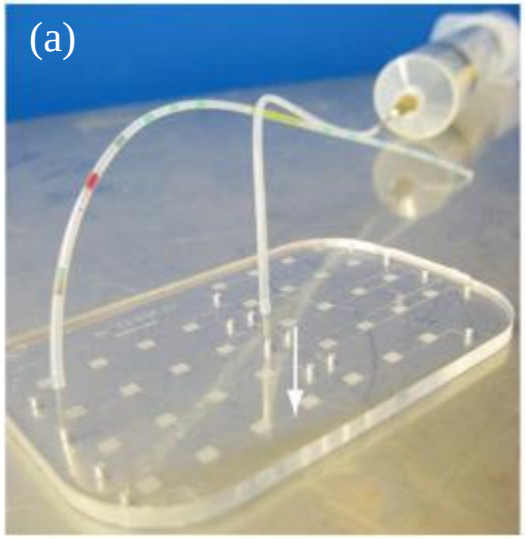

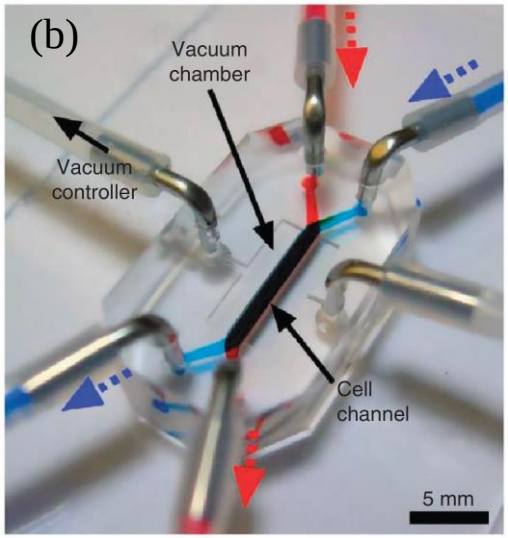

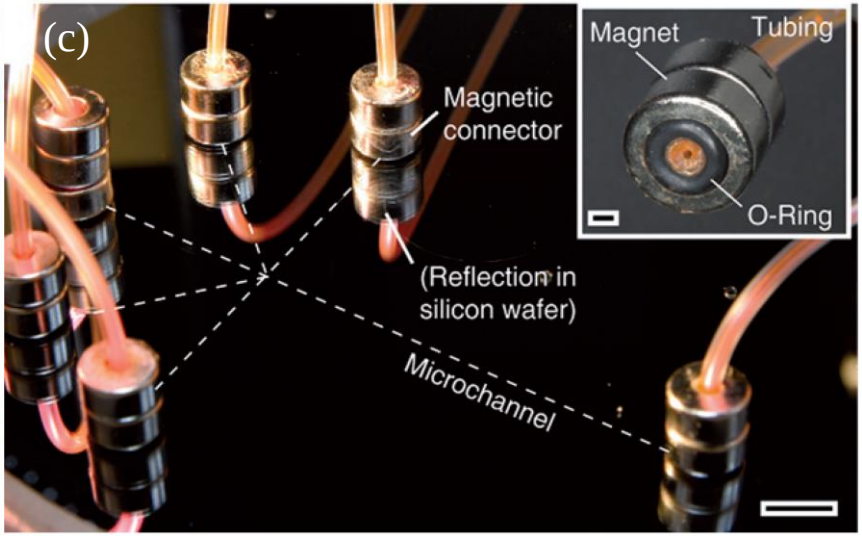

(a) Tubing is directly inserted into polymeric chip or (b) connected to polymer chip using a stainless steel tubing first to connect to external pumping systems. (c) A removable connector design is to use magnetic connector made of a ring magnet with a hole that accommodates tubing or a needle and second magnet placed on the back side of the chip to prevent leakage. (d) NanoPorts™ for Lab-on-a-Chip.

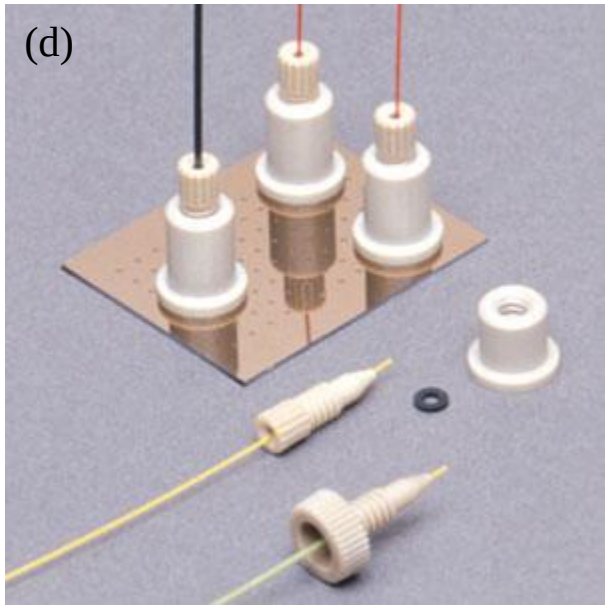

1. C. D. Chin et al, *Nature medicine*, 2011, **17**, 1015-1019.
2. D. Huh et al, *Nature protocols*, 2013, **8**, 2135-2157.
3. J. Atencia et al, *Lab on a Chip*, 2010, **10**, 246-249.

Anatomy of a simple microfluidic chip

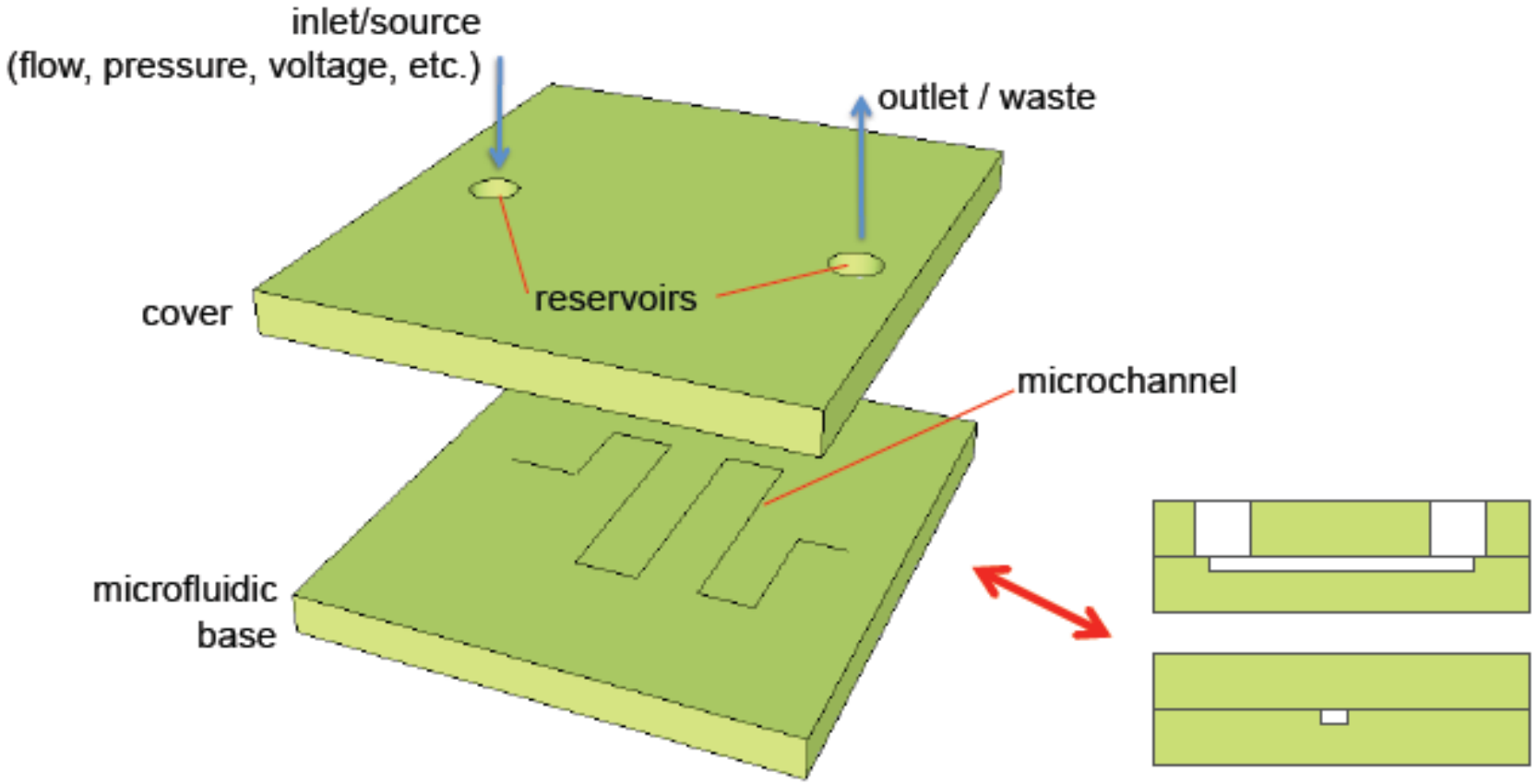

- Channels must (typically) be sealed with a cover plate
- high surface/volume ratio in microchannel
- large reservoirs (world-to-chip interfacing is a challenge

World-to-chip Interface

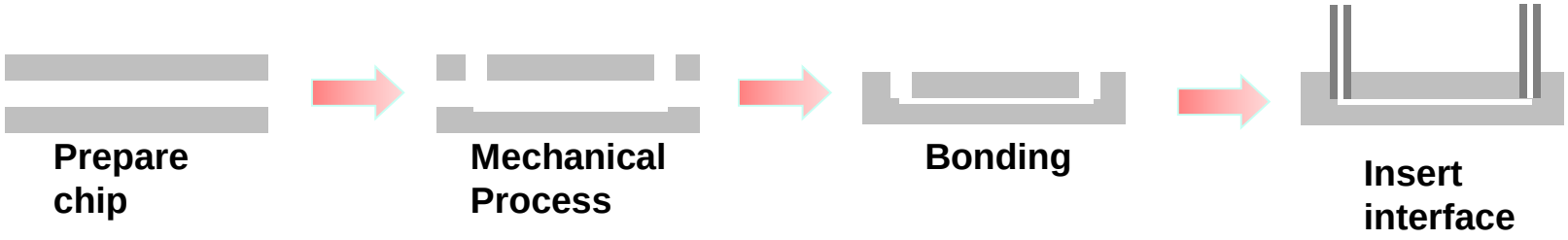

Flow channel volume

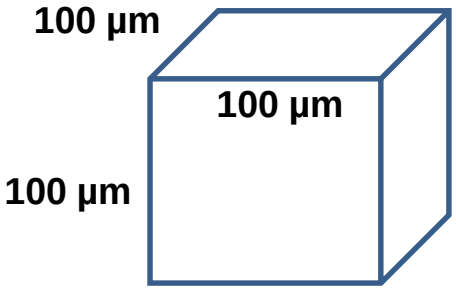

100 µm x 100 µm x 100 µm = 1 nL

If the channel length is 1 cm…

V channel = 100 nL

Reservoir

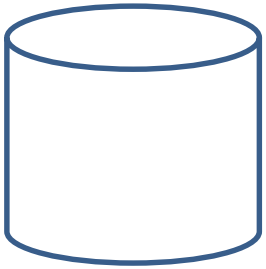

V = π x (1 mm)^2 x (2 mm) = 6 µL

Chip Base Solid Phase Extraction – Liquid Chromatography System

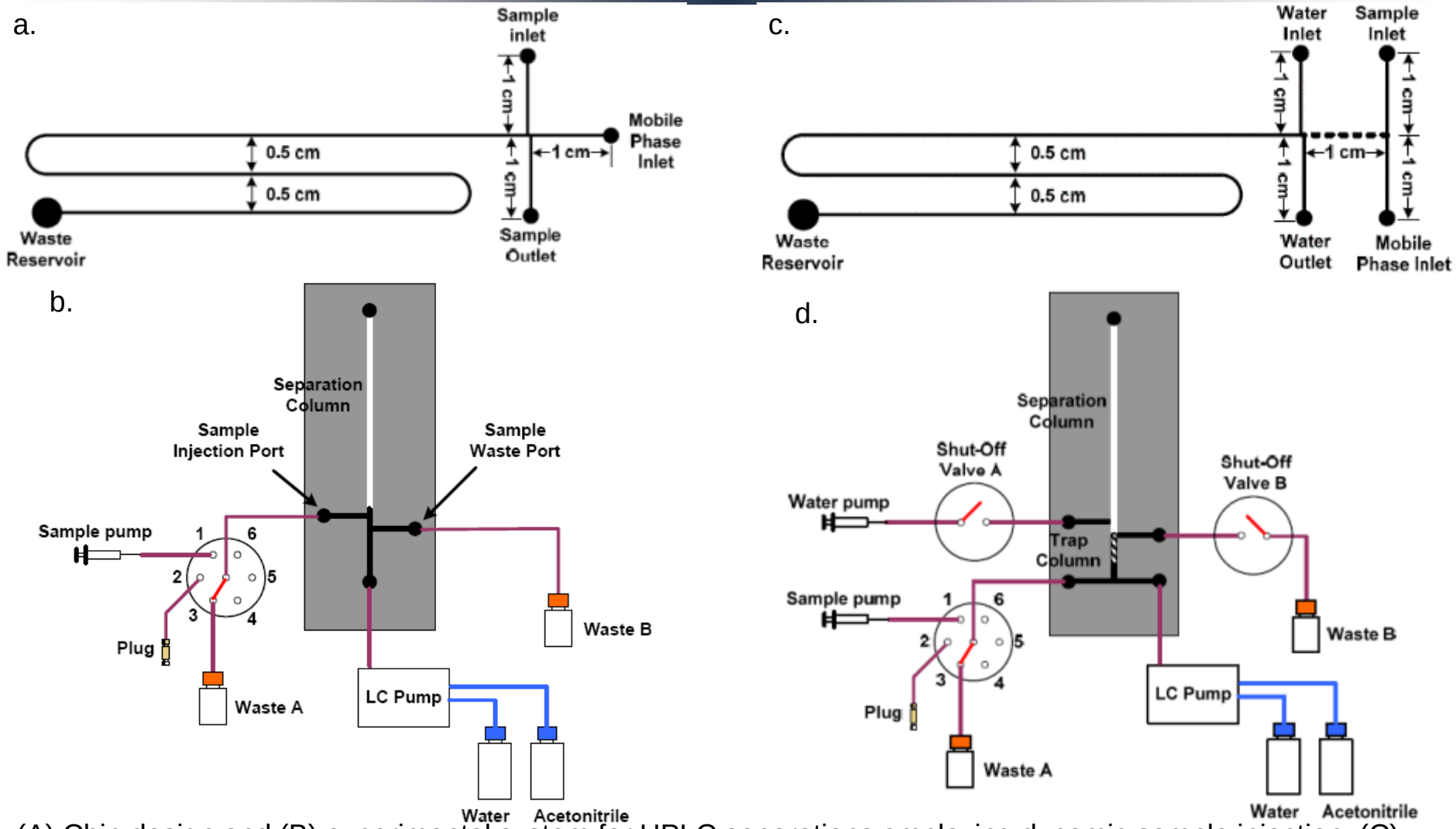

(A) Chip design and (B) experimental system for HPLC separations employing dynamic sample injection; (C) Chip design and (D) experimental system for on-line sample cleanup/enrichment-HPLC separations, with an integrated 5 mm long SPE trap column used for on-line sample cleanup and enrichment. The total length of the serpentine separation channels is 17 cm in both chip designs.

Separation Result of Model Peptides

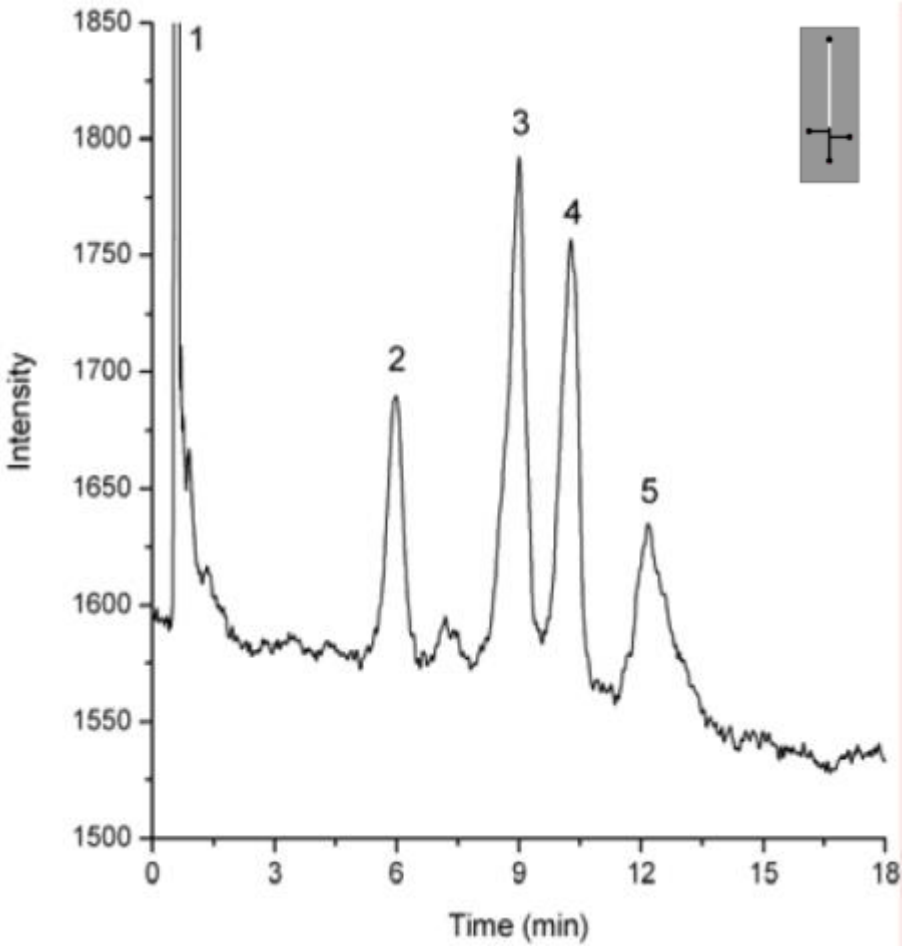

Separation of a mixture of 4 FITC labeled model peptides. Peak elution order is: (1) FITC, (2) angiotensin II, (3) [leu5]-enkephalin, (4) neurotensin,and (5) bradykinin.

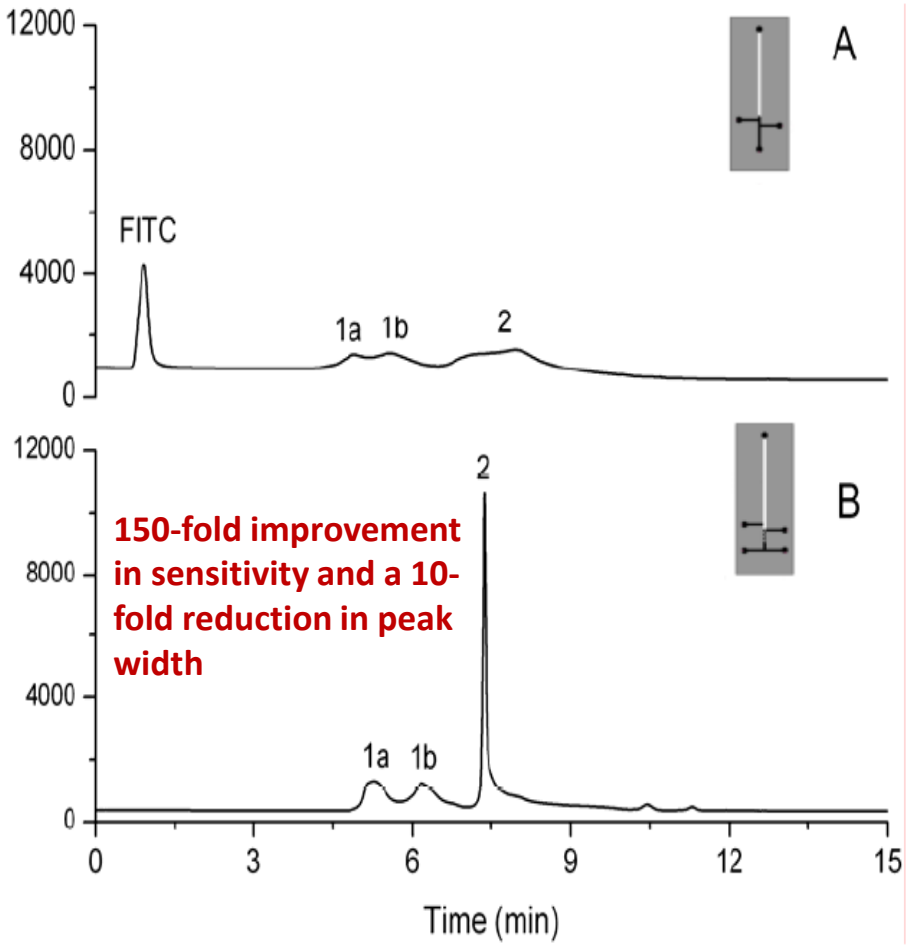

HPLC separation of FITC labeled ribonuclease A (1a, 1b) and cytochrome C (2) using (A) dynamic sample injection and (B) online sample cleanup/enrichment prior to HPLC separation.

J. Liu et al., *Analytical Chemistry*, 2009

IEF-mRPLC Polymer Chip

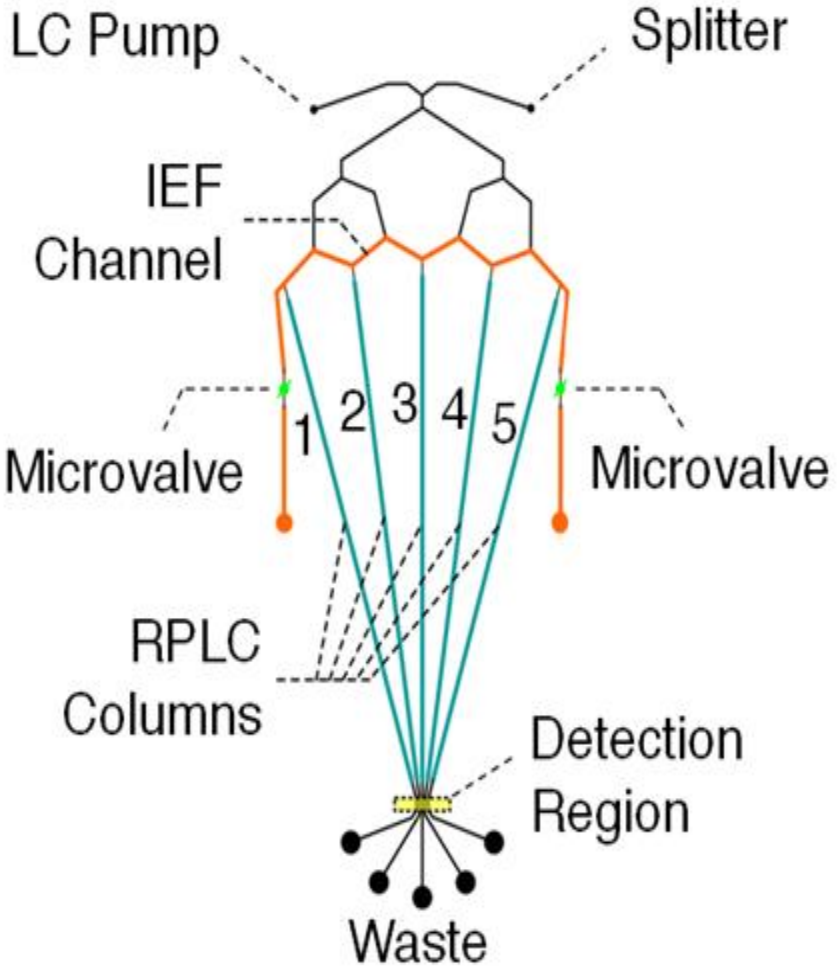

Photograph of the IEF-mRPLC chip.

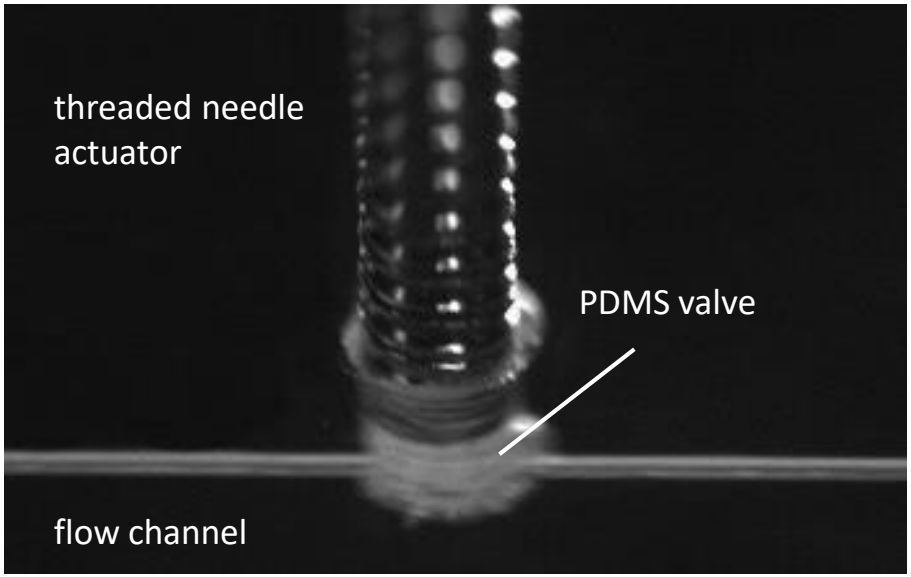

PDMS microvalve actuated by a threaded needle

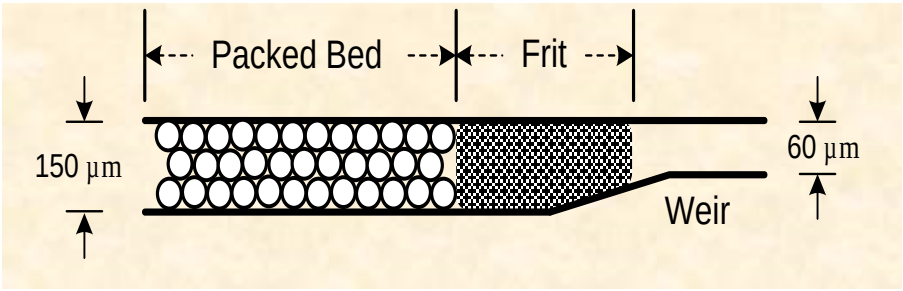

Silica beads packed against monolith frit

Test Results of µRPLC and IEF

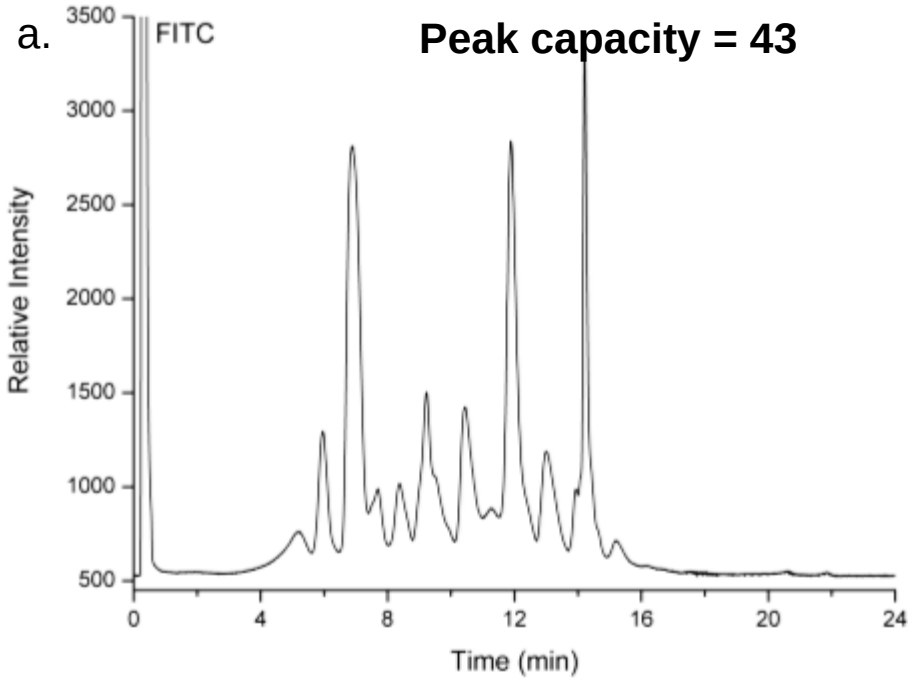

(a) µRPLC separation of 0.2 mg/mL FITC-cytochrome c digest. 0.4% HPMC was used to coat the IEF channel in order to reduce non-specific interactions between the channel walls and sample components.

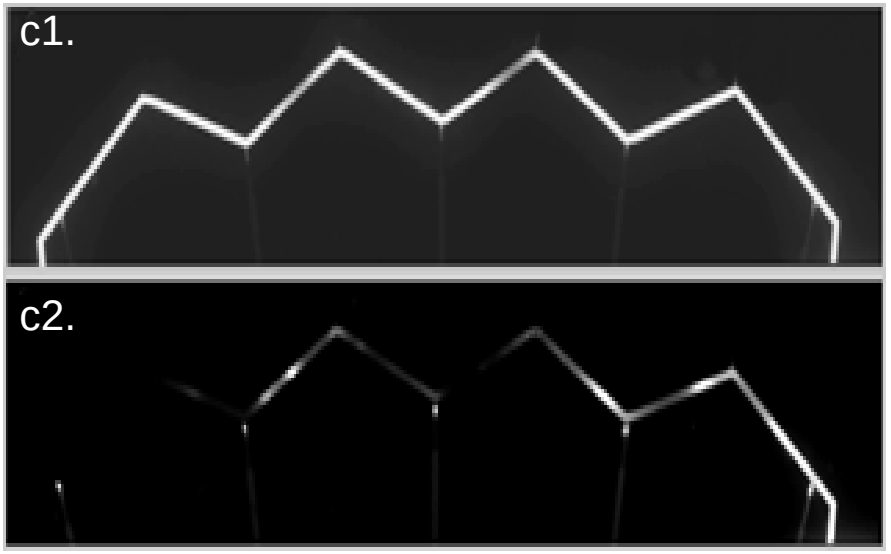

(c) Focusing of FITC-BSA digest in the IEF channel. (c1) Sample introduction; (c2) 30 min IEF of the digest. Catholyte: 35 mL of 0.5 M NaOH; anolyte 35 mL of 0.5 M H_3PO_4; power: 1000 V

J. Liu et al., *Lab on a Chip*, 2010

Test Results of IEF-mRPLC

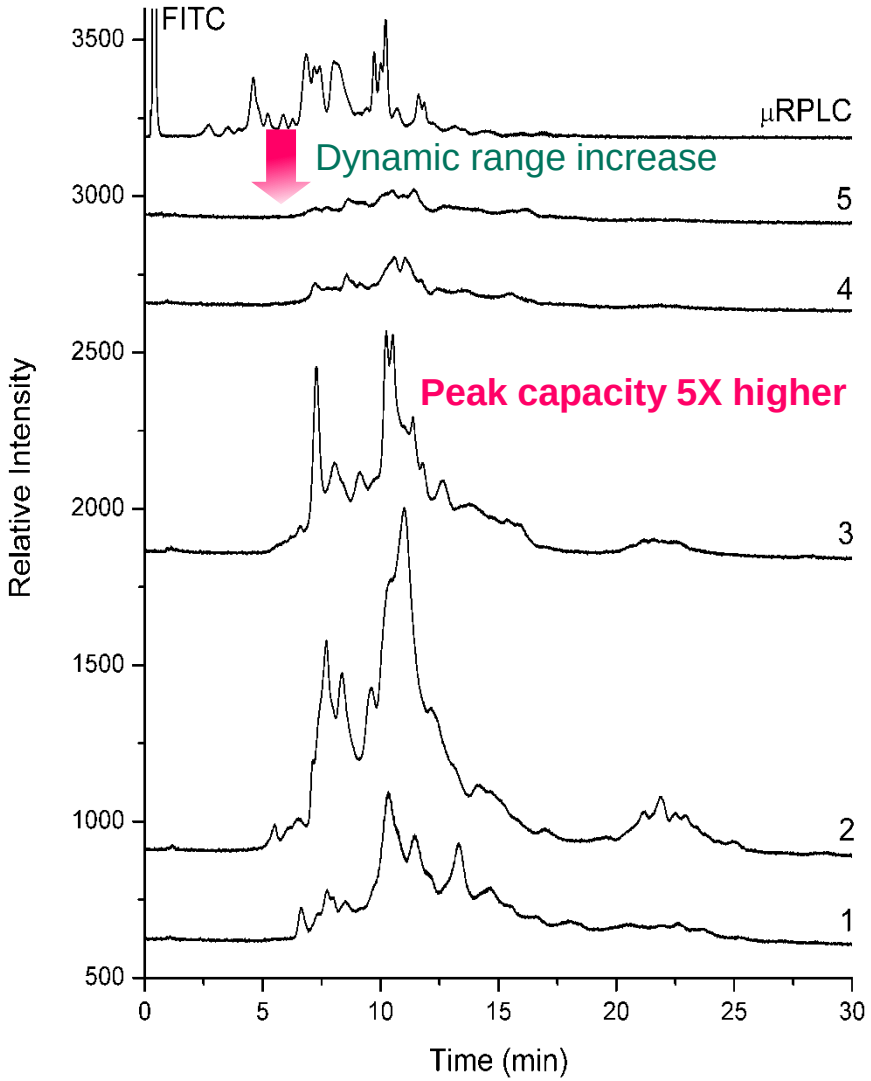

μRPLC and μIEF-mRPLC of 0.25 mg/mL FITC-BSA digest.

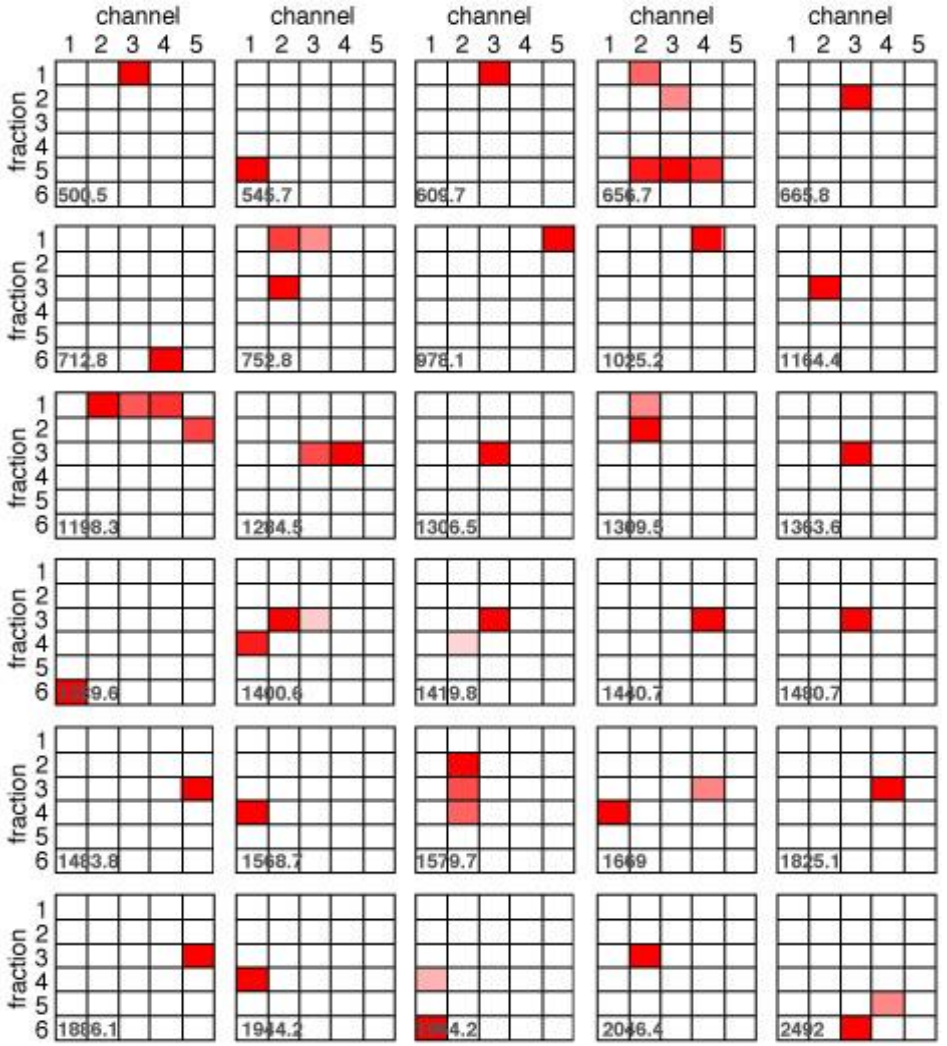

Locations of top 30 peptides identified from BSA digest by mRPLC fraction and channel. Mass tolerance: 1Da, m/z cut-off: 500 Da **~80% coverage**

Polymer Monoliths with Exchangeable Chemistries

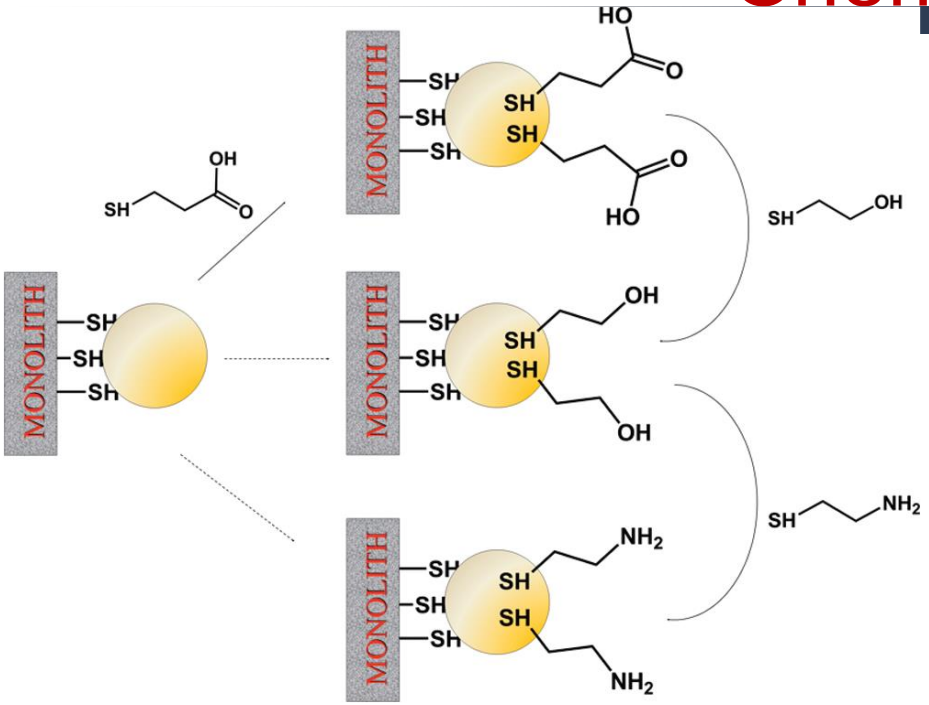

Scheme of surface modifications of a single poly(glycidyl methacrylate-co-ethylene dimethacrylate) monolith reacted with cysteamine and containing gold nanoparticles. First, the column is treated with 3-thiopropionic acid, then with mercaptoethanol, and finally with cysteamine. The dashed arrow indicates that the same functionality can also be prepared via direct reaction of the gold nanoparticles containing the monolith with the respective thiol group containing compound.

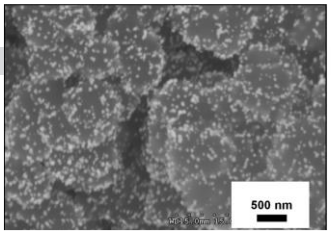

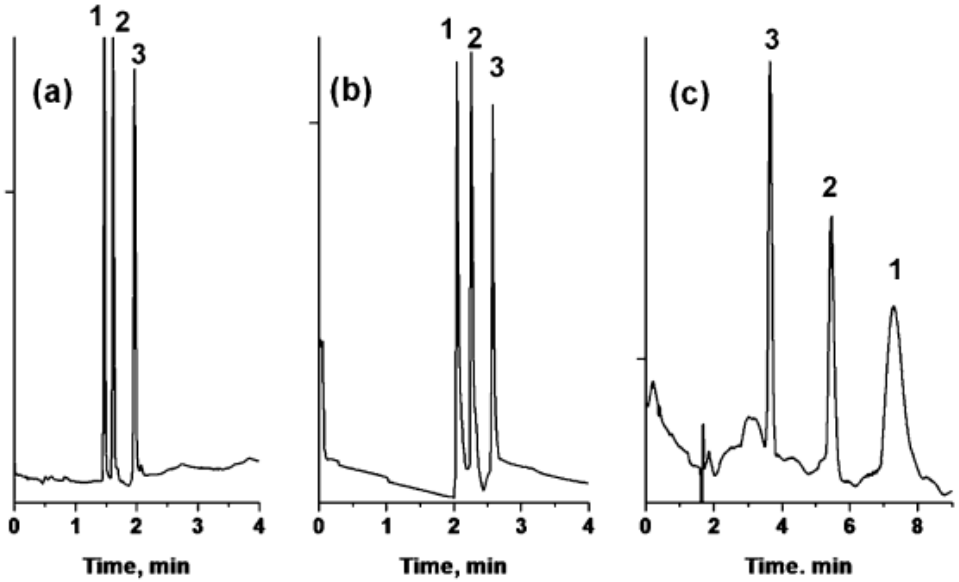

Separation of peptides in capillary electrochromatographic mode using a single poly(glycidyl methacrylate-co-ethylene dimethacrylate) monolithic column reacted with cysteamine and containing gold nanoparticles functionalized consecutively with 3-thiopropionic acid (a), mercaptoethanol (b), and cysteamine (c).

Anal. Chem. 2010, *82,* 7416–7421

Immunoassay

Lateral Flow Immunoassay (LFA; LFIA)

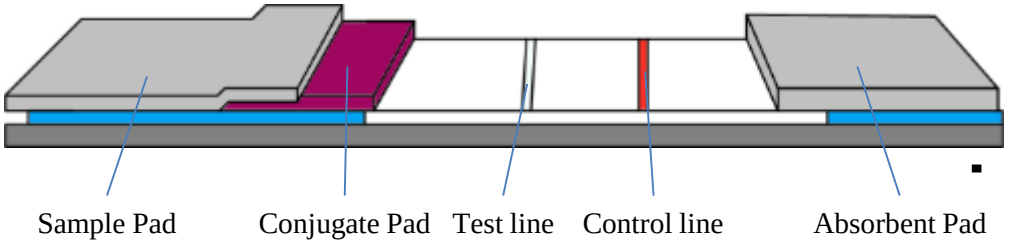

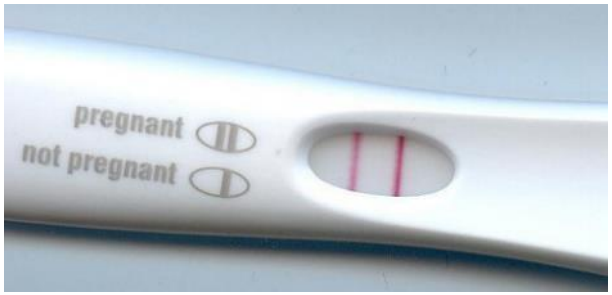

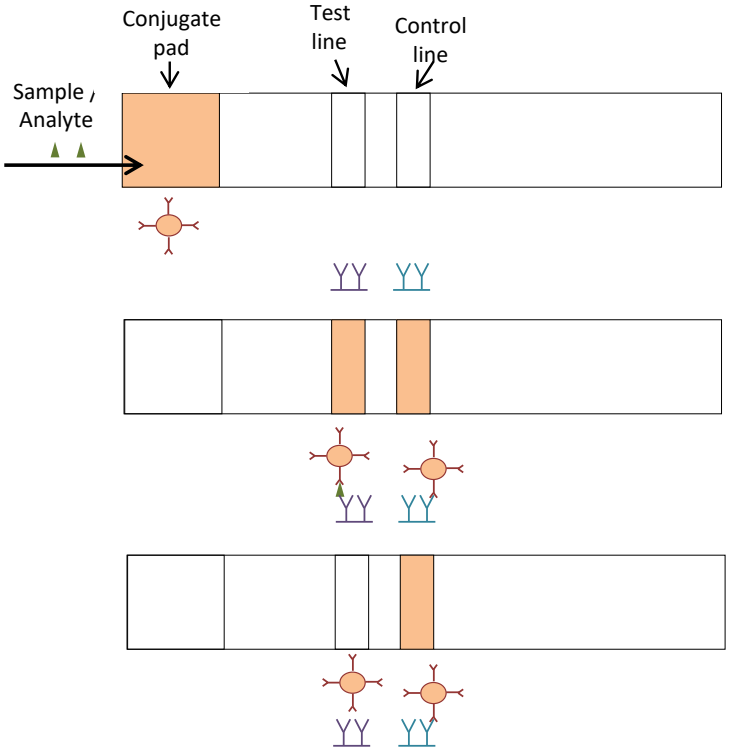

Direct solid-phase immunoassay

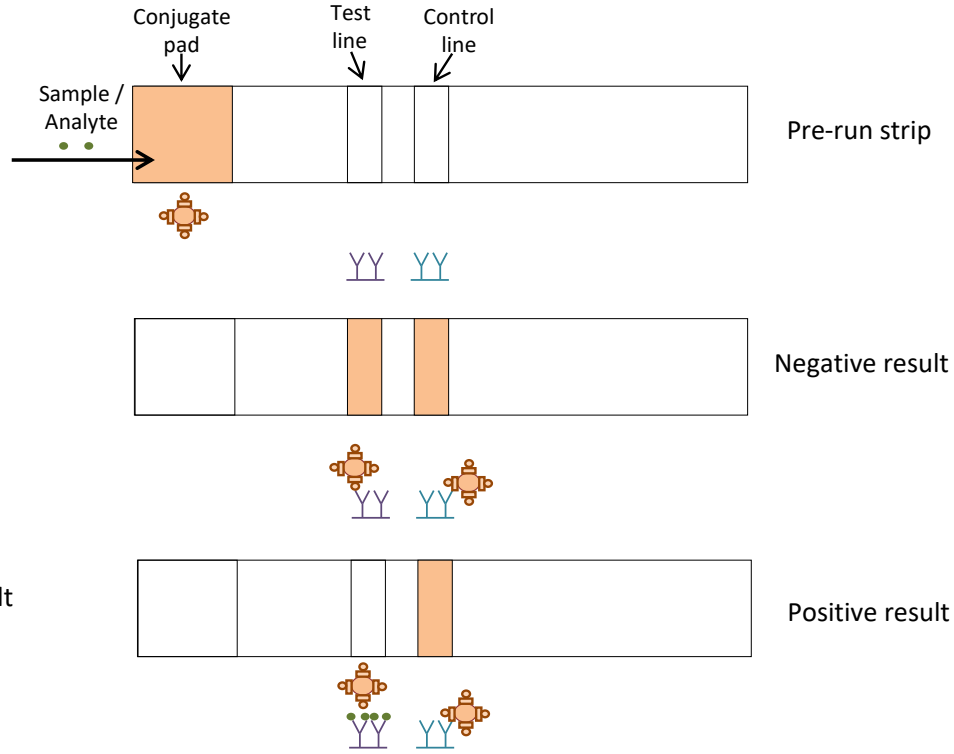

Competitive solid-phase immunoassay

Immunoassay Detection Platforms

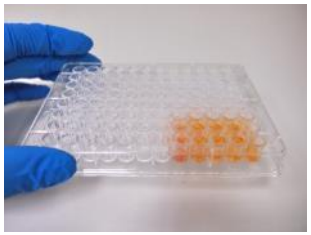

Conventional
ELISA
Microtiter plate
&
Plate reader

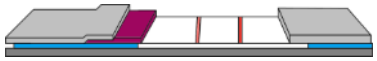

Lateral flow
immunoassay

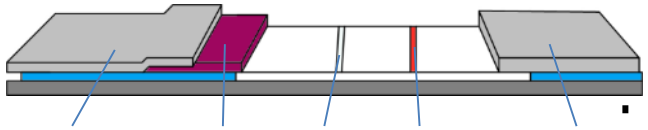

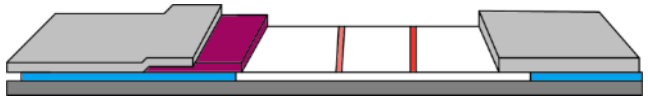

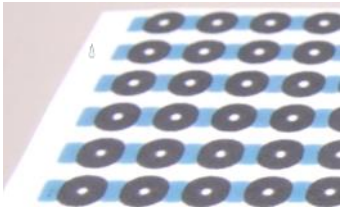

µPAD

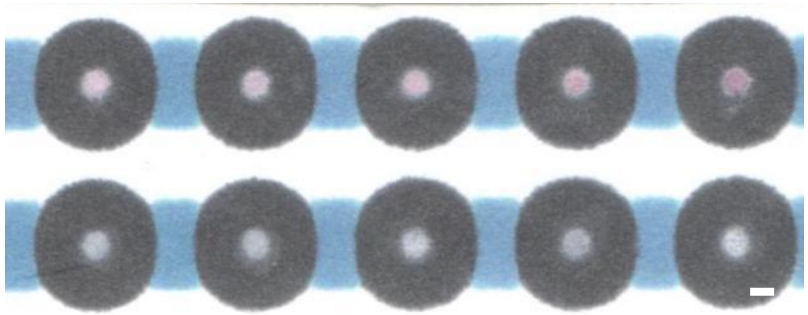

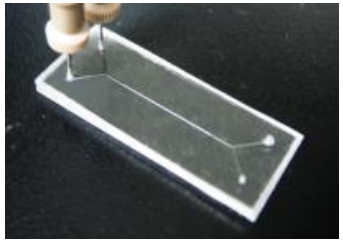

Flow through
immunoassay

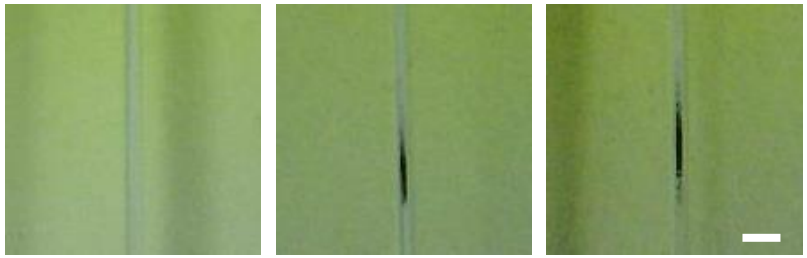

Scale bar: 1 mm

Flow Through Immunoassay

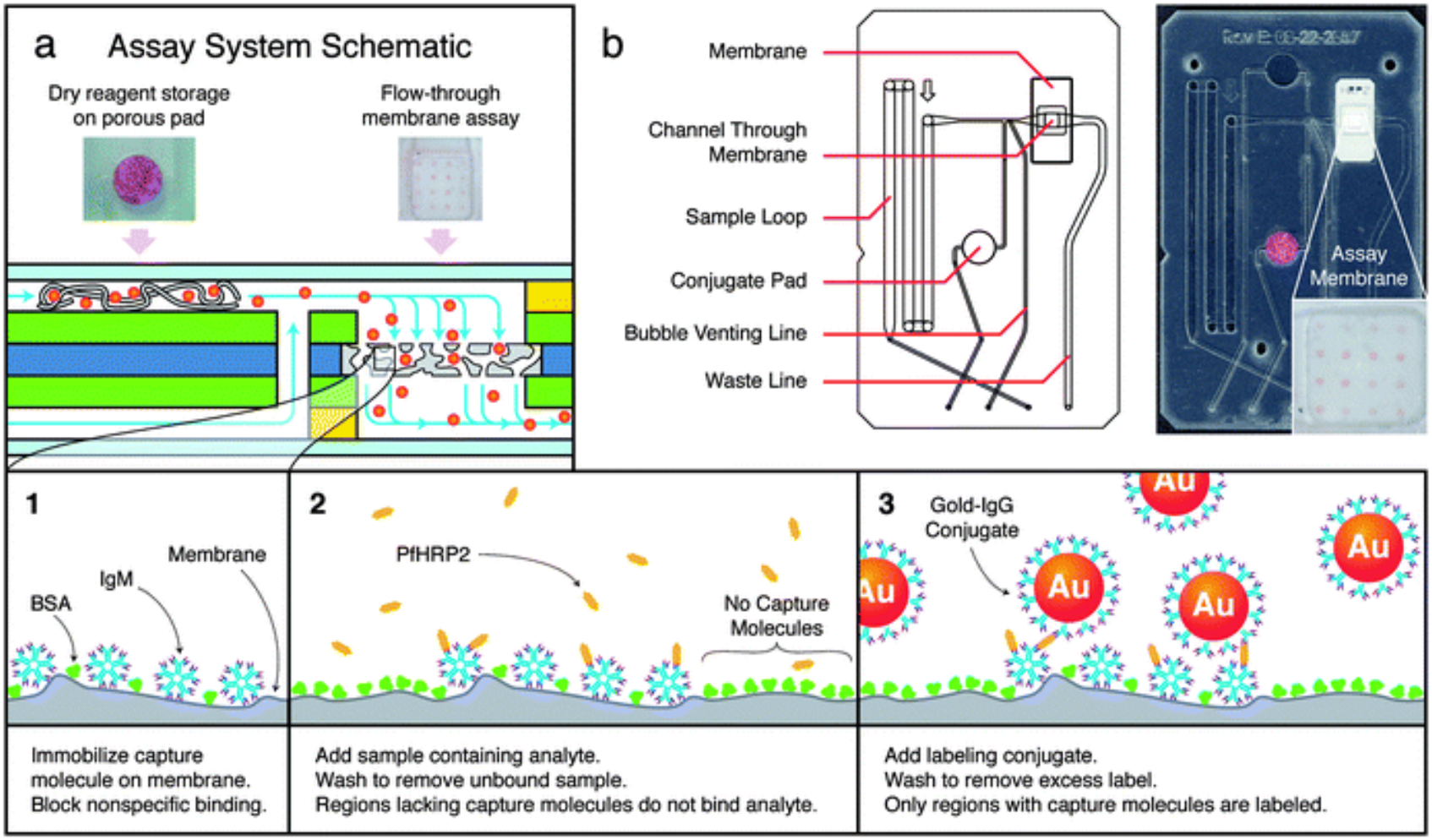

(a) Cross-section and close-up schematic of the flow-through membrane assay format. (b) Design and image of assembled, 10-layer assay card. The card is pictured before use, with the red gold–antibody conjugate present in the pad. The inset image shows the pattern of capture regions visible on the membrane after completion of the assay.

D. Y. Stevens, C. R. Petri, J. L. Osborn, P. Spicar-Mihalic, K. G. McKenzie and P. Yager, *Lab on a Chip*, 2008, **8**, 2038-2045.

Disposable Immunoassay Chips for Infectious Diseases Monitoring

I. Manual screw pump

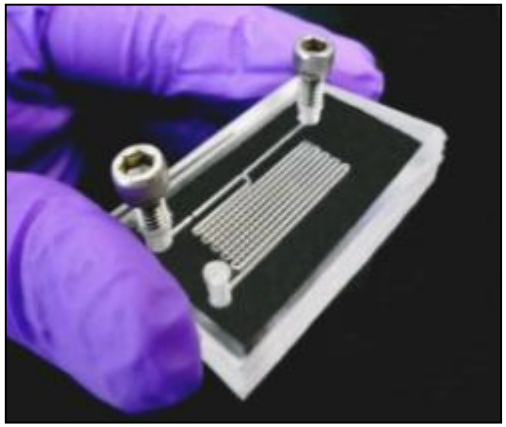

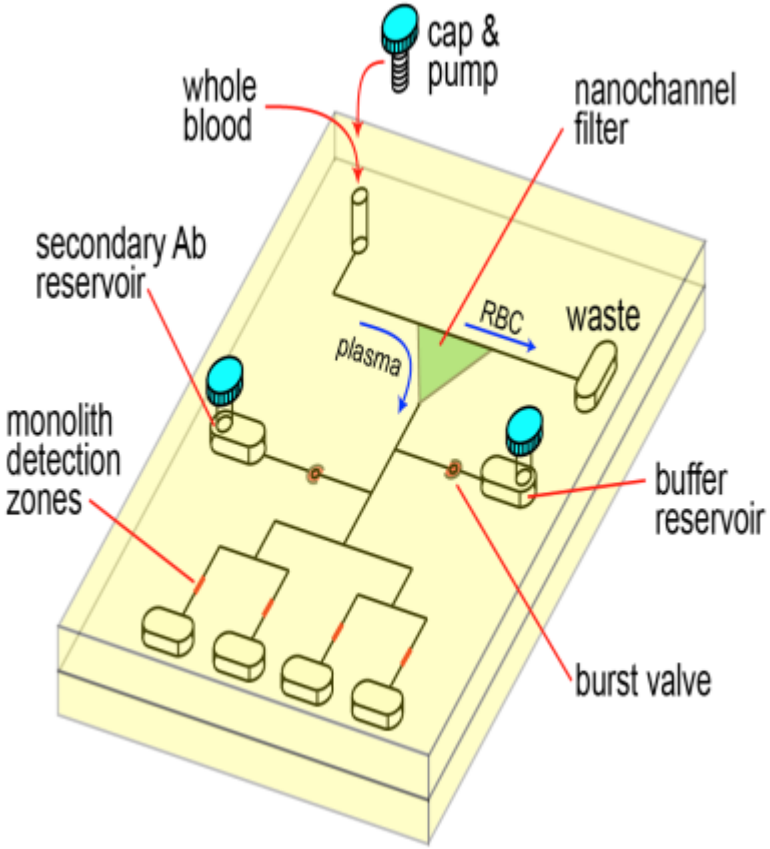

II. Cell/plasma separation

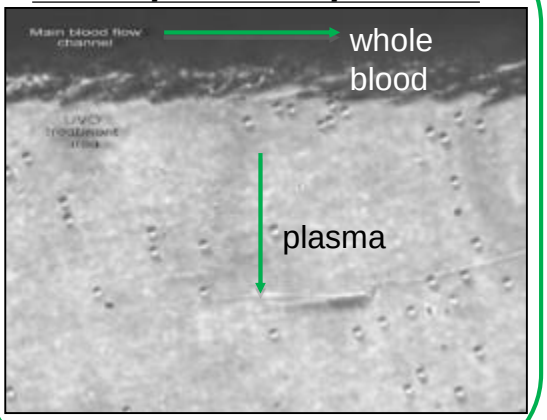

III. Micro/Nano channels fabrication

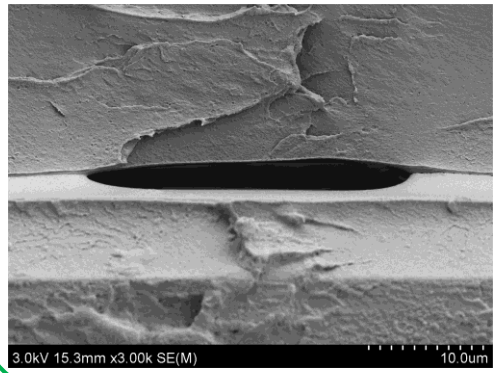

IV. Solution storage interface

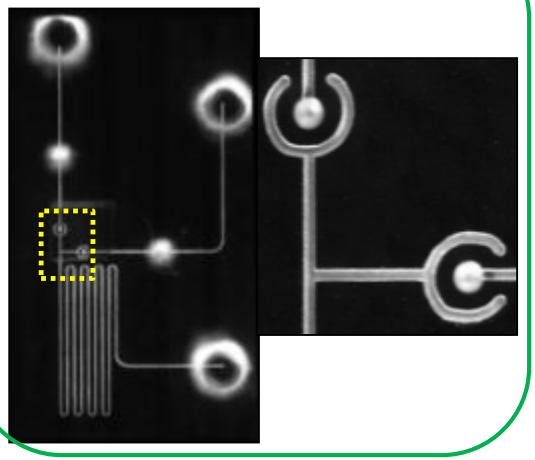

V. Porous monoliths for immunoassay detection

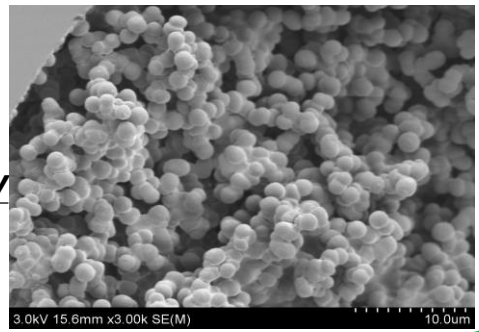

Flow-Through Immunosensors Using Antibody-Immobilized Polymer Monoliths

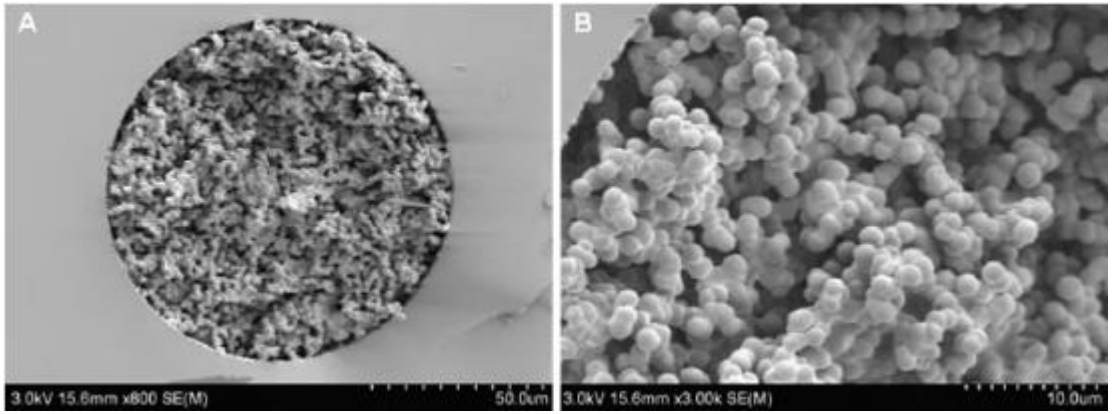

Far field and close up SEM images of a GMA-SR454 monolith.

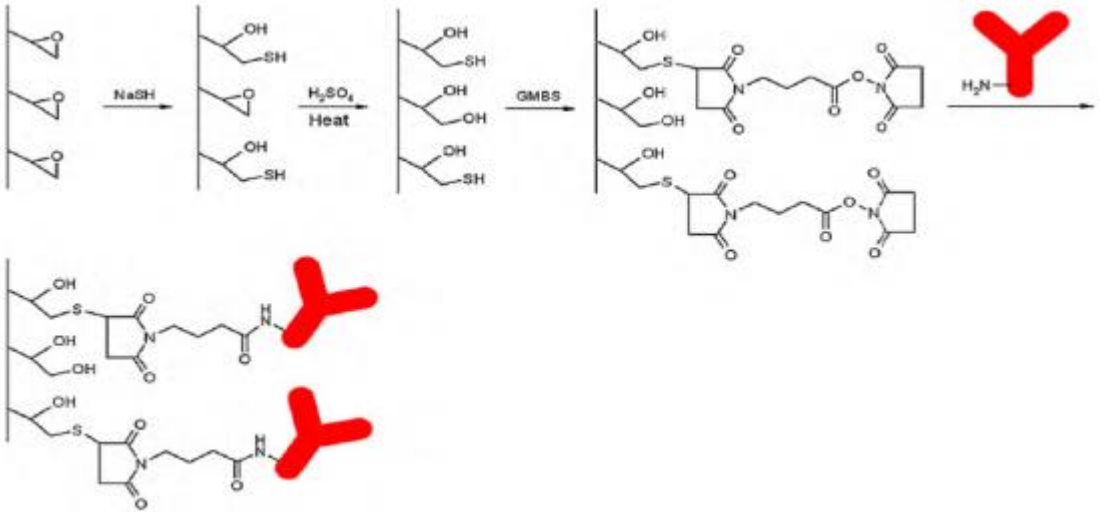

Immobilization of antibodies on GMA-SR454 monolith surface. Thiol groups are introduced by attacking epoxide groups with NaSH, and residual epoxide groups are eliminated in the following acid hydrolysis. GMBS spacer is then grafted to the thiolated monolith, enabling antibody capture through the reaction of succinimidyl ester functionality in GMBS with primary amine of antibodies.

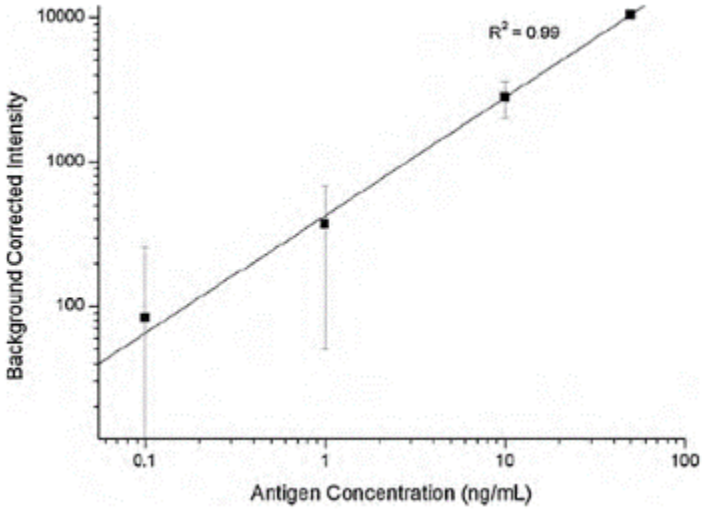

Dilution study using FITC-labeled rabbit IgG as an antigen to monolith immobilized anti-rabbit IgG. The intensity in the fitted linear equation yields a predicted concentration limit of detection (LOD) of 5 ng/mL for the chosen flow rate and infusion time.

J. Liu, *Biosensor and Bioelectronics*, 2010

Colorimetric Immunosensing Using Surface-Modified Porous Monoliths and Gold Nanoparticles

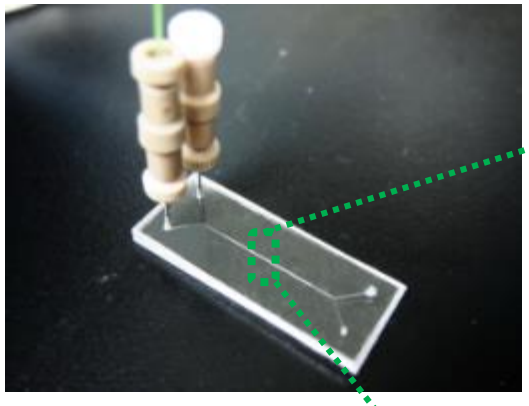

Flow through immunoassay

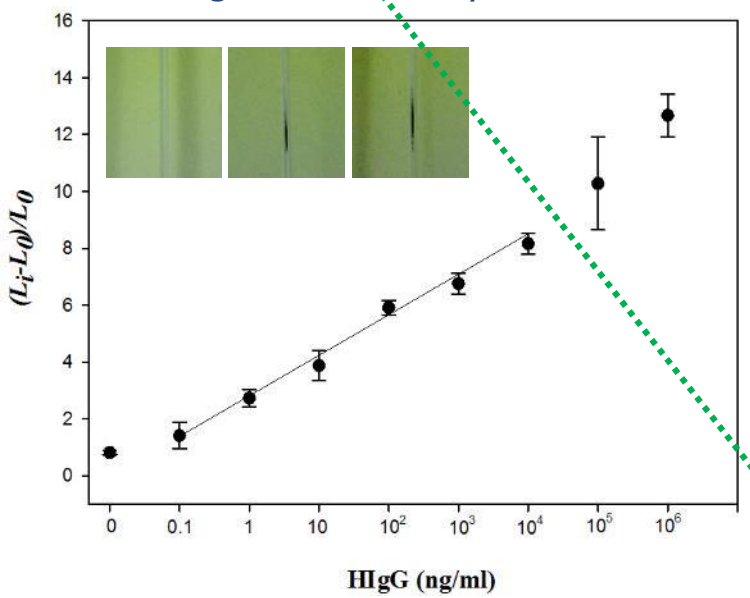

Porous monoliths-based colorimetric immunoassay combining AuNPs probes for the detection of HIgG

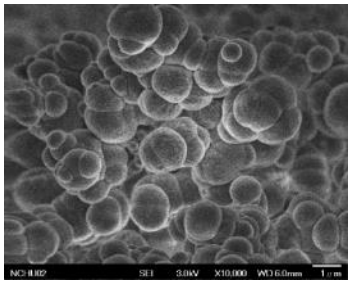

Monoliths

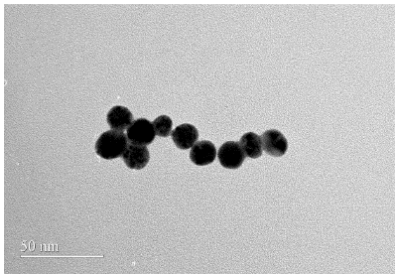

AuNPs

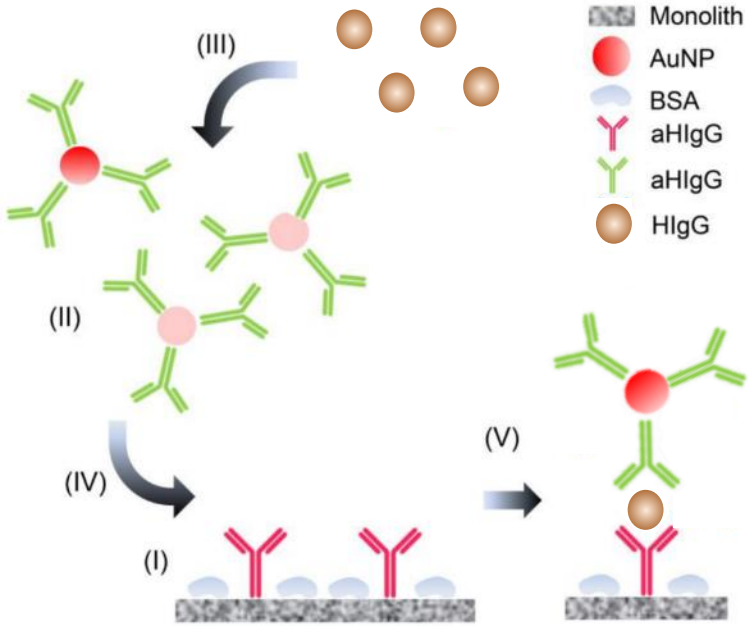

The sandwich immunosensing strategy using porous monolith and AuNPs probes.

S. H. Chuang, *Sci. Tech. Adv. Mater.*, 2013

Blood Tests

Licensed nurse staff

Painful

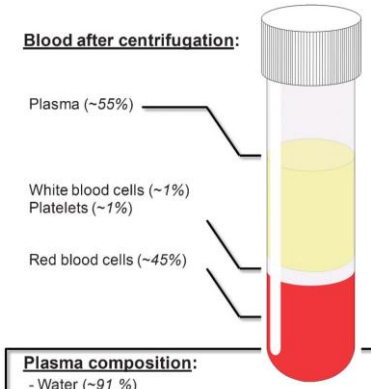

Plasma composition:
- Water (~91 %)
- Proteins (~7 %)
- Bacteria, Fungi and Micro-organisms (*traces*)
- Viruses (*traces*)
- Metabolites (*traces*)
- Circulating Nucleic Acids (*traces*)
  - In healthy patients:
    - DNA (~1.8-35 ng/mL)
    - RNA (~2.5 ng/mL)
  - Depending on conditions:
    - Tumor DNA (cancer)
    - Viral DNA (infection)
    - Fetal DNA (pregnancy)
    - Donor DNA (transplantation)
  - 5 most abundant in healthy patients:
    - Glucose (5 mM)
    - Total cholesterol (5 mM)
    - Melanin (5 mM)
    - Urea (4 mM)
    - ATP (3 mM)
    - Hormones (TSH, T4, Testosterone, Estradiol).

Lab Chip, 2013, 3323-3346.

Expensive

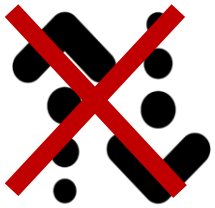

Inconvenient

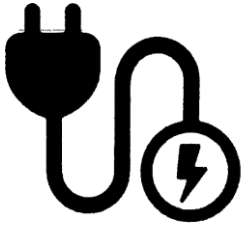

Electricity power

Finger prick

Traditional blood typing tests in hospital

- Conventional blood typing tests are reliable and accurate, but they also **require well-trained personnel and sophisticated equipment to obtain results**.
- In addition, typical agglutination tests require a blood sample of **more than 1 mL**, which cannot be obtained using low invasive methods, such as finger pricking.

- **Column agglutination**

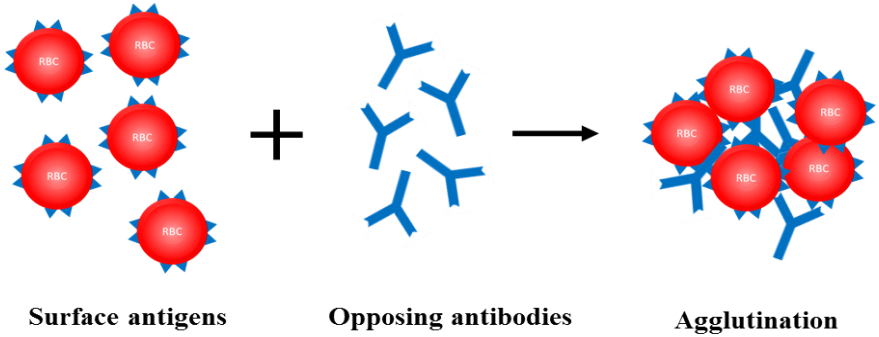

2 USD

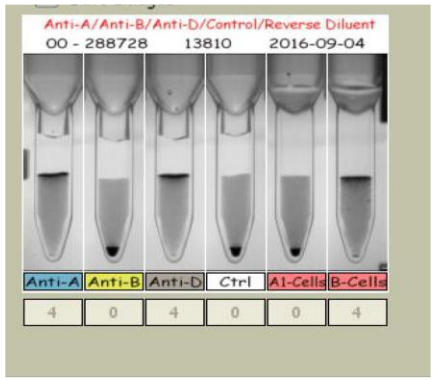

Rapid, accurate, and inexpensive blood typing tests are necessary for clinical confirmation on the battle filed or for infants that can't extract regular amount of blood.
How about other blood disease diagnosis?

A multifunctional microfluidic device for blood typing and blood disease screening

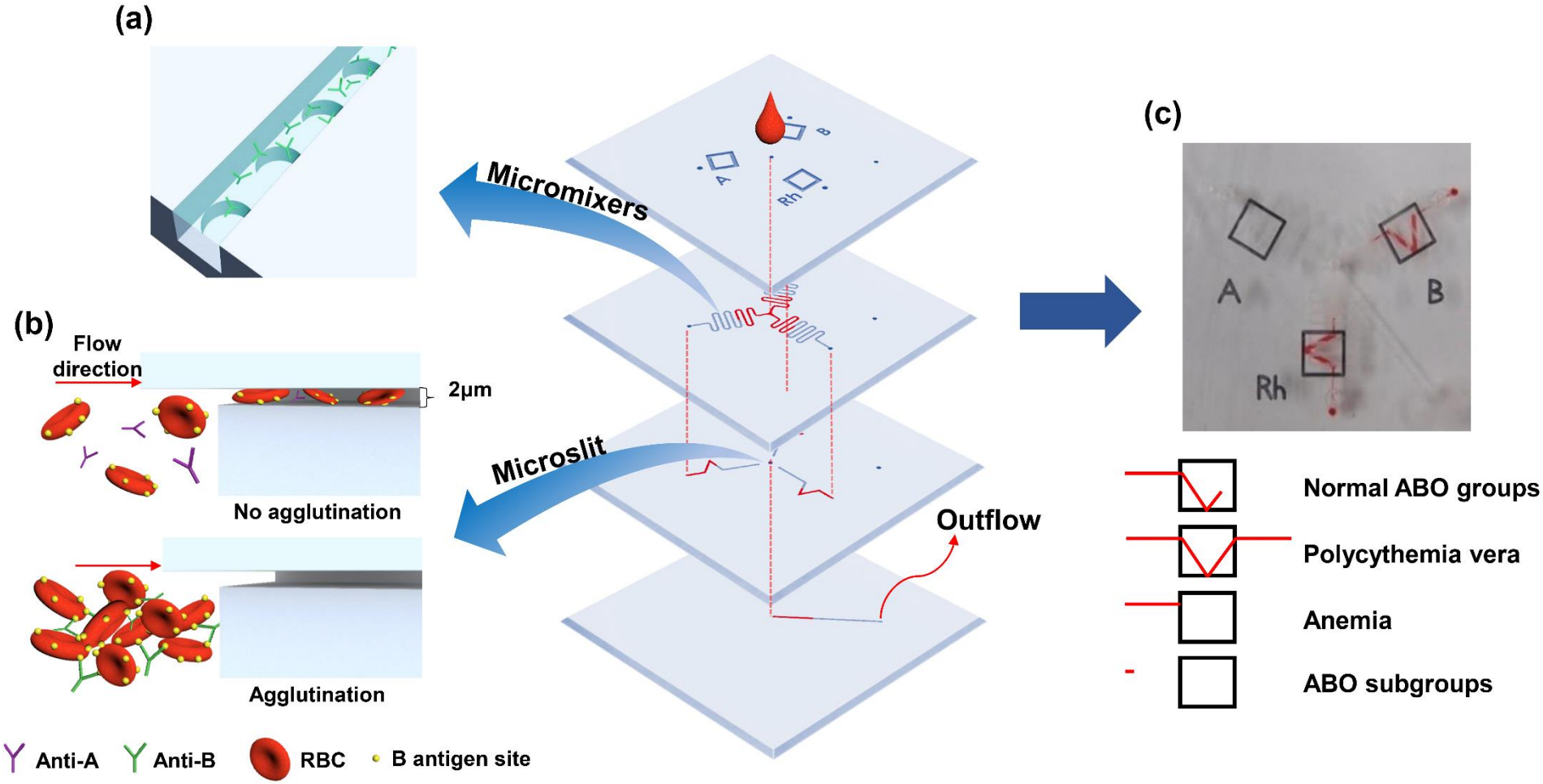

Illustration of the blood type and disease primary screening process. A drop of blood flows sequentially through the four-layer microfluidic chip from the top to bottom layer, (a) dividing the RBCs into three serpentine reaction channels where they can react with preloaded antibodies in the micromixers. (b) Agglutinated RBCs that result from the specific antibody-antigen interaction are blocked by the microslits, (c) resulting in red lines that appear in the observation area. Based on the location and length of these red lines in the microchannels, the blood type and disease can be easily distinguished.

A multifunctional microfluidic device for blood typing and blood disease screening

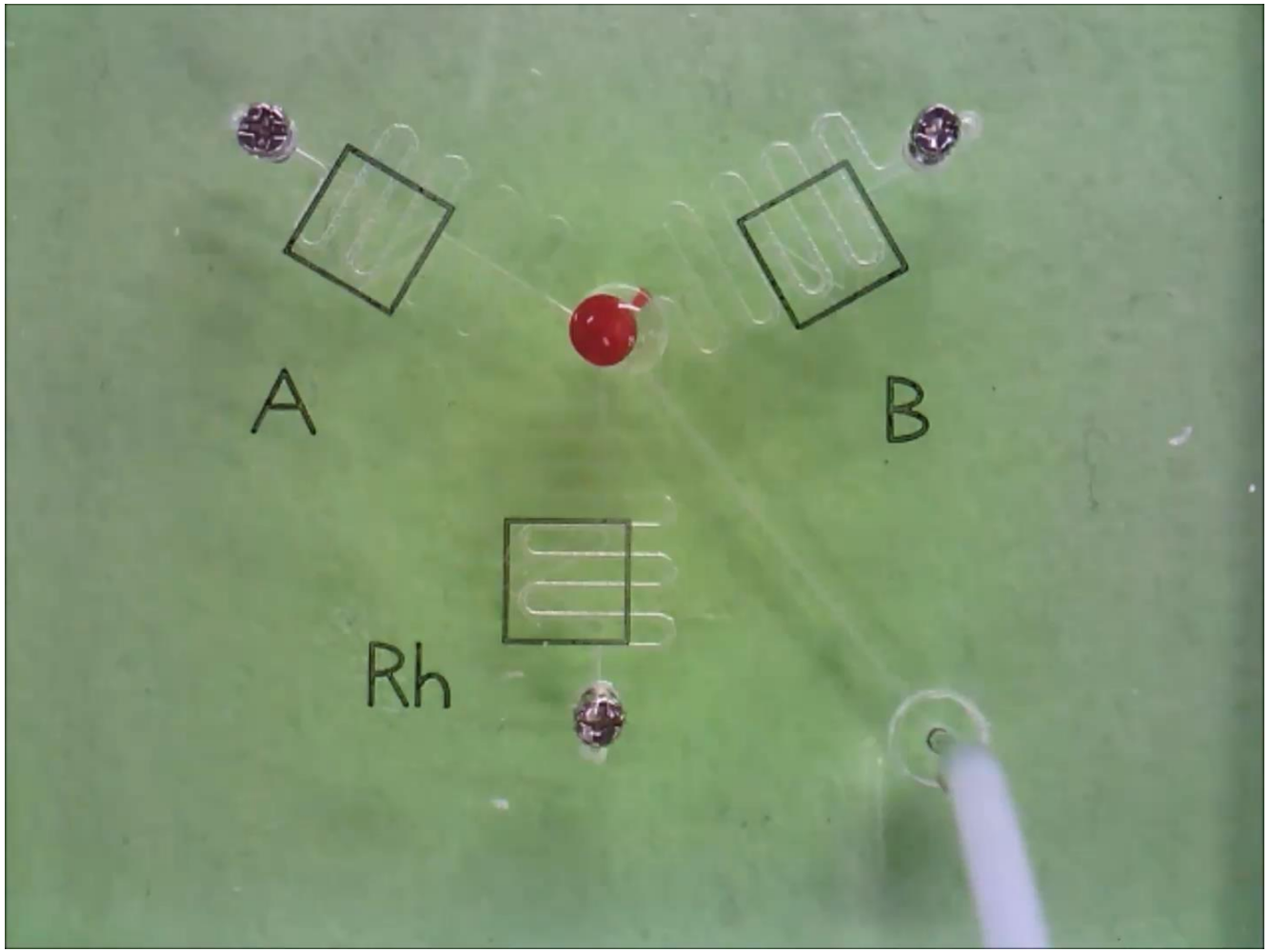

The fabrication process of the microfluidic chip using the selective solvent swelling method

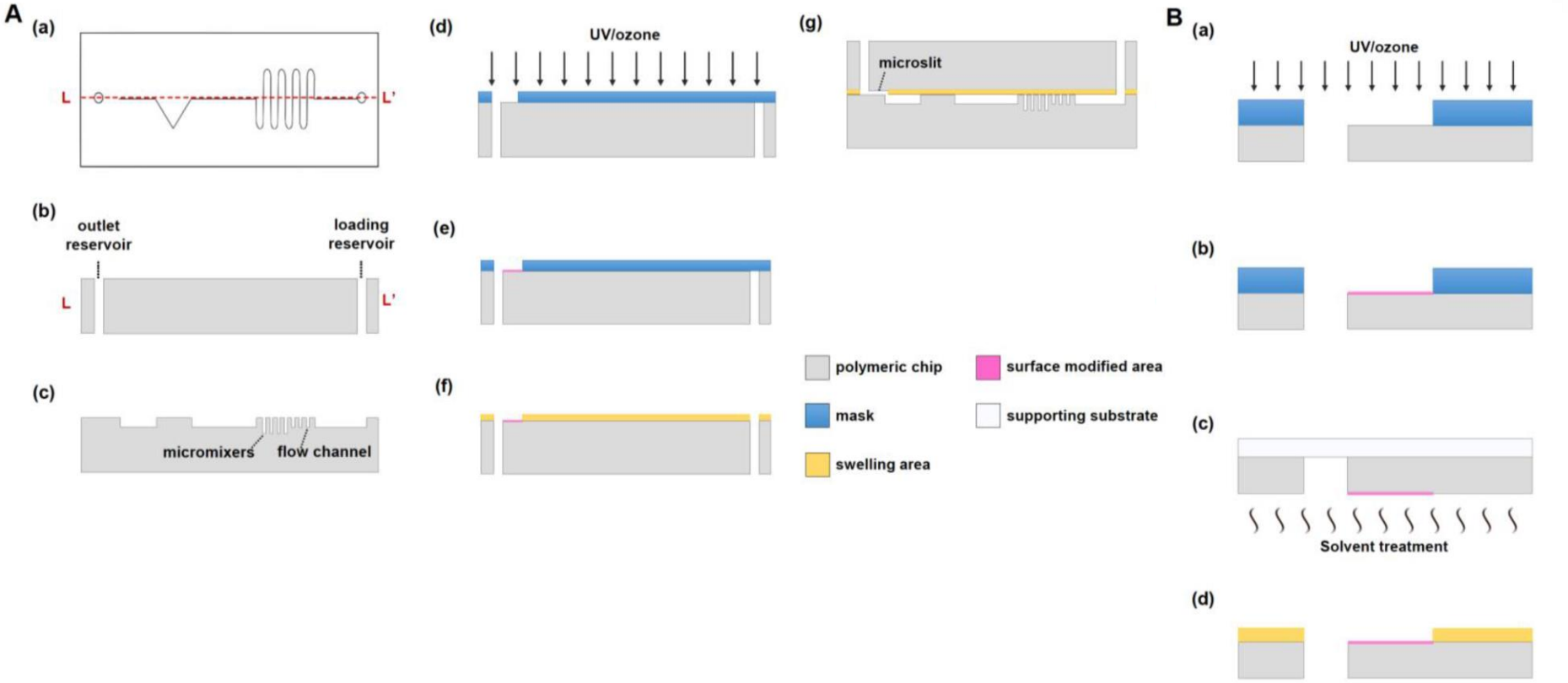

(A) The fabrication process of the chip. (a) Top view of the single-channel chip. (b) The top cover chip is drilled to form two holes for a loading reservoir and an outlet reservoir. (c) The bottom chip is milled to form the serpentine microchannels and micromixers. (d)(e) The top cover chip is masked with tape and exposed to UV/ozone to form the surface-modified area. (f) After removing the mask, the top cover chip is swelled with cyclohexane vapor. (g) The top and bottom chips are sealed into a single-channel chip by pressing them at room temperature. (B) The selective solvent swelling method is used to form a microslit. (a)(b) After exposing the masked region of the polymeric chip surface to UV/ozone, the unmasked region is modified with hydrophilic groups. (c)(d) The chip surface is treated with cyclohexane vapor, causing the unmodified region of COP chip to absorb the non-polar solvent and swell, while the modified surface resists the absorption of solvent vapor.

Blood typing test results

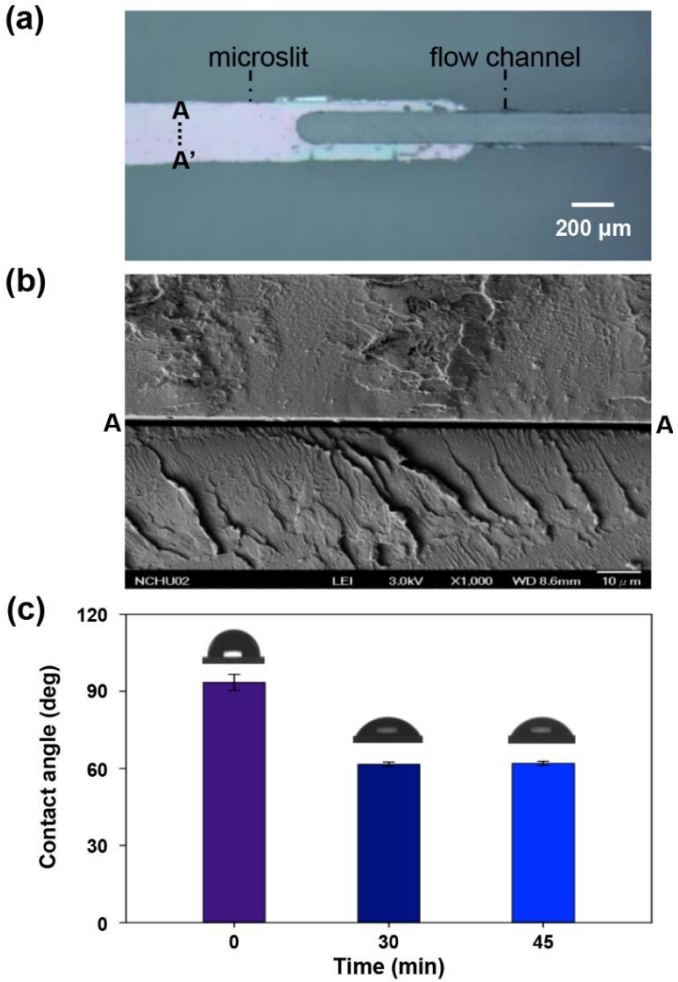

(a) Top view microscopic image of the 300 μm wide microslit. (b) SEM image of the A-A' cross-section of the microslit, which was formed using a UV/ozone pretreatment and followed by selective solvent swelling. (c) The contact angle of water measured on the surface of the COP at different UV exposure times (N = 3).

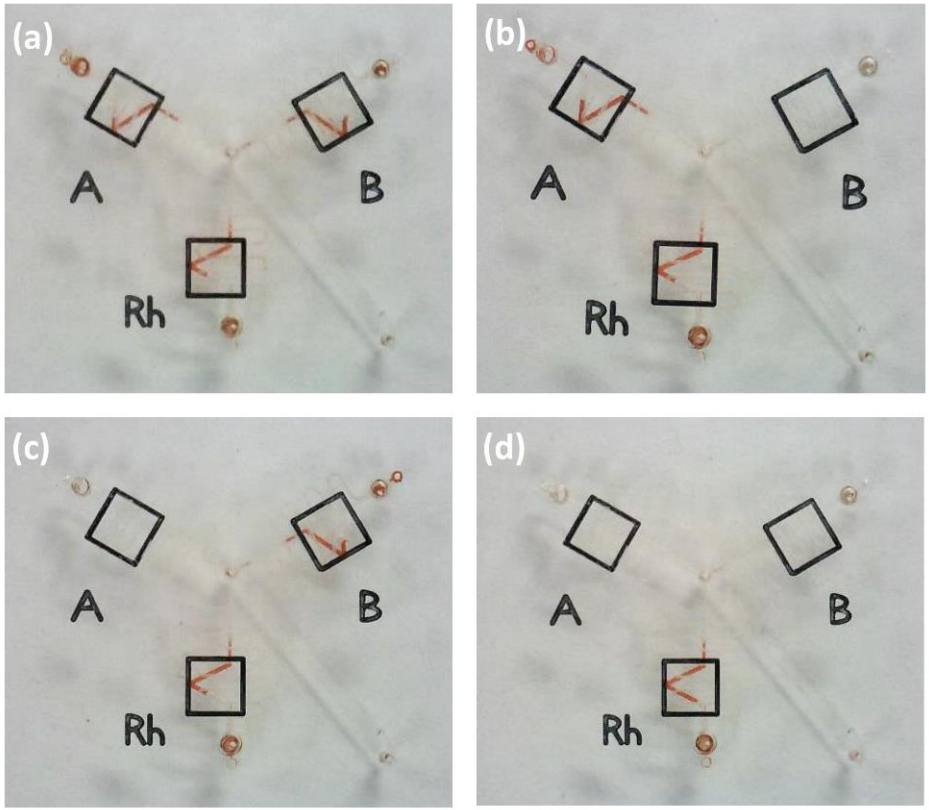

Representative chip test results are shown for (a) AB Rh+, (b) A Rh+, (c) B Rh+, and (d) O Rh+ blood types. These results are clearly visualized by the red lines corresponding to the A, B, and Rh symbols on the top of the chip.

Hematocrit values and the levels of blood agglutination can be used for blood disease screening

Table 1. Comparison of sensing strategies for blood typing and blood disease primary screening.

Method	Normal ABO groups	PV	Anemia	ABO subgroups
Hematocrit level (%)	Male: 39-47 Female 36-46	Male: > 49 Female: > 48	Male: < 39 Female: < 36	-*
Diagnostics in clinical center	Tube or gel method	Complete blood count	Complete blood count	Tube or gel method
This work Length of the red line in the device (cm)[b, c]	0.89 ± 0.04	1.24 ± 0.21	0.38 ± 0.10	0.03 ± 0.02

* ABO subgroups are not related to the hematocrit level.
[a] Standard deviations based on three independent measurements.
[b] The cross-section of the microchannel is 200 µm × 140 µm.

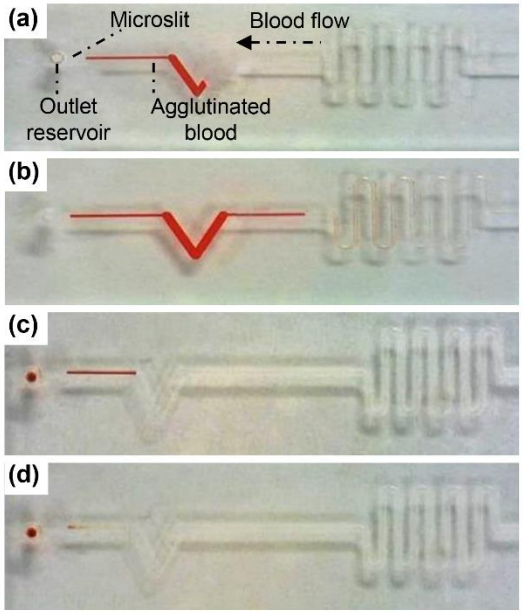

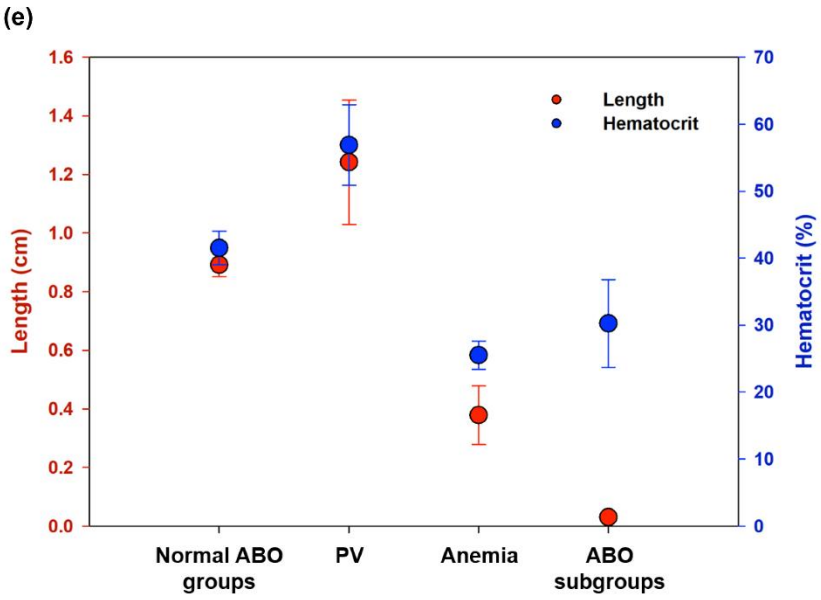

The red line caused by the hemoagglutination reactions between different blood samples and anti-D antibody (a-c) and anti-A antibody (d). The samples featured include (a) normal, (b) PV, (c) anemia Rh+ blood, and (d) the A3 subgroup type. (e) The length of agglutinated red line in the microchannel versus the level of hematocrit for different blood samples. N = 8 for normal ABO groups, anemia, PV, and N = 6 for ABO subgroups.

A portable device for blood typing and primary screening of blood disease

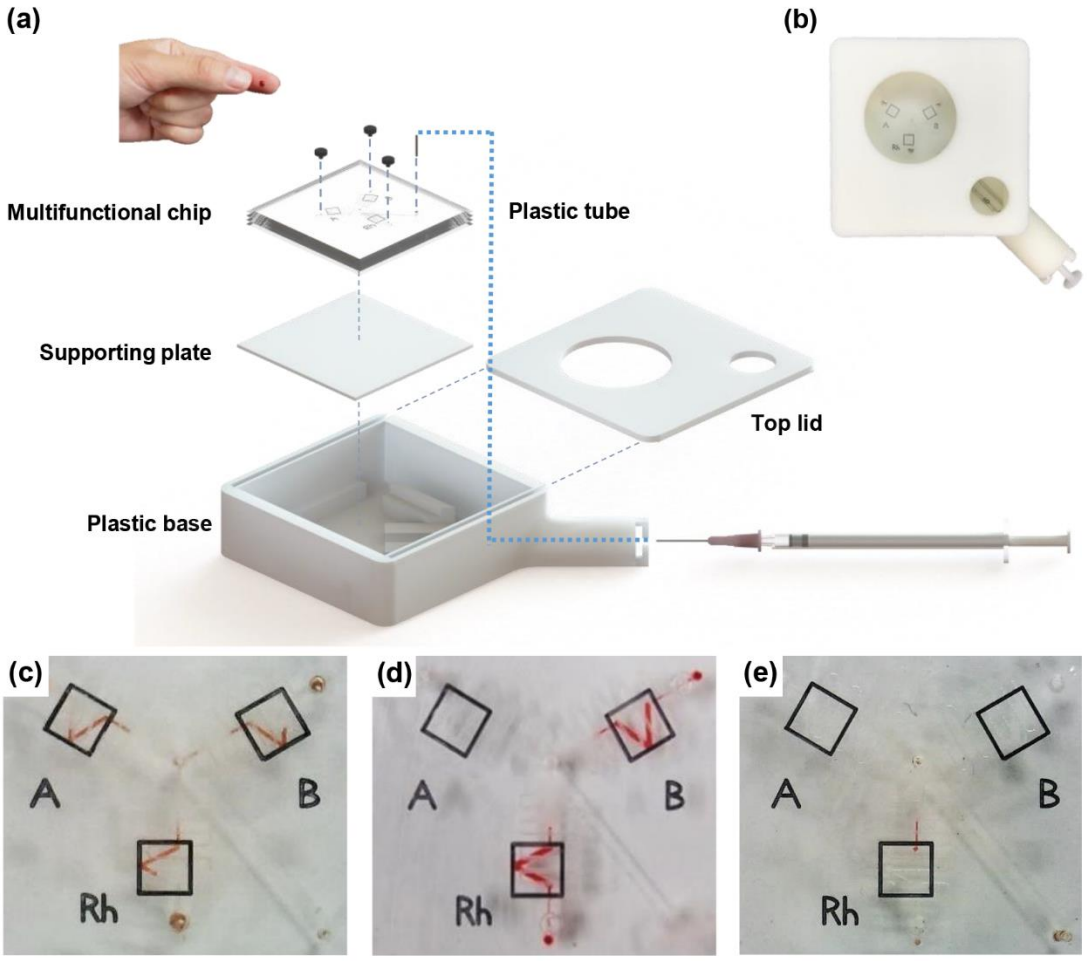

(a) multichannel microfluidic device, the top-view of which is shown in (b). A drop of blood is obtained by a finger-prick and dropped into the loading reservoir, followed by 10 μL of PBS buffer solution. The rod of the syringe pump is pulled backward to create negative pressure that drives the blood flow through the microchannels and react with pre-loaded antibodies. The agglutinated RBCs (the red lines) indicate the identity of the blood type and blood disease (PV, anemia, or subgroup). Representative test results are shown for (c) AB Rh+ (normal ABO group), (d) B Rh+ (PV), and (e) O Rh+ (anemia).

Lab on a Disk

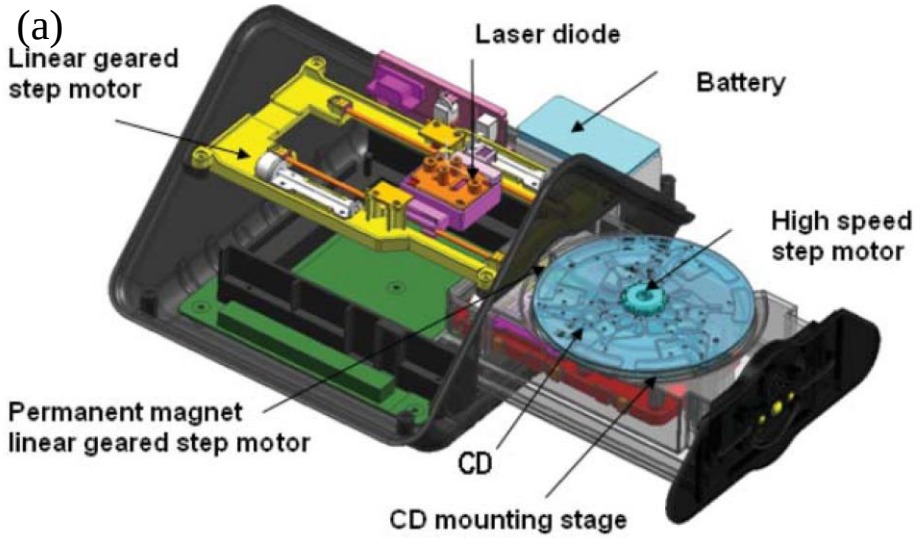

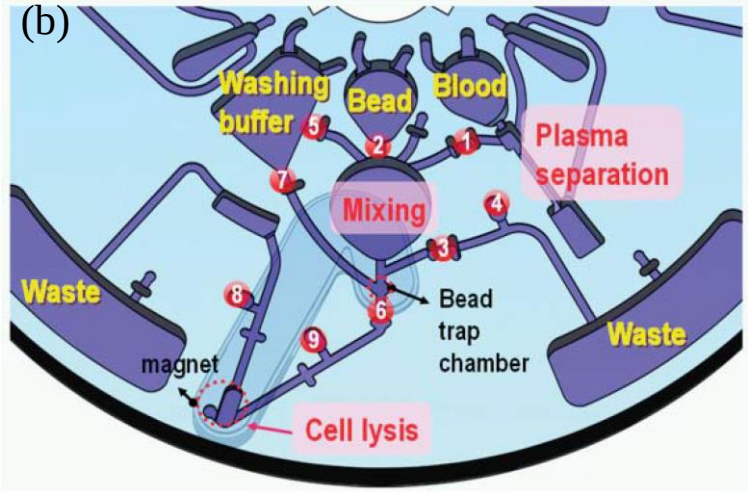

(a) Schematic diagram of the portable lab-on-a-disc device. (b) The detailed microfluidic layout and functions of the polymeric disc.

Y.-K. Cho, J.-G. Lee, J.-M. Park, B.-S. Lee, Y. Lee and C. Ko, *Lab on a Chip*, 2007, **7**, 565-573.

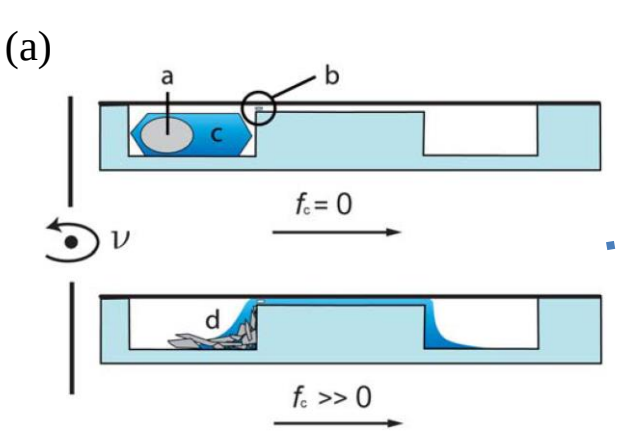

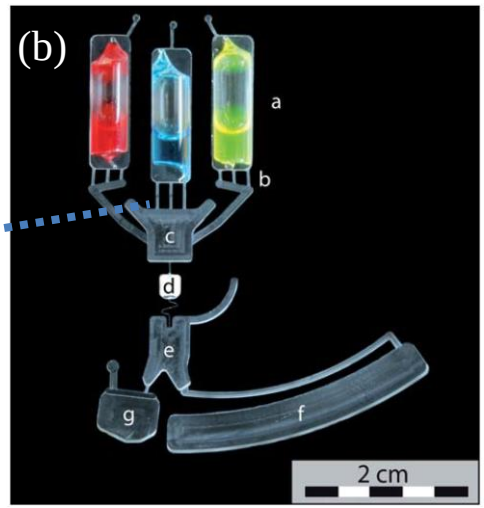

(a) Schematics of storage and release within a centrifugally operated LoaC system. Reagents can be long term stored in the glass ampoule before usage. (b) Image of the cartridge for on-chip DNA extraction featuring required buffers pre-stored in three glass ampoules.

1. J. Hoffmann et al, *Lab on a Chip*, 2010, **10**, 1480-1484.

Cell/Plasma Separation

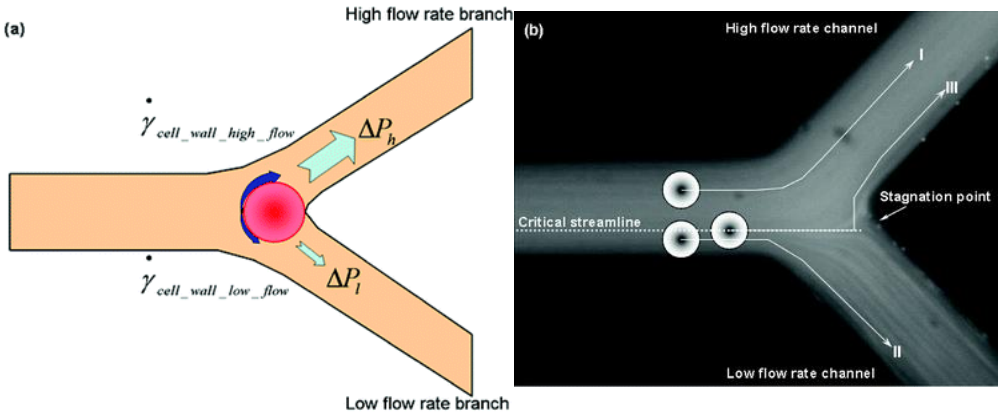

Scheme depicting plasma separation from a finger prick of blood by harnessing the Zweifach-Fung effect. Multiple DNA-encoded antibody barcode arrays are patterned within the plasma-skimming channels for in situ protein measurements.

R. Fan et al, *Nature biotechnology*, 2008, 26, 1373-1378.

(a) Schematic of the Zweifach–Fung effect; red blood cells have a tendency to travel into the higher flow rate daughter vessel with no cells travelling to the lower flow rate daughter vessel when the flow rate ratio is more than 2.5 and the cell-to-vessel diameter ratio is of the order of 1. The primary reason for this effect are because of differential pressure drops and shear forces acting on a cell. (b) An illustration of the critical streamline; A particle (I) whose centroid is beyond the critical streamline will travel into the high flow rate channel.

2006, Lab Chip

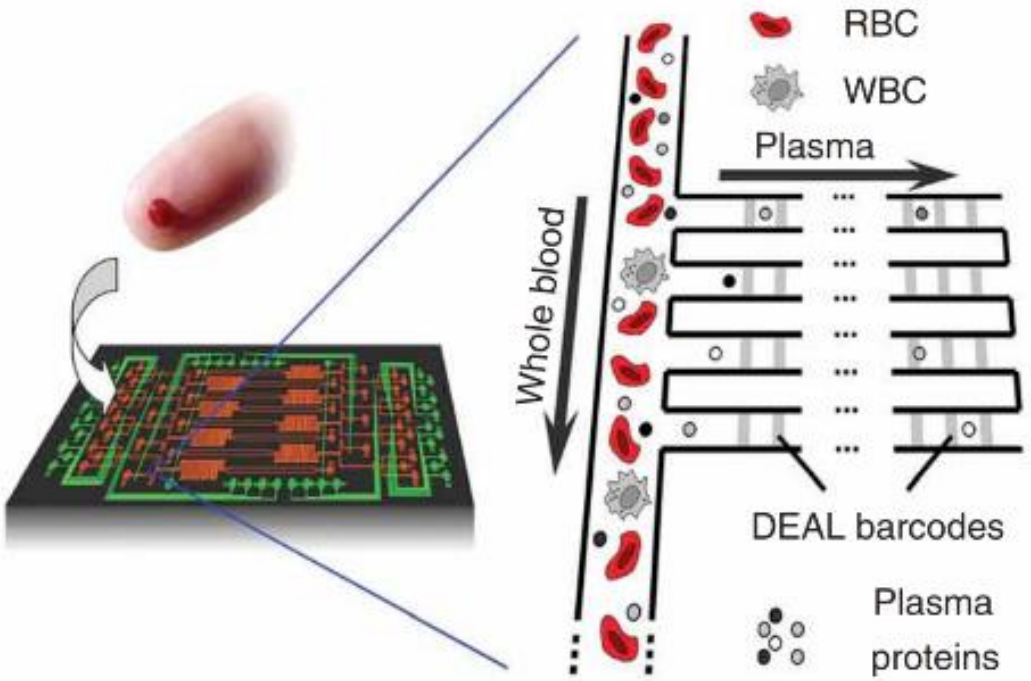

V-Chip ELISA

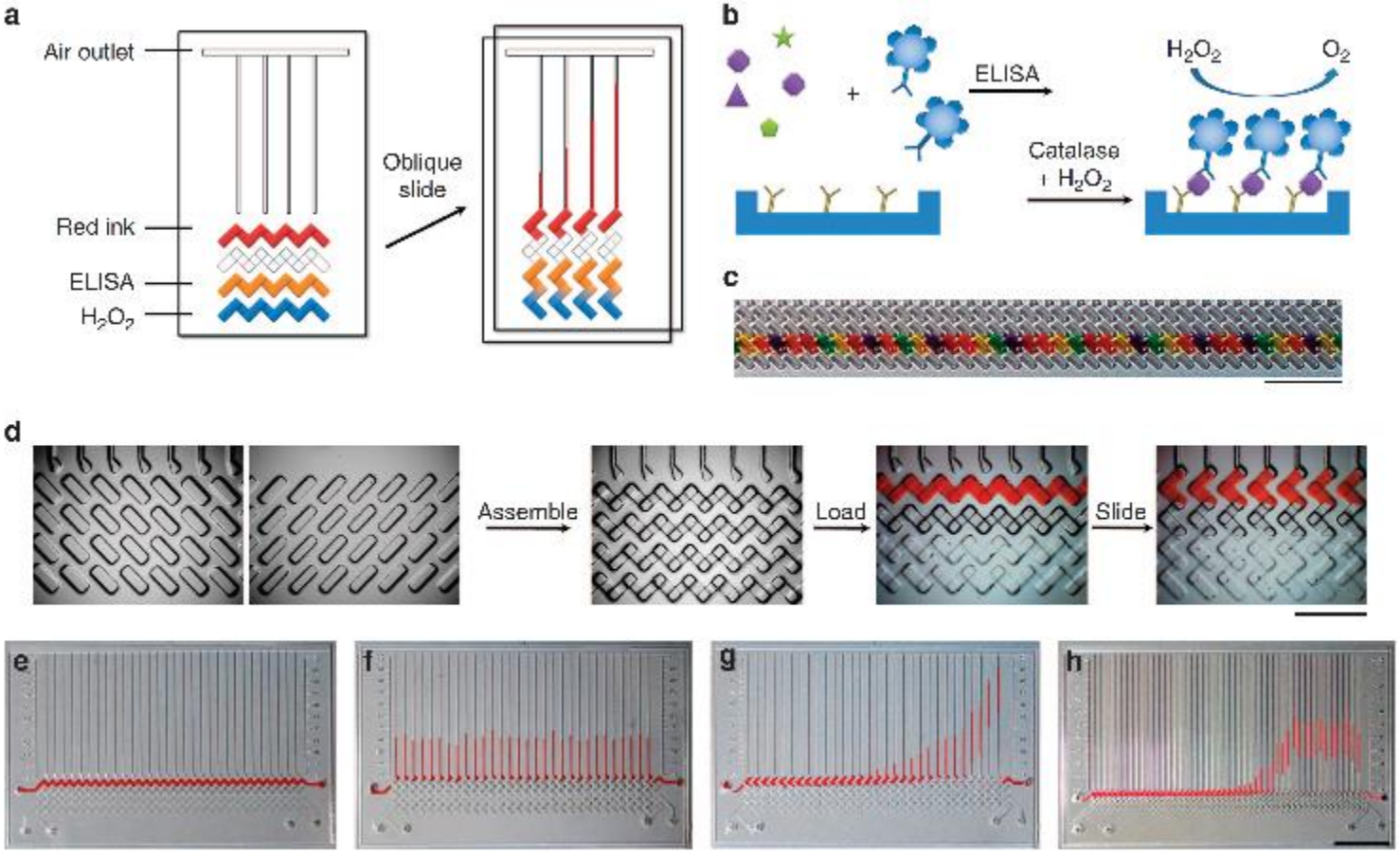

1. Y. Song et al, *Nature communications*, 2012, **3**, 1283.

(a) Schematic view of a typical V-Chip. On the left is an assembled V-Chip with the flow path at the horizontal position. Ink and H_2O_2 can be preloaded and the ELISA assay can be performed in the designated lanes. An oblique slide changes the flow path on the right, causing catalase and H_2O_2 to react and push the inked bars. (b) V-Chip ELISA reaction scheme. (c) Image of sample wells loaded with different colored food dyes. Scale bar is 0.5 cm. (d) Zoomed microscopic images of as-fabricated bottom and top plates, device assembly, reagent loading and assay operation in a V-Chip. Scale bar is 2.5 mm. (e) A V-Chip loaded with the red ink and reagents. (f) Uniform ink advancement image resulting from the application of equal concentrations of catalase. (g,h) Visualized ink advancement in 30- and 50-channel V-Chips generated by the 3- and 6-h diffusion of catalase from the drilled holes on the right to the ELISA lane. Scale bar, 1 cm in e, f, g and h.

Droplet Microfluidics

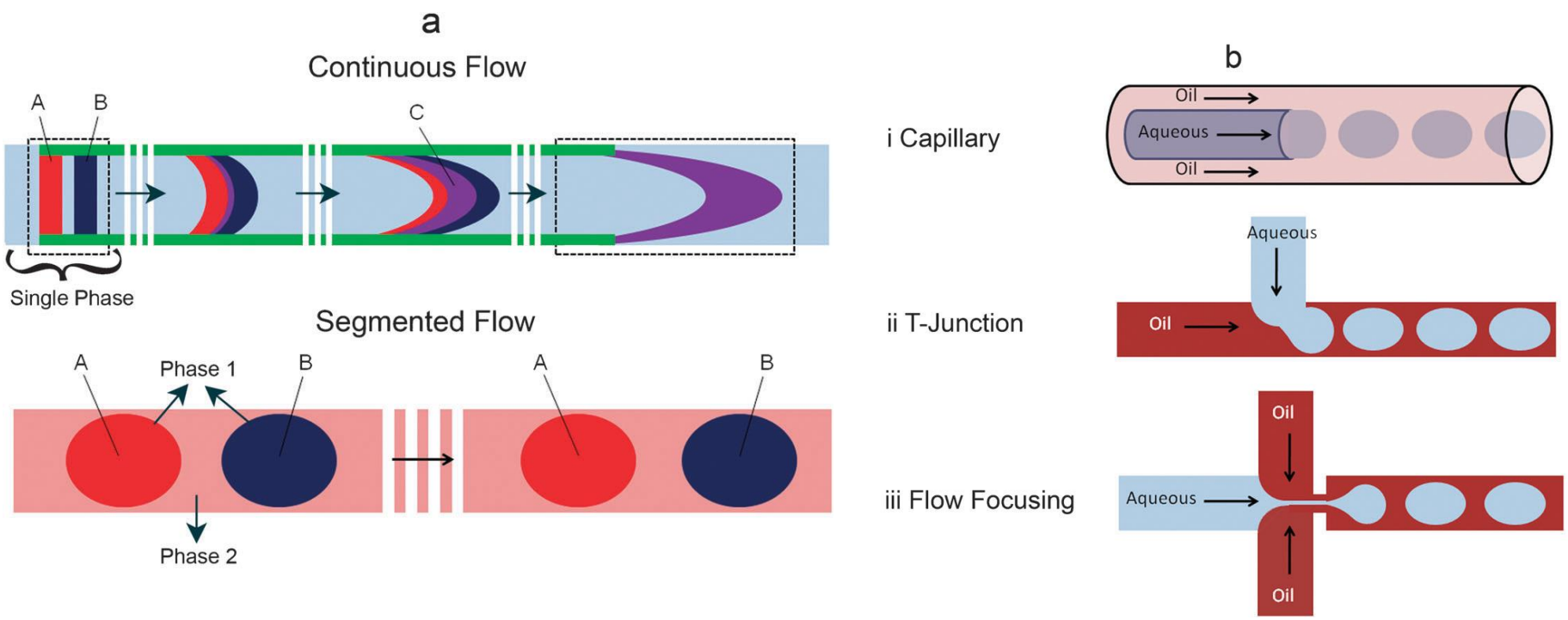

(a) Comparison between continuous and segmented flow microfluidics: microfluidic droplets elegantly address several issues of continuous flow, such as Taylor dispersion of reagents due to parabolic flow: the enlargement of the dotted area illustrates this spreading effect; crosscontamination: the single continuous phase allows diffusion between different fluid portions—in this case A and B eventually combine and become C (radial diffusion is omitted for the sake of simplicity); and reagent adsorption on channel walls (illustrated as green channel edges) leading to reagent loss and cross-contamination. (b) Droplet generation strategies: (i) co-flow in a capillary format; (ii) T-Junction in a planar chip format; (iii) flow focusing in a planar chip format.

Chem. Comm., 2011, 1936-1942.

Operating procedure of the proposed loop-mediated isothermal amplification (ddLAMP) assay

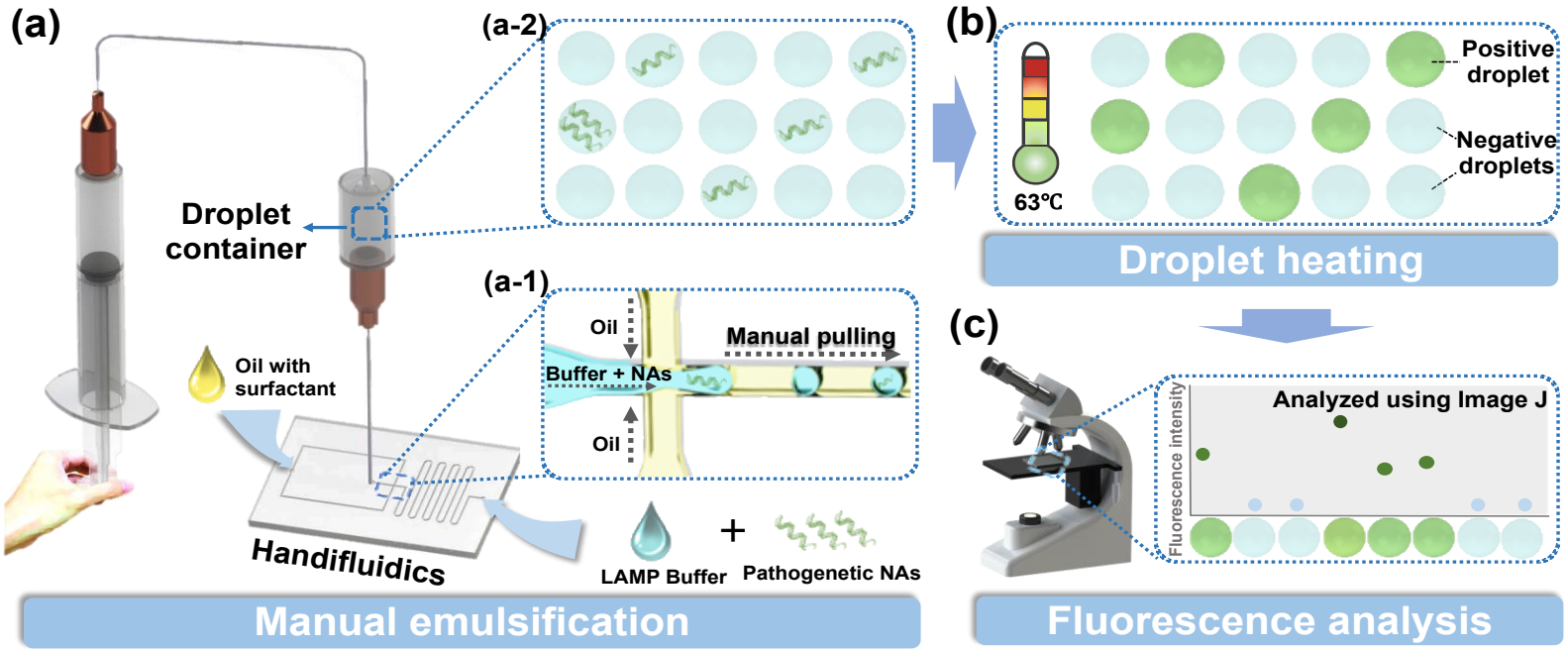

Schematic of the operating procedure of the proposed ddLAMP assay (a) Schematic of the manual emulsification process. The LAMP mixture (containing LAMP buffer and pathogenetic nucleic acids (NAs)) is emulsified into monodisperse droplets (a-1) and collected into a droplet container (a-2) by manually drawing a syringe to generate a negative pressure that drives the Handifluidics system, in which the resulting droplets contain the target DNA in a Poisson distribution. (b) Schematic of the droplet heating process. To conduct the LAMP reaction, the droplets inside the container are heated at 63 ˚C for 1 h using a water bath. (c) Schematic of the droplet fluorescence analysis. After performing the LAMP reaction, the droplets are extruded into a 12-well plate for imaging under a fluorescence microscope. The resulting images are analyzed using ImageJ to obtain the fluorescence intensity of the droplets.

Multi-sample detection processes and results

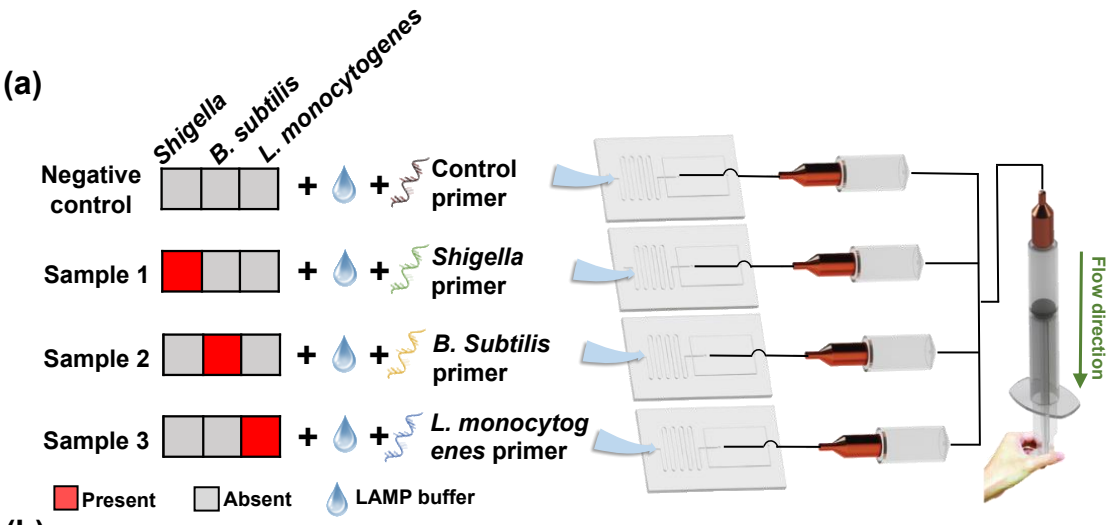

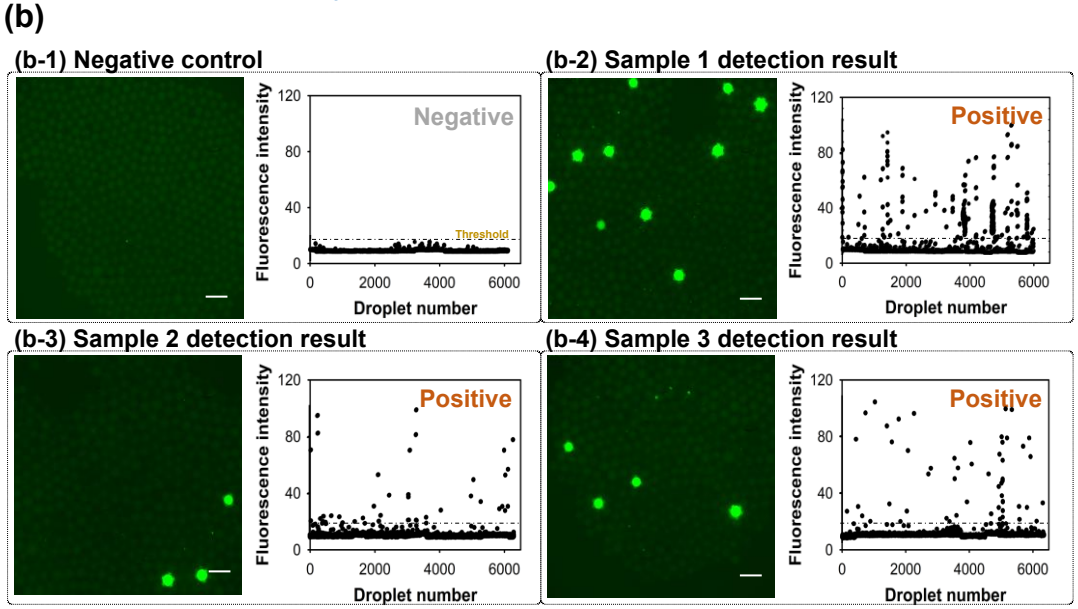

(a) Schematic of the multi-sample detection process using the proposed system. The system consists of a splitter and four Handifluidics devices connected with four droplet containers. Samples containing no DNA (negative control), Shigella (sample 1), B. subtillis (sample 2), and L. monicytogenes (sample 3) DNA were firstly mixed with LAMP buffers and control primer, and then loaded into different inner phase inlets of the Handifluidics devices, while mineral oil with 2.5 wt% EM 90 was loaded into the outer phase inlets. When manually pulling the splitter, the samples and the oil are introduced into the corresponding devices to generate droplets. (b) Results for multi-sample detection. The fluorescence micrographs and plotted intensity of the droplets after performing the LAMP reaction for the samples that contained (b-1) no target gene, and those that contained (b-2) sample 1, (b-3) sample 2, and (b-4) sample 3. Scale bars are 100 µm.

Concluding Remarks

- The advantages of droplet-based microfluidics, including low sample volumes, the facile integration of different functionalities and an exquisite control of heat and mass transport, whilst overcoming problems related to Taylor dispersion, surface–molecule interactions and slow mixing that plague continuous-flow (or single-phase) microfluidic systems, the ability to define and form ultra-small assay volumes, negligible cross-contamination and sample adsorption, enhanced mixing due to chaotic advection, and exceptionally high droplet generation frequencies (up to hundreds of kHz).

Chem. Comm., 2019, 9895-9903.